IL
NUOVO CIMENTO
ORGANO DELLA SOCIETÀ ITALIANA DI FISICA
SOTTO GLI AUSPICI DEL CONSIGLIO NAZIONALE DELLE RICERCHE

VOL. I, N. 2 *Serie decima* 1° Febbraio 1955

The Effects of Dislocations on X-Ray Diffraction. (*)

A. J. C. WILSON

Viriamu Jones Laboratory, University College - Cardiff, Wales

(ricevuto il 15 Novembre 1954)

Summary. — No satisfactory general theory of the effect of dislocations on X-ray diffraction exists. The treatment of WILSON [1] provides integral breadths for a powder consisting of long cylindrical particles each with a single axial screw dislocation. The actual expressions are complex, but lead to breadths increasing practically linearly with l, the index of reflexion corresponding to the dislocation axis. The results can be generalized to give approximate expressions for similar particles with edge dislocations [2,3] but expressions for (i) the line profile for a crystal with a single dislocation, and (ii) breadths and profile for crystals with more than one dislocation have not been obtained. The approximate theory of STOKES and WILSON [4] can be used for this purpose; the accuracy obtained is open to some question. The « tails » of the line profile so found are not particularly pronounced, and the « Cauchy » line profile found experimentally for cold-worked metals by WILLIAMSON *et al.* [5,6] may be a consequence of the general considerations discussed by EASTABROOK and WILSON [7], and not of anything particularly characteristic of dislocations.

1. – Introduction.

No satisfactory theoretical treatment of the diffraction of X-rays by a dislocated crystal exists. The elastic field of an edge dislocation is extremely complex, and the only exact treatment, for the restricted case of a powder consisting of long cylindrical crystals, each with a single axial dislocation, is

(*) Substance of a paper given at a meeting of the X-Ray Analysis Group of The Institute of Physics, London, 23 October 1954.

based on the comparatively simple displacement caused by a screw dislocation ([1,8]). It is possible to extend this slightly to give an approximate solution for edge dislocations ([2,3]), but I shall not deal with this extension here.

2. – Reciprocal-Lattice Representation.

We consider a cylindrical crystal of radius A with a single screw dislocation along its centre, and choose axes so that $\boldsymbol{c}$ is parallel to the dislocation axis. Each unit cell is then shifted by an amount $n\psi\boldsymbol{c}/2\pi$, where ψ is an angle measured from some fixed direction perpendicular to $\boldsymbol{c}$, and n is an integer determining the « pitch » of the screw (the displacement experienced in moving once round the dislocation axis on what appears to be a lattice plane).

Mathematical analysis shows that the points of the reciprocal lattice are extended into discs perpendicular to $\boldsymbol{c}$, and in fact for the points other than those with $l=0$ the discs are rings with zero intensity at the centre. The amplitude of reflexion as a function of horizontal distance ϱ from a reciprocal lattice point is

$$G = i^{nl} \cdot FZ \cdot \pi A^2 C^{-1} \; K_{nl}(2\pi\varrho A) \,, \tag{1}$$

where

$$K_m(x) = -2x^{-1}J_{m-1}(x) - 4mx^{-2} \sum_{g=1}^{\frac{1}{2}(m-1)} J_{m-2g}(x) - 2mx^{-2}J_0(x) + 2mx^{-2} \tag{2}$$

for m even and

$$K_m(x) = -2x^{-1}J_{m-1}(x) - 4mx^{-2} \sum_{g=1}^{\frac{1}{2}(m-1)} J_{m-2g}(x) + 2mx^{-2} \int_0^x J_0(x)\,\mathrm{d}x \tag{3}$$

for m odd; the J's are Bessel functions. Tables of the integral terminating equation (3) exist ([9]).

3. – Integral Breadths.

These expressions for G are complicated, and the line profiles on a Debye-Scherrer photograph have not been obtained. It has, however, been possible

([1]) A. J. C. WILSON: *Acta Crystallogr.*, **5**, 318 (1952).
([2]) A. J. C. WILSON: *Research, Lond.*, **3**, 387 (1950).
([3]) Y. Y. LI: Private communications (1954).
([4]) A. R. STOKES and A. J. C. WILSON: *Proc. Phys. Soc., Lond.*, **56**, 174 (1944).
([5]) G. K. WILLIAMSON and W. H. HALL: *Acta Metallurg.*, **1**, 22 (1953).
([6]) G. K. WILLIAMSON and R. E. SMALLMAN: *Acta Crystallogr.*, **7**, 574 (1954).
([7]) J. N. EASTABROOK and A. J. C. WILSON: *Proc. Phys. Soc., Lond.*, B **65**, 67 (1952).
([8]) A. J. C. WILSON: *Research, Lond.*, **2**, 541 (1949).
([9]) A. N. LOWAN and M. ABRAMOWITZ: *Journ. Math. Phys.*, **22**, 2 (1943).

to obtain series expressions for a quantity inversely proportional to the integral breadths. After allowing for a fore-shortening factor depending on the indices of reflexion (compare [10], p. 71), the integral breadths are inversely proportional to

$$H_0 = \frac{8A}{3\pi} NF^2 \sum_{g=0}^{\infty} \frac{\Gamma(g + nl + \frac{1}{2})\,\Gamma(g + \frac{1}{2})}{(2g + nl + 2)\Gamma(g + nl + 1)g!} . \tag{4}$$

The series can be reduced to a finite sum for all values on nl except, apparently, $nl = 1$. For nl even it becomes

$$\frac{\pi nl}{n^2l^2 - 1} + \frac{(nl)!\,\pi^{\frac{1}{2}}}{2^{nl-1}(nl-1)} \sum_{g=0}^{\frac{1}{2}nl} \frac{(-)^{nl-g+1}}{(nl - 2g + 1)g!\,\Gamma(nl - g + \frac{1}{2})} , \tag{5}$$

and for odd values of nl from 3 onwards it becomes

$$\frac{[\frac{1}{2}(nl-3)]!\,\Gamma(\frac{1}{2})}{2\Gamma(nl + \frac{1}{2})} \sum_{g=0}^{\frac{1}{2}(nl-3)} \frac{\Gamma(nl - g - \frac{1}{2})g!}{[\frac{1}{2}(nl-3) - g]!\,\Gamma(g + \frac{3}{2})} . \tag{6}$$

In spite of the complexity of these expressions, the integral breadths, plotted in Fig. 1 for values of nl up to 7, are practically a linear function of nl. The point for $nl = 0$ gives also the particle-size broadening for a long cylindrical non-dislocated crystal. The equation for the straight line is approximately

$$\beta_{nl} = \beta_0(1 + 1.30nl) . \tag{7}$$

FRANK [11] has advanced a simple argument that leads to the expression

$$\beta_{nl} = \beta_0(1 + 1.17nl) . \tag{8}$$

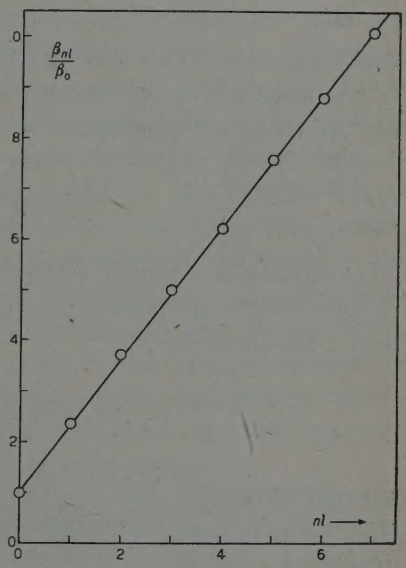

Fig. 1. – Line broadening for a crystal with a screw dislocation, plotted as a function of nl. The straight line represents $\beta_{nl}/\beta_0 = 1 + 1.30nl$; the point for $nl = 1$ is more accurate than that shown in Fig. 1 of WILSON [1].

[10] A. J. C. WILSON: *X-Ray Optics* (London, 1949).
[11] F. C. FRANK: *Research, Lond.*, **2**, 542 (1949).

4. – Stokes-Wilson Approximation.

In the approximate treatment of strain broadening given by STOKES and WILSON [4] strain gradients are neglected. To this approximation the line profile, as a function of distance measured in radians from the centre of the line, is given by

$$\frac{I(-e\,\mathrm{tg}\,\theta)}{I(0)} = \frac{\varphi_{hkl}(e)}{\varphi_{hkl}(0)}\,, \tag{9}$$

where $\varphi_{hkl}(e)\,\mathrm{d}e$ is the fraction of the crystal for which the tensile strain in the hkl direction lies between e and $e+\mathrm{d}e$. For a cylindrical crystal with an axial screw dislocation the displacement is given by

$$\boldsymbol{u} = \frac{\psi}{2\pi}\, n\boldsymbol{c}\,,$$

and it is easy to show that the tensile strain in the hkl direction at the point $\boldsymbol{r}$ is

$$e_{hkl} = |\boldsymbol{s}|^{-2}\boldsymbol{s}\cdot\nabla\boldsymbol{u}\cdot\boldsymbol{s} \tag{10}$$

$$= \frac{nl}{2\pi}\,\frac{\boldsymbol{s}\cdot(\boldsymbol{k}\times\boldsymbol{r})}{s^2 r^2}\,, \tag{11}$$

where $\boldsymbol{s} = h\boldsymbol{a}^* + k\boldsymbol{b}^* + l\boldsymbol{c}^*$ is the position vector in reciprocal space and $\boldsymbol{k}$ is a unit vector in the direction of $\boldsymbol{c}$. The contours of constant strain in the hkl direction are thus given by

$$\boldsymbol{r}\cdot\left\{\boldsymbol{r} - \frac{nl\boldsymbol{s}\times\boldsymbol{k}}{2\pi s^2 e_{hkl}}\right\} = 0\,. \tag{12}$$

This represents a family of circles with radii inversely proportional to e_{hkl} and tangent to the projection of $\boldsymbol{s}$ on the plane perpendicular to the dislocation axis. The contours for

$$e_{hkl} = 0,\ \tfrac{1}{4},\ \tfrac{1}{2},\ 1,\ 2,\ \ldots \cdot \left\{\frac{nl\,|\boldsymbol{s}\times\boldsymbol{k}|}{2\pi s^2 A}\right\}$$

are represented in Fig. 2. The expression in brackets represents the largest value attained by the strain on the circumference of the cylindrical crystal (radius A). Expressed in terms of φ, the angle between $\boldsymbol{c}^*$ and $\boldsymbol{s}$, this characteristic strain is

$$E = \frac{nl\sin\varphi}{2\pi s A}\,. \tag{13}$$

Note that E and e_{hh} vanish both for $l = 0$ (reflexions from planes parallel to the dislocation axis) and for $\varphi = 0$ (reflexions from planes perpendicular to the dislocation axis).

To obtain $\varphi_{hkl}(e)$ it is necessary to calculate what fraction of the total area of cross-section lies between circles of radii corresponding to e_{hh} and $e_{hh} + \mathrm{d}e_{hh}$. This is easily found to be

$$\varphi(e)\,\mathrm{d}e = \frac{E^2}{2e^3}\,\mathrm{d}e \tag{14}$$

for $e > E$, and with somewhat more difficulty to be

$$\varphi(e)\,\mathrm{d}e = \left\{\frac{E^3}{2e^3} - \frac{E^3}{\pi e^3}\arccos\frac{e}{E} - \frac{E^2\sqrt{E^2 - e^2}}{\pi e^2}\right\}\frac{\mathrm{d}e}{E} \tag{15}$$

for $e < E$.

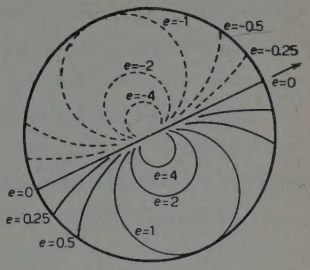

Fig. 2. – Contours of constant strain in the *hkl* direction in a cylindrical crystal with a screw dislocation. The arrow shows the projection of the *hkl* direction on to a plane perpendicular to the dislocation axis.

The rather curious line profile resulting from these expressions is shown in Fig. 3. As already pointed out, the regions of high intensity in reciprocal space are ring-shaped, so the dip in the middle is not unexpected. This part of the curve, however, is due to the part of the crystal which would be most influenced by dislocations in neighbouring parts of the crystal, and it may be of no practical significance, even if it is not an artifact generated by the approximations made in the Stokes-Wilson treatment. The tails of the line profile, however, correspond to the part of the crystal in the immediate neighbourhood of the dislocation axis, and one would not expect them to be greatly affected by the presence of the dislocations within the same crystal. They fall off as the inverse cube of e, and so approach zero more quickly than do the tails of the Cauchy distribution.

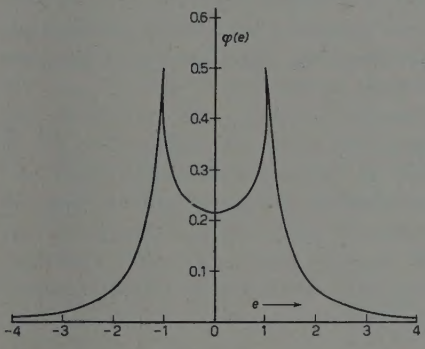

Fig. 3. – Line profile corresponding to Fig. 2, according to the approximate theory of STOKES and WILSON [4].

For comparison with the results of the more exact calculation in section 3 it is of interest to calculate the integral breadth corresponding to the line

---

[12] W. H. HALL: *Ph. D. Thesis* (Birmingham), and private communications (1950).

profile just derived. The limit of equation (15) as $e \to 0$ is

$$\varphi(0) = \frac{2}{3\pi E}, \tag{16}$$

so (equations (2) and (3) of Stokes and Wilson)

$$\left\{ \begin{aligned} \beta &= \frac{2 \operatorname{tg} \theta}{\varphi(0)} \\ &= 3\pi E \operatorname{tg} \theta, \\ &= \frac{3nl\lambda \sin \varphi}{4A \cos \theta}, \end{aligned} \right. \tag{17}$$

after making the substitution $s = 2 \sin \theta / \lambda$.

The approximation may be improved somewhat by adding the breadth corresponding to the particle-size broadening for a cylinder of radius A:

$$\beta = \frac{\lambda}{\varepsilon \cos \theta},$$

where ([8]), equation (5) and discussion after equation (6))

$$\varepsilon = \frac{16A}{3} \cos \varphi, \tag{18}$$

so that

$$\beta = \frac{3\pi\lambda \sin \theta}{16A \cos \theta} \left[1 + \frac{4}{\pi} nl \right], \tag{19}$$

$$\beta_{nl} = \beta_0 [1 + 1.27nl]. \tag{20}$$

The coefficient of nl differs from that in equation (7) by less than 3%.

5. – General Remarks.

I shall close with a few remarks on the general problem of interpreting the line profiles observed with cold-worked metals. WILLIAMSON and his collaborators ([5,6]) have found that these are approximately of the Cauchy form.

This tends to zero rather slowly, as the inverse square of the distance from the centre of the line, and WILLIAMSON and his collaborators have suggested that this long tail is associated with the region of high distortion near the dislocation axis. The approximate treatment in the preceding section offers no support for this; it suggests an approach to zero as the inverse cube of the distance from the centre of the line. EASTABROOK and WILSON [7] have devised general arguments to show that, if the distorted crystal is large enough to contain several positive and negative cycles of strain, the line profile is likely to be one of the Cauchy type. In all probability, therefore, the Cauchy distribution does not specifically indicate the effect of dislocations.

RIASSUNTO (*)

Non è nota alcuna teoria generale soddisfacente dell'effetto delle dislocazioni sulla diffrazione dei raggi X. La trattazione di WILSON [1] fornisce larghezze integrali per una polvere formata da lunghe particelle cilindriche che presentino ciascuna una singola dislocazione assiale del genere « screw ». Le espressioni risultanti sono complesse, ma conducono a larghezze crescenti in pratica linearmente con l, l'indice di riflessione corrispondendo all'asse della dislocazione. I risultati si possono generalizzare per ottenere espressioni approssimate per particelle simili con dislocazioni del tipo « edge » [2,3], ma non si è riusciti ad ottenere espressioni (1) per il profilo del limite della dislocazione per un cristallo con un'unica dislocazione e (2) larghezze e profili per cristalli con più di una dislocazione. La teoria approssimata di Stokes e Wilson [4] serve a questo scopo; l'esattezza ottenibile è passibile di qualche osservazione. Le « code » della linea di profilo così trovate non sono particolarmente pronunciate e la linea di profilo di Cauchy trovata sperimentalmente da WILLIAMSON *et al.* [5,6] per metalli lavorati a freddo può dipendere dalle condizioni generali discusse da EASTABROOK e WILSON [7] e non da alcuna circostanza riferentesi particolarmente alle dislocazioni.

(*) *Traduzione a cura della Redazione.*

Associated Production of a τ-Meson and a Charged Hyperon.

K. Gottstein

Max-Planck-Institut für Physik - Göttingen

(ricevuto il 4 Dicembre 1954)

Summary. — In a stack of stripped emulsions an example of associated production of a positively charged τ-meson and of a hyperon decaying in flight into a charged L-meson was observed. The mass of the hyperon is found to be $2374 \pm \frac{29}{37}\ m_e$, assuming the decay scheme $Y^{\pm} \to \pi^{\pm} + n + Q$. For the τ-meson one obtains from range measurements $m_\tau = 963 \pm 0.5\ m_e$, all three secondaries coming to rest in the emulsion. A possible reason is suggested why some authors might have slightly overestimated the mass of their τ-mesons.

1. – Introduction.

Recent investigations have given evidence for the associated production of heavy mesons and hyperons, a process which had already been considered in the theoretical field [1]. Lal *et al.* [2] observed one event in photographic emulsions in which a τ-meson is emitted together with a charged hyperon which decays in flight into a L-meson and one or more neutral particles. The lower limit for the rest mass of the hyperon is given as 1570 electron masses. Cloud-chamber experiments yielded a few further examples for the pair production of heavy unstable particles (Λ^0 with θ^0, and possibly Λ^- with K^+), both by 1.5 GeV π^--mesons from the Brookhaven Cosmotron [3], and by particles from the Cosmic Radiation [4]. The Bristol group [5], in a systematic

[1] M. Gell-Mann and A. Pais: *Proceed. of the Intern. Physics Conf., Glasgow*, July 1954. Further references are given there and in [3].

[2] D. Lal, Yash Pal and B. Peters: *Proc. Ind. Acad. of Sci.*, **38**, 398 (1953).

[3] W. B. Fowler, R. P. Shutt, A. M. Thorndike and W. L. Whittemore: *Phys., Rev.*, **93**, 861 (1954).

[4] R. W. Thompson, J. R. Burwell, R. W. Huggett and C. J. Karzmark: *Phys., Rev.*, **95**, 1576 (1954).

[5] C. Dahanayake, P. E. Francois, Y. Fujimoto, P. Iredale, C. J. Waddington, and M. Yasin: *Phil. Mag.*, **45**, 855 (1954).

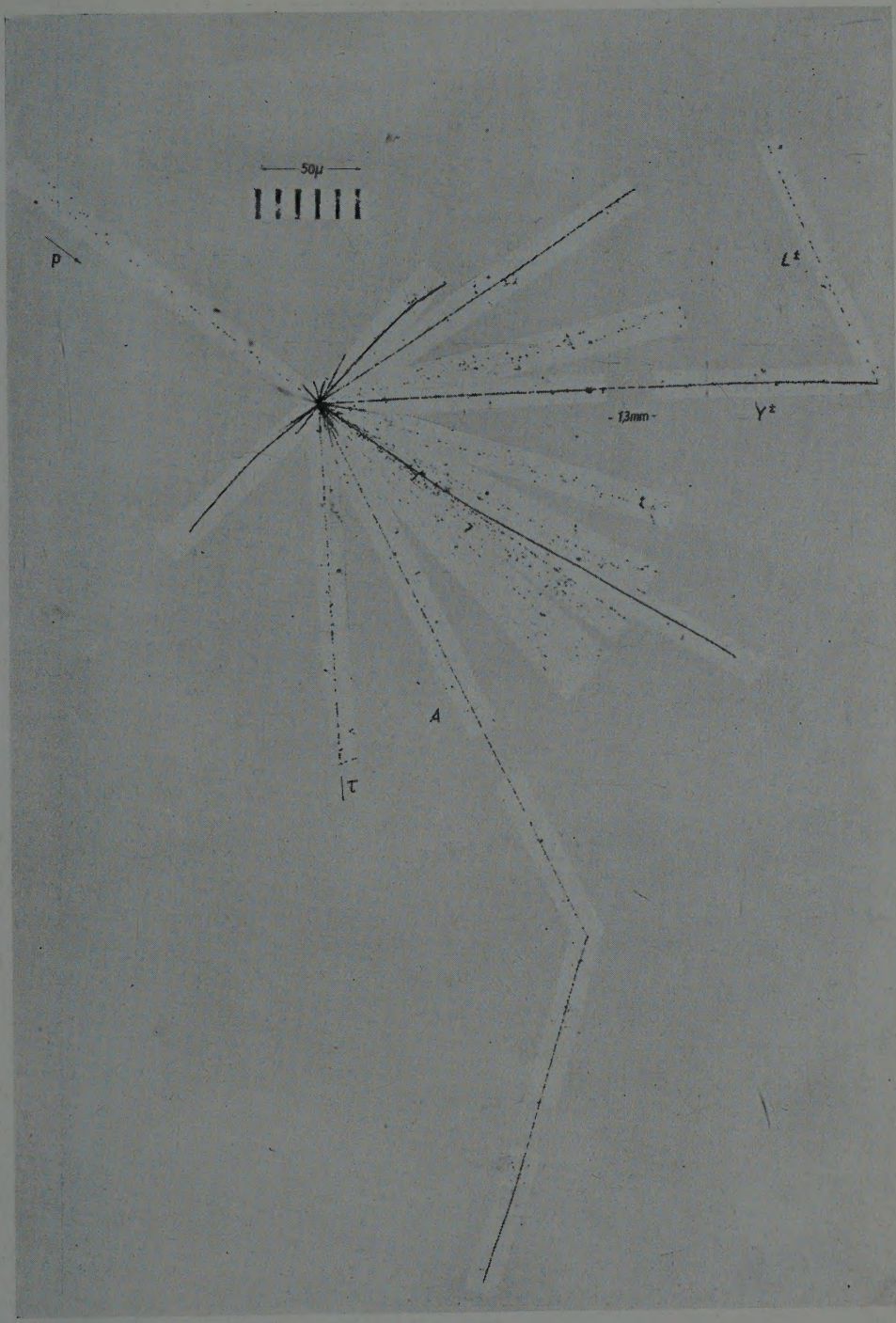

a

Fig. 1*a* – Microphotograph of the associated production of a positively charged τ-meson and a charged hyperon.

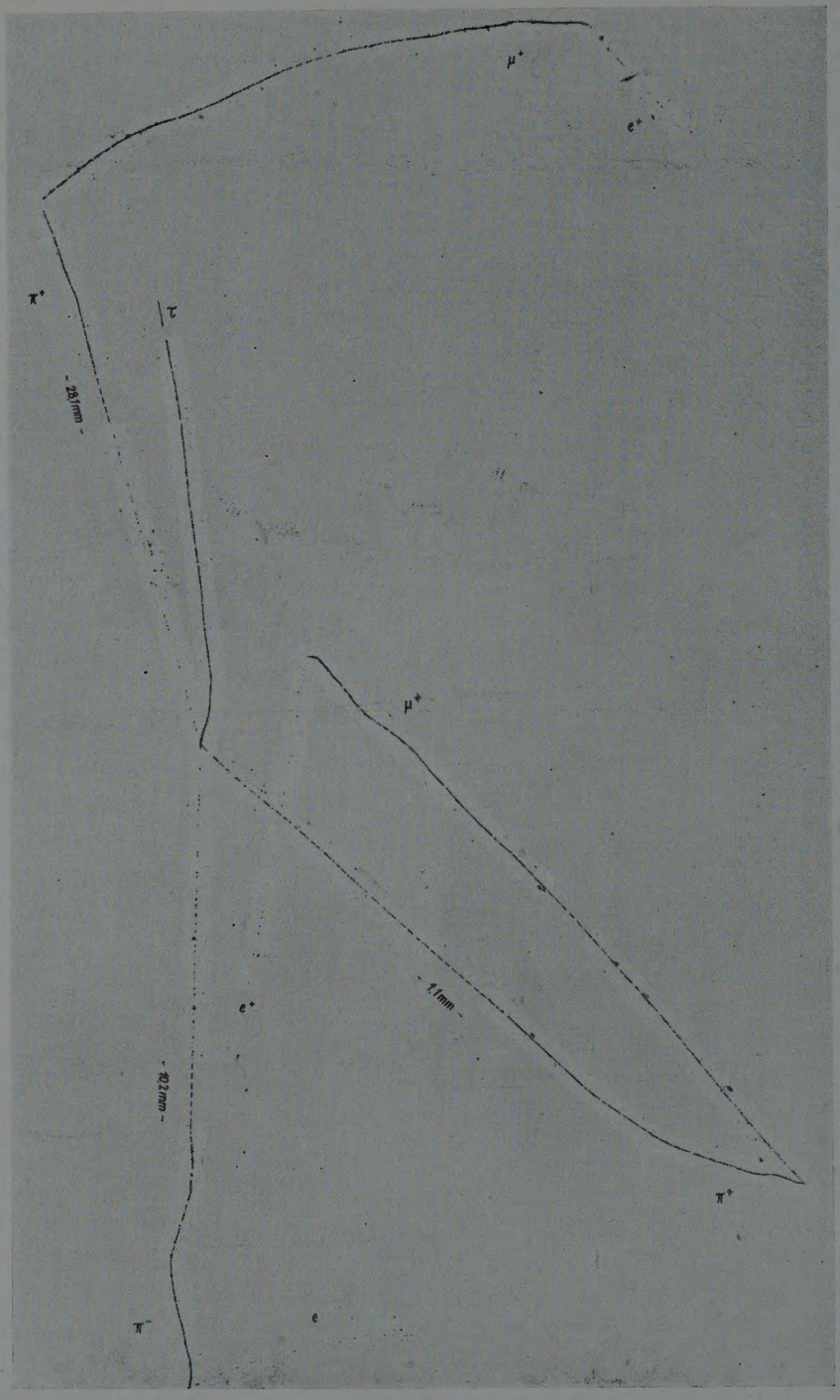

b

Fig. 1*b* – Microphotograph of the associated production of a positively charged τ-meson and a charged hyperon.

study of the particles emitted from nuclear disintegrations, found two cases of associated emission of a K-particle (decaying at rest) and a hyperon (decaying in flight). A neutral V-event (Λ^0 or θ^0) originating from a disintegration from which also a K-meson emerges, and the associated production of a τ-meson and an unstable fragment were reported by DEBENEDETTI *et al.* [6].

This note describes an event of the type observed by LAL *et al.* [2]. In the present case, however, the experimental conditions allow more accurate measurements to be made.

2. – Details of the Event.

In the course of general scanning of the emulsions of an Ilford G5 « stripped » stack of 40 layers, each 600 μ thick, exposed for seven hours at an average height of 27 km in Sardinia, summer 1953, a τ-meson decay was found. One of the three secondaries showed a typical π-μ-e-decay after a track length of 1.4 mm within the same emulsion layer in which the τ-decay occurred. Another secondary could be followed into the adjoining sheet where, after a total track length in emulsion of 28.3 mm, it also underwent decay, the μ-meson track again being visible in the emulsion over its whole length with the electron track originating from its end. The third secondary particle leaves the sheet, entering the adjoining one, but returns to it and comes to rest after having traversed a total of 10.4 mm in emulsion. A slow electron the track of which is at least 160 μ long can be seen to have been emitted from where the particle had stopped. Thus it appears that the meson has been captured by a heavy nucleus of the emulsion. The track of the τ-meson, when followed backwards, was found to have a total length of 23 mm in three emulsion sheets, and to come from a « star » of type 28 +29 p. In a search for further associated unstable particles all tracks of this « star » with grain-density above plateau were followed, and one event was found which can be explained as representing the decay in flight of a charged hyperon. The hyperon track has a length of 1.6 mm in three emulsions, the secondary leaves the stack having traversed 34 emulsion sheets in which its total track length is 23.1 mm.

Fig. 1*a* and *b* shows a microphotograph of the event.

3. – Measurements and results.

3·1. *General remarks.* – All length measurements in the emulsion plane were made using our Leitz Koordinatenkomparator which allows the reading

(6) A. DEBENEDETTI, C. M. GARELLI, L. TALLONE, and M. VIGONE: *Nuovo Cimento*, **12**, 369 (1954); **12**, 467 (1954).

of lengths of several centimetres with an accuracy of the order of 1 μ. Shrinkage factors were determined by measuring the lengths of steeply dipping μ-meson tracks from π-μ-decays. The « true » length was then calculated by approximating the tracks (which in reality are not straight but slightly scattered) by a polygon.

For grain-densities higher than three times the plateau value the range-energy relation calculated by FAY *et al.* ([7]) was used, for lower grain-densities the one obtained by the Rome group ([8]) from interpolation between the range-energy relations for aluminium and lead ([9]). Before these relations could be applied it had to be considered, however, that they are valid for dry emulsion whereas the Sardinian stacks had been exposed at a relative humidity of approximately 55% ([10]). According to LEES *et al.* ([11]) the increase in range at 60% relative humidity is 4% for G5 emulsions and for protons of 10 MeV energy. It was assumed that this is also true for the somewhat higher energies occurring here. Moreover, the Rome relation refers to C2-emulsion the stopping power of which is smaller by 1% than the stopping power of G5-emulsion ([12]). Apart from these corrections it was taken into account that the emulsions had been exposed with thin sheets of tissue paper (~ 1 mg/cm^2 corresponding to the stopping power of about 5 μ of emulsion) between them.

Grain-densities were always normalized with regard to the plateau value in the respective region of the emulsion which was determined by measuring the grain-densities on the tracks of electron-positron pairs at equal depth.

3·2. *The τ-meson.* – The three secondary tracks of the τ-meson are coplanar within 1 degree.

Table I shows the kinetic energies E_{kin} of the secondaries, as resulting from range measurements, under the assumption that all three of them are π-mesons.

The mass of the τ-meson which one thus obtains (963 ± 0.5 m_e) agrees not too well with the values given by some other workers ([13-15]), most of whom,

---

([7]) H. FAY, K. GOTTSTEIN and K. HAIN: *Nuovo Cimento, Suppl.*, **11**, 234 (1954).

([8]) G. BARONI, C. CASTAGNOLI, G. CORTINI, C. FRANZINETTI and A. MANFREDINI: *Communication BS 9, European Council for Nuclear Research*, July 1954.

([9]) S. BISWAS, E. C. GEORGE and B. PETERS: *Proc. Ind. Acad. Sci.*, **38**, 418 (1953).

([10]) M. W. FRIEDLANDER: *Communication BS 1, European Council for Nuclear Research*, May 1954.

([11]) C. F. LEES, G. C. MORRISON and W. G. V. ROSSER: *Proc. Phys. Soc.*, A **66**, 13 (1953).

([12]) J. ROTBLAT: *Nature*, **167**, 550 (1951).

([13]) M. BALDO, G. BELLIBONI, M. CECCARELLI, M. GRILLI, B. SECHI, B. VITALE and G. T. ZORN: *Nuovo Cimento*, in press.

([14]) E. AMALDI, G. BARONI, C. CASTAGNOLI, G. CORTINI and A. MANFREDINI: *Bagnères-Report*, p. 157 (1953).

([15]) C. F. POWELL: *Nuovo Cimento, Suppl.*, **11**, 165 (1954).

however, appear to have not taken into account the moisture content of their emulsions. For comparison the value following from the application of the range-energy relation for dry emulsion is also given (967 m_e), which is almost exactly the result quoted by these authors.

TABLE I.

(R_{Em} = Range in emulsion, R_P = Range corresponding to the path in paper, R_T = Total range).

Track	R_{Em} (μ)	$R_{Em} \times 0.96$ (μ)	R_P (μ)	R_T (μ)	$R_T \times 1.01$ (μ)	R_{Dry} (*) (μ)	E_{kin} (MeV)
τ	23009	22090	90	22180	22400		62.8
						23330	64.4
Secondary No. 1	1364	1309	0				7.3
							7.4
Secondary No. 2	10408	9992	105	10097	10198		23.5
						10618	24.1
Secondary No. 3	28323	27190	47	27237	27509		43.1
						28654	44.1

Q (MeV) = **73.9** (75.6)
m_τ (m_e) = **963** (967)

(*) $R_{Dry} = (R_{Em} + R_P) \cdot 1.01$ (The Factor 1.01 in this and in the preceding column is due to the difference in stopping power between G 5- and C 2- emulsion).

The τ-meson is found to have been emitted with a kinetic energy of 63 MeV, its track forming an angle of 130 degrees with respect to that of the primary of the disintegration.

The assumption that all three secondaries are π-mesons is verified by ionization-range measurements; Fig. 2 shows the relation between specific energy loss and range derived from the range-energy relation ([8]) for protons. The experimental values obtained on the τ-meson and its secondaries have been adapted to this diagram by multiplying the ranges by the ratio m_p/m_τ, and m_p/m_π. respectively, and by normalizing the grain-densities with regard to the « plateau » value 0.6 keV/μ. One notices that also the points for the negative particle, No. 2, fit the curve rather well. The fit is considerably worse

if the ranges are multiplied by m_p/m_π. Moreover, the momenta of the three particles add up to zero ((0.4 ± 1.6) MeV/c) only if all of them are π-mesons. The time of flight of the τ-meson, in its own frame of reference, is $2 \cdot 10^{-10}$ s.

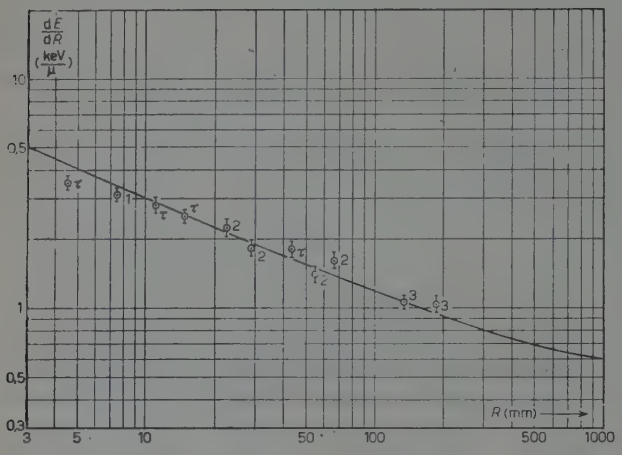

Fig. 2. – Relation between specific energy loss and range. ———: Curve calculated from the range-energy relation ([8]) for protons. The numbers on the experimental points refer to the numbers of the secondaries (Comp. Table I). (Ranges have been multiplied by m_p/m, grain-densities normalized with respect to the « plateau » value).

3·3. *The Hyperon.* – The particle which is subsequently shown to be a hyperon is emitted under an angle of 118° with respect to the direction of the primary and of 90° with respect to that of the τ-meson. Its track is too steep for scattering measurements to be feasible. Grain-density measurements, however, indicate that the particle has not come to rest at the point where the thin track of the secondary particle appears. The grain-density has, in fact, (1.2 ± 0.35) times the plateau value although some systematic error due to the steepness of the track might have caused it to be somewhat underestimated.

TABLE II.

m_{sec}	(m_e)	273	207
$\left(E_{kin}\right)_{sec\ L}$	(MeV)	53^{+11}_{-8}	40^{+8}_{-6}
$\left(E_{kin}\right)_{sec\ C}$	(MeV)	112^{+14}_{-18}	84^{+11}_{-14}
$\left(E_{kin}\right)_{N\ C}$	(MeV)	23^{+4}_{-5}	13^{+4}_{-5}
$m_Y(m_{el})$		$2\,374^{+29}_{-37}$(*)	$2\,235^{+21}_{-27}$

(*) If the neutral decay product was assumed to be a Λ^o-particle one would obtain: $m_Y = 2710\ m_e$.

The secondary is emitted backwards, its track forming, in the laboratory system, an angle of 27.7 ± 0.7 degrees with the hyperon track. Its mass as derived from the variation of ionization with range is 271^{+195}_{-106} electron masses. It is thus either a π- or a μ-meson. Assuming a two-body decay the mass of the parent particle can be calculated from the conservation laws on these two premises, under the further assumption that the neutral particle is a neutron. This mass value constitutes a lower limit in the case of a more-body decay. Table II contains the results of the calculations. In the estimation of the errors both the statistical deviations and a possible systematic underestimation by 30% of the grain-density of the parent particle have been taken into account. The subscripts L and C refer to the laboratory and to the centre-of-mass system.

The experimental evidence is thus compatible with either of the two interpretations:

$a)$ $\qquad Y^{\pm} \to \pi^{\pm} + n + (135^{+15}_{-19})$ MeV ,

$b)$ $\qquad Y^{\pm} \to \mu^{\pm} + n + (\ 97^{+12}_{-15})$ MeV .

The interpretation $a)$ is, however, more likely to be correct. The corresponding mass value fits in with the results obtained by other laboratories on charged hyperons decaying, in fligth ([16-19]) as well as at rest ([20-21]), into charged light mesons.

Between emission and decay the hyperon has lived for approximately $1.5 \cdot 10^{-11}$ s, in its own frame of reference. It was emitted with a kinetic energy of (87 ± 10) MeV.

3·4. *Further Observations.* – The two planes defined, respectively, by the directions of flight of the τ-particle and the hyperon, and the hyperon and the secondary L-meson, form an angle of 28° with each other. (See remark in ([3]) and in ([5])).

In following the tracks from the disintegration an event was found which could be considered to represent the inelastic scattering of a proton, or, more generally, a « star » of type $1+0p$. If, however, it is to be interpreted in

([16]) D. Lal, Yash Pal and B. Peters: *Phys. Rev.*, **92**, 438 (1953).
([17]) M. Ceccarelli and M. Merlin: *Nuovo Cimento*, **10**, 1207 (1953).
([18]) P. H. Barrett: *Phys. Rev.*, **94**, 1328 (1954).
([19]) M. W. Friedlander: *Phil. Mag.*, **45**, 418 (1954).
([20]) A. Bonetti, R. Levi-Setti, M. Panetti and G. Tomasini: *Nuovo Cimento*, **10**, 1736 (1953).
([21]) D. T. King, N. Seeman and M. M. Shapiro: *Phys. Rev.*, **92**, 838 (1953).

terms of the scheme

$$Y^- \rightarrow p + \pi^0 + Q\,,$$

the parent particle would have to have a mass of $2530\ (\pm 40)\ m_e$. The particle causing it (track A in Fig. 1) was emitted under an angle of about 30° with respect to the track of the τ-meson, and then traversed two emulsion sheets. It is too steep for direct mass measurements.

3·5. *Conclusions.* – While it is as yet too early to say whether hyperons and heavy mesons are exclusively produced in pairs it is interesting to note that in those cases in which pair production does occur, τ-mesons as well as $\varkappa$-mesons can take the place of the heavy meson. In addition to their similar mass this is another property which these two types of particles have in common whereby further support is lent to the tentative suggestion made at Bagnères-de-Bigorre, that the different decay scheme is, in fact, the only difference between τ and $\varkappa$.

The author's thanks are due to Miss M. AHRENS who found the τ-meson described, and to Mr. L. VON LINDERN and Mrs. H. BAUMBACH for the microphotograph.

RIASSUNTO (*)

In un pacco di emulsioni strappate fu osservato un esempio del decadimento in volo di un mesone τ con carica positiva e di un iperone in un mesone L carico. La massa dell'iperone fu determinata in $2374\ ^{+29}_{-37}\ m_e$; assumendo un decadimento secondo lo schema $Y^{\pm} \rightarrow \pi^{\pm} + n + Q$. Per il mesone τ si ottiene da misure di range $m_\tau = 963 \pm 0{,}5\ m_e$, con arresto dei tre secondari nell'emulsione. Si dà un plausibile motivo del fatto che alcuni autori possano avere stimato leggermente in eccesso la massa dei loro mesoni τ.

(*) *Traduzione a cura della Redazione.*

The Decay of ^{185}W.

A. Bisi, S. Terrani and L. Zappa

Istituto di Fisica Sperimentale del Politecnico - Milano

(ricevuto il 5 Dicembre 1954)

Summary. — The β- and γ-radiations from ^{185}W have been investigated by means of an intermediate image β-spectrometer, a proportional counter spectrometer and a scintillation spectrometer. The disintegration has been found to be complex. It was found that the maximum energy of the main β-spectrum (90 per cent) was 426 keV and that the β-transition goes to the ground state of ^{185}Re. A faint γ-ray of 55.6 keV was detected and found to correspond to an excited level in ^{185}Re. The γ-ray arises from a magnetic dipole transition. Spin and parity have been assigned; a decay scheme is proposed.

1. – Introduction.

A β^--activity of about 75 days half-life induced in tungsten by slow neutrons bombardment was discovered and assigned to ^{185}W by Minakawa [1] and by Fajans and Sullivan [2]. The β-decay was found to be simple by many investigators, the upper energy limit of the electrons being 428 keV. The allowed shape of the β-spectrum down to energies somewhat less than 150 keV was put in evidence by Shull [3].

As yet no direct proof of the existence of γ-rays following β-decay has been obtained. In spite of the negative results of earlier investigations, a brief report on the occurrence of two electron lines in the ^{185}W decay was given by Cork, Keller and Stoddard [4]. These lines, if interpreted as an *L-M* combination should yield a single γ-ray at 133.7 keV. Bunyan, Lundby and

(1) O. Minakawa: *Phys. Rev.*, **57**, 1189 (1940).
(2) K. Fajans and W. H. Sullivan: *Phys. Rev.*, **58**, 276 (1940).
(3) F. B. Shull: *Phys. Rev.*, **74**, 917 (1948).
(4) J. M. Cork, H. B. Keller and A. E. Stoddard: *Phys. Rev.*, **76**, 575 (1949).

WALKER (5) in the course of a search for short-lived nuclear isomers were not able to confirm the assumption of CORK *et al.*. Quite recently MIJATOVIĆ (6) has carried out a preliminary investigation of the electromagnetic radiation from ^{185}W by means of a scintillation spectrometer. An intense peak was observed at about 60 keV and attributed to X-radiation, while a weak and broad peak at higher energies was identified as a 134 keV γ-ray.

Table I summarizes the results of the previous investigations on the decay of ^{185}W as far as we know.

TABLE I.

Half-life d	Energy of radiation in MeV β^-	γ	$\frac{\gamma}{\beta}$	References
77	0.4 –0.5 abs.	γ	—	MINAKAWA (1)
74.5	0.55–0.65 abs.	—	—	FAJANS and SULLIVAN (2)
	0.64–0.72 cl. ch.	—	—	
	0.55 abs.	no γ	$\frac{\gamma}{\beta} < 3.3 \cdot 10^{-4}$	SULLIVAN (8)
		no γ	—	COLEMAN, NUDENBERG and POOL (9)
	0.43 spect.	no γ	—	PEACOCK and WILKINSON (10)
73.2	0.43 spect.	—	—	SAXON (11)
	0.428 spect.	—	—	SHULL (3)
76	—	0.134 spect. conv.	—	CORK, KELLER and STODDARD (4)
		no γ	—	BUNYAN, LUNDBY and WALKER (5)
		0.134 scint. spect.	$\frac{X+\gamma}{\beta} = 0.09$	MIJATOVIĆ (6)

The adopted symbols and abbreviations are taken off from the Table of Isotopes of HOLLANDER, PERLMAN and SEABORG (*Rev. Mod. Phys.* **25**, 467 (1953)).

(5) D. E. BUNYAN, H. LUNDBY and D. WALKER: *Proc. Phys. Soc.*, A **57**, 253 (1949).
(6) A. M. MIJATOVIĆ: *Bull. Inst. Nuclear Sci. «Boris Kidrich»*, **4**, 75 (1954).
(7) J. E. MACK: *Rev. Mod. Phys.*, **22**, 64 (1950).
(8) W. H. SULLIVAN: *Phys. Rev.*, **68**, 277 (1945).
(9) K. D. COLEMAN, R. NUDENBERG and M. L. POOL: *Phys. Rev.*, **72**, 164 (1948).
(10) C. L. PEACOCK and R. G. WILKINSON: *Phys. Rev.*, **74**, 297 (1948).
(11) D. SAXON: *Phys. Rev.*, **74**, 1264 (1948).

Spin and magnetic moment for the ground state of ^{185}Re have been measured ([7]).

This paper discusses the results of our research to clarify the decay of ^{185}W. A new decay scheme is suggested, through a detailed investigation of β- and γ-spectra.

2. – Experimental Apparatus.

A high transmission intermediate image beta spectrometer ([12,13]) was used for investigating the β-spectrum. The baffles in the spectrometer were adjusted for a resolving power of 4 per cent.

The γ- and X-radiations were analysed using a single crystal spectrometer (NaI-Tl) and a proportional counter spectrometer ([14,15]). After amplification the pulse size was measured by means of a twenty channel electronic pulse analyser ([16]).

3. – Beta-Spectrum.

The samples of ^{185}W were obtained by neutron irradiation of tungsten oxide in the Harwell pile. Samples from which the ^{185}W β-spectrum was measured were prepared by evaporating a few drops of $(NH_4)_2WO_4$ on a Formvar foil less than 0.1 mg/cm² thin.

The Fermi plot of the β-spectrum is shown in Fig. 1. The upper limit of the electrons energy was found to be:

$$E = 426 \pm 3 \text{ keV} .$$

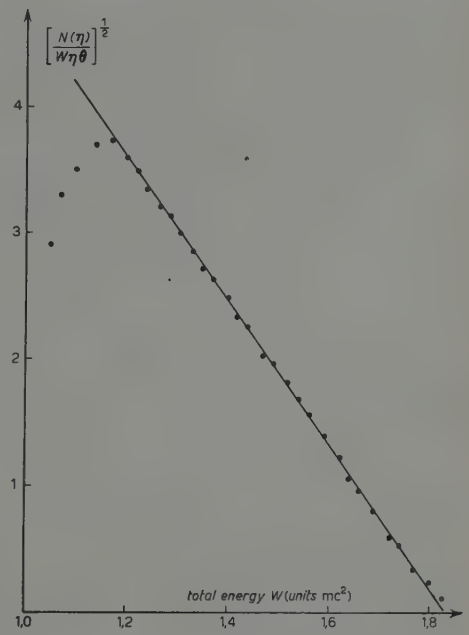

Fig. 1. – Fermi plot of the β-spectrum of ^{185}W.

The plot is substantially a straigh line from the upper end-point down to about 85 keV. No evidence was found of a complex decay, neither was there of conversion lines superimposed on the β-spectrum down to energies of about 50 keV.

([12]) H. Slätis and K. Siegbahn: *Ark. Fys.*, **1**, 339 (1949).
([13]) G. Bolla, S. Terrani and L. Zappa: *Nuovo Cimento*, **12**, 875 (1954).
([14]) G. Bertolini, A. Bisi and L. Zappa: *Nuovo Cimento*, **10**, 1424 (1953).
([15]) A. Bisi and L. Zappa: *Nuovo Cimento*, **12**, 539 (1954).
([16]) E. Gatti: *Nuovo Cimento*, **11**, 153 (1954).

4. – X- and γ-Radiation.

Careful investigations of X- and γ-radiation by means of the scintillation spectrometer and of the proportional counter spectrometer show the presence of two peaks at 9 keV, and about 57 keV (Fig. 2, 3); no evidence at all was found of radiations at higher energies. The peak at 9 keV can be interpreted as LX-radiation characteristic of Re.

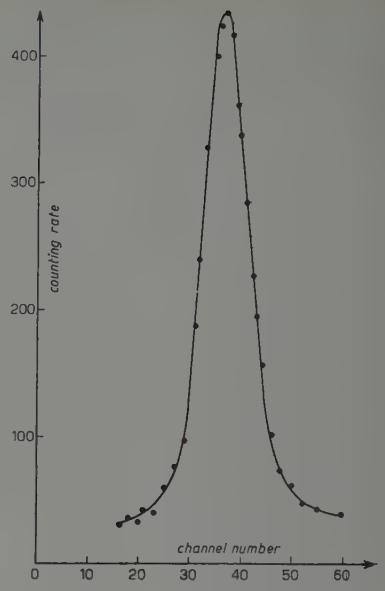

Fig. 2. – L X-rays from ^{185}W.

The interpretation of the peak at about 57 keV is difficult without an accurate measurement of its energy, owing to the fact that the KX-radiation from Re, if produced in the disintegration of ^{185}W, will give a peak at nearly the same energy (60.7 keV). The energy calibration in the proportional counter spectrometer was carried out by using soft γ-rays or KX-rays following K-capture or K-internal conversion. The sources were placed outside a window in the counter. The calibrating energies are listed in the Table II where for K_α energy we have used the weighted mean of the K_{α_1} and K_{α_2} energies derived from the table of HILL, CHURCH and MIHELICH [17].

As shown in Fig. 4 the energy can be determined with an accuracy better that 0.5 per cent. In this way the unknown energy was found to be:

$$E = 55.6 \pm 0.1 \text{ keV}.$$

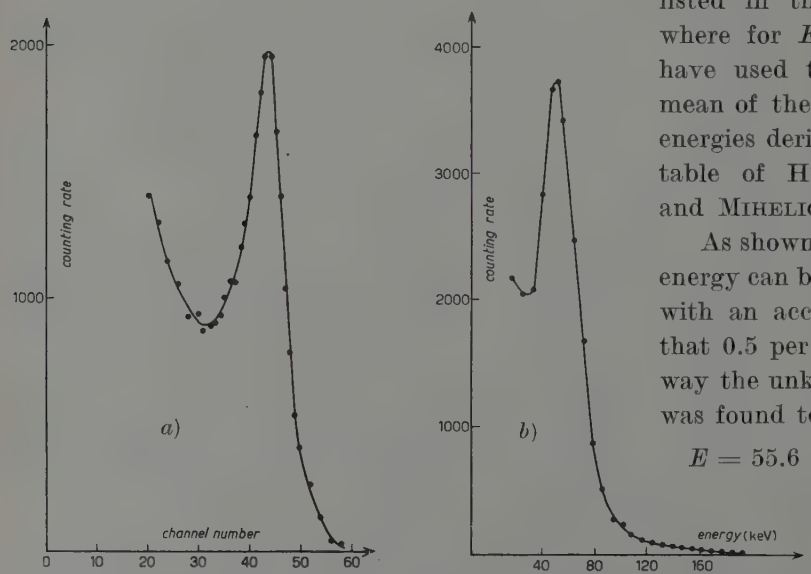

Fig. 3. – 55.6 keV γ-ray from ^{185}W: *a*) proportional counter spectrometer; *b*) scintillation spectrometer.

[17] R. D. HILL, E. L. CHURCH and J. W. MIHELICH: *Rev. Sci. Instr.*, **23**, 523 (1952).

TABLE II.

Isotope	Mode of decay	K_α energy (keV)	γ energy (keV)
^{109}Cd	E.C., γ	22.10	—
^{137}Cs	β^-, γ	32.05	—
^{210}Pb (RaD)	β^-, γ	—	46.7
^{195}Au	E.C., γ	66.20	—

Obviously the observed peak cannot be attributed to KX-rays from Re (60.7 keV), W (58.8 keV), or Ta (57.2 keV). Therefore we interpret the peak at 55.6 keV as a γ-ray arising from the disintegration of ^{185}W. Our assumptions supported from the following arguments:

a) The β-spectrum was investigated 5 months after the irradiation of the sample, when the short-lived activities had practically disappeared. Therefore the only difficulty in the interpretation of the peak at 55.6 keV could arise from the KX-radiation of Ta following K-capture in ^{181}W ($T_{\frac{1}{2}} = 140$ d). On the basis of the present knowledge of the relative isotopic abundance, of the cross-sections for neutron capture and of the half-lives, the ^{181}W abundance relative to ^{185}W should be somewhat less than 0.5%. As it will become clear in the following section this percentage cannot explain the observed ratio I_γ/I_β.

b) The γ-ray intensity, observed for about 50 days, decays with a halflife of nearly 85 d. This value is almost the same as the halflife of the β-decay (*).

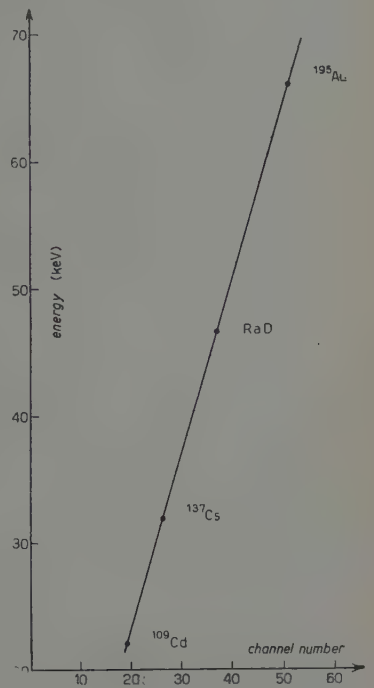

Fig. 4. – Energy calibration of the proportional counter spectrometer.

5. – Intensity Measurements and Internal Conversion Coefficient.

The measurement of γ-ray intensity relative to β-spectrum intensity was carried out as follows. Using the proportional counter spectrometer the γ-ray

(*) *Note added in proof*: A direct comparison between the γ-rays from ^{185}W and the KX-rays from ^{181}W shows that the two peaks have different energy in agreement with our preceding discussion.

intensity was deduced from the area under the peak after subtracting the background and after correction for the detection efficiency of the spectrometer ([18]). Using the β-spectrometer the β-spectrum intensity was obtained from the area of an ideal allowed Fermi distribution after correction for the transmission of the spectrometer; thus:

$$\frac{I_\gamma}{I_\beta} = 0.024 .$$

Because of the small intensity of the γ-radiation, the γ-emission cannot arise in cascade with a simple β-transition. Thus the presence of this γ-ray suggests a complexity in the β-spectrum.

The usual method cannot give the relative intensities of the β-transitions in this case, owing to the fact that the two β-components differ very slightly in energy and because of the small percentage of the β-component of lower energy. We, therefore, attempt to measure the internal conversion coefficient of the γ-ray.

The relative intensities of the *LX*-radiation and the γ-ray from the measurements with the proportional counter spectrometer was found to be:

$$\left(\frac{I_L}{I_\gamma}\right)^* = 0.71 .$$

The obtained ratio must be corrected for the presence of the *LX*-radiation characteristic of tungsten excited by β-particles in the source. The correction was deduced as follows:

a) the thickness of the sample was estimated from the deviation from a straight line at low energy of the Fermi plot;

b) approximate expression of the probability of the *L*-shell ionization by electron impact was taken from MOTT and MASSEY ([19]) taking into consideration the fluorescence yield of W;

c) the Fermi distribution of the energy of the electrons was taken into account. The corrected ratio I_L/I_γ becomes, then:

$$\frac{I_L}{I_\gamma} \cong 0.3 .$$

([18]) A. BISI and L. ZAPPA: *Nuovo Cimento*, **12**, 211 (1954).

([19]) N. F. MOTT and H. S. W. MASSEY: *The Theory of Atomic Collisions*, Cap. XI (Oxford, 1949).

The internal conversion coefficient is now:

$$\alpha_L = \frac{1}{\omega_{LL}} \frac{I_L}{I_\gamma} ,$$

where ω_{LL} is the L fluorescence yield of Re. The fluorescence yield was deduced from the partial yields ω_{L_i} and from the relative excitations u_i of the three L levels. The adopted values of the partial yields are ([20]) (*):

$$\begin{aligned} \omega_{L_I} &= 0.085 \\ \omega_{L_{II}} &= 0.35 \\ \omega_{L_{III}} &= 0.21 . \end{aligned}$$

As regards the relative excitations u_i of the three L subshells from internal conversion, we have for an $M1$ transition ([21]):

$$\begin{aligned} u_1 &= 0.90 \\ u_2 &= 0.08 \\ u_3 &= 0.02 . \end{aligned}$$

Thus:

$$\omega_{LL} = 0.11$$

and

$$\alpha_L \cong 3 .$$

Our value is consistent with the value deduced from calculations of GELLMAN, GRIFFITH and STANLEY ([22]) for an $M1$ transition:

$$(\alpha_L)_{\text{theor}} \cong 5 .$$

On the other hand no reasonable agreementb etween experimental and theoretical value of α_L can be achieved with $E1$ or $E2$ transition. It appears therefore that the 55.6 keV γ-ray arises from a magnetic dipole transition.

Finally we note that the measured intensities of the γ- and L X-radiations were not corrected for the presence of the radiations from ^{181}W whose decay

---

([20]) B. B. KINSEY: *Canad. Journ. Res.*, A **26**, 404 (1948).

(*) For Re ($Z=75$) the transition of the Coster Kronig type ($L_I \to L_{III} M_{IV}$, M_V) are energetically impossible according to the reviewed table of the critical X-ray absorption energies given by HILL, CHURCH and MIHELICH ([17]). However, as Kinsey's calculation of the partial fluorescence yields for heavy elements was consistent with the occurrence of the $L_I \to L_{III} M_{IV}$ transition for $Z > 73$, a revision of this calculation was made. It was found that the partial fluorescence yields differ slightly from Kinsey's values; only the Coster Kronig widths are generally reduced.

([21]) M. RIOU: *Journ. Phys. et Rad.*, **13**, 593 (1952).

([22]) H. GELLMAN, B. A. GRIFFITH and J. P. STANLEY: *Phys. Rev.*, **85**, 944 (1952).

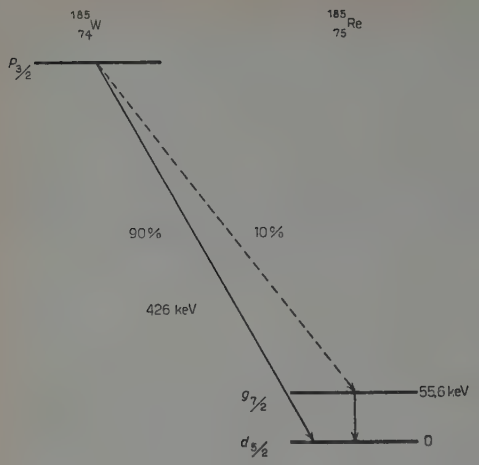

Fig. 5. – The proposed decay scheme of ^{185}W.

scheme is unknown. Nevertheless no uncertainty in assigning the multipole order of γ-ray arises.

6. – Decay Scheme.

The results of the preceding sections suggest a decay scheme of the type shown in Fig. 5, for ^{185}W. The assignement of the orbital to the excited state of ^{185}Re is based on the multipole order of the 55.6 keV γ-transition.

From the relative intensities of the β-components, we found, using f-values computed by FEENBERG and TRIGG ([23]), the log ft values listed in Table III.

TABLE III.

β-transition energy	Rel. Int.	log ft	Classification of the β-transition.
426 keV	0.90	7.6	$\Delta I = 0, 1$. Yes, first forbidden
370 keV	0.10	8.3	$\Delta I = 2$. Yes, first forbidden

The classification of the β-transitions is given according to MAYER, MOSZKOWSKI and NORDHEIM ([24]).

For further support of the proposed decay scheme, a detailed investigation of the disintegration of ^{185}Os would be desirable.

The kind interest of Prof. G. BOLLA and a useful discussion with Prof. B. FERRETTI are gratefully acknowledged.

([23]) E. FEENBERG and G. TRIGG: *Rev. Mod. Phys.*, **22**, 399 (1950).
([24]) M. G. MAYER, S. A. MOSZKOWSKI and L. W. NORDHEIM: *Rev. Mod. Phys.*, **29**, 1315 (1951).

RIASSUNTO

Le radiazioni β e γ emesse dal ^{185}W sono state studiate con uno spettrometro β a immagine intermedia, uno spettrometro a contatore proporzionale ed uno spettrometro a scintillazione. Si trova che il decadimento è complesso. La componente principale del decadimento conduce allo stato fondamentale del ^{185}Re ed ha energia massima pari a 426 keV. Si osserva la presenza di una debole radiazione γ di energia $E_\gamma = 55.6$ keV corrispondente ad una transizione di dipolo magnetico. Si assegnano spin e parità dei livelli e si propone uno schema di decadimento.

Penetrating Showers from Hydrogen and Other Elements.

M. Cervasi, G. Fidecaro (*), L. Mezzetti

Istituto di Fisica dell'Università - Roma
Istituto Nazionale di Fisica Nucleare - Sezione di Roma

(ricevuto il 7 Dicembre 1954)

Summary. — The production of penetrating showers (p.s.) in Paraffin, Graphite, Iron and Lead by the fast nucleons of the Cosmic Radiation at 3500 m above sea level has been investigated. The apparatus consists of a large area p.s.-detector and a large hodoscope of Geiger counters; its main features, as compared with the arrangements recently used by other Authors, are a better angular resolution for the particles of the showers and the use of very thin production layers. The validity of the «difference method» to obtain the interactions in Hydrogen from the comparison of the rates obtained with Paraffin and Carbon is discussed. From the rates obtained for Hydrogen through this analysis and those found for Graphite, Iron and Lead, the ratios of the interaction mean free paths for p.s. production are deduced. The cross-sections appear to follow closely the $A^{\frac{2}{3}}$ law (A = mass number), corresponding to the geometrical cross-section of the nuclei involved. Also the apparent cross-section for Hydrogen is found to be little less than «geometrical» ($60 \cdot 10^{-27}$ cm^2), in disagreement with what was found by other Authors: the discrepancy is believed to be due to the differences in instrumental bias. The rates of the p.s. which appear to be generated in Hydrogen by charged and neutral primaries are compared and discussed. The experimental results do not show any striking difference between the two cases, but an interpretation in terms of the elementary cross-sections for the pp and np interactions appear to be premature.

1. – Introduction.

In this paper we report on the preliminary results of some measurements carried out at the Laboratory of Testa Grigia (3500 m above sea level) from

(*) Now at University of Liverpool.

the Fall of 1953 to the Fall of 1954. An arrangement of Geiger counters recorded penetrating showers generated in thin layers of materials (in particular Graphite and Paraffin) by the high energy nucleons of the Cosmic Radiation.

A comparative study of the interactions produced by these nucleons in a hydrogenous material such as Paraffin, and in the corresponding non-hydrogenous material, can, in principle, give some information about the cross-sections of the elementary processes n–p and p–p. This method, which is here called « the difference method », has often been applied in recent years for the study of meson production ([1-6]).

With respect to other techniques (for example, cloud chambers filled with compressed hydrogen) the combination of the technique of Geiger counter hodoscopes with the difference method allows one to obtain, without too great difficulty, much higher counting rates. This advantage is particularly important when the flux of useful primaries for the interactions being studied is relatively low, as in the case of the high energy nucleons of the Cosmic Radiation; but it is often more than counterbalanced by a considerable difficulty in the interpretation of the results, due essentially to three causes:

a) the relatively small amount of information contained in each single observation (characteristic of Geiger counter techniques);

b) the fact that the detection efficiency can be sensibly different for the interactions in hydrogen and for those in a heavier material (carbon); and, more serious, the fact that the characteristics of the interactions which are attributed to hydrogen with the difference method (and the corresponding detection efficiency) can be sensibly altered by the presence of the nuclei of the other material;

c) the presence of spurious effects of various kinds, whose identification and correction is generally possible (as a consequence of point *a*)) only by statistical methods.

These remarks definitely suggest:

1) the use of thin targets (that is, thin with respect to the mean free paths of the interactions being studied) for the generating material of penetrating showers;

([1]) D. Froman, J. Kenney and V. H. Regener: *Phys. Rev.*, **91**, 707 (1953).

([2]) C. B. A. McCusker, N. A. Porter and B. G. Wilson: *Phys. Rev.*, **91**, 384 (1953).

([3]) W. D. Walker and N. M. Duller: *Phys. Rev.*, **90**, 320 (1953).

([4]) H. Schultz: *Zeits. Naturforsch.*, **9***a*, 419 (1954).

([5]) R. Rediker: *Phys. Rev.*, **95**, 526 (1954).

([6]) P. Colombino, S. Ferroni, G. Ghigo and G. Wataghin: *Nuovo Cimento*, **12**, 819 (1954).

2) the comparison of the results obtained with various thicknesses (but always « small »).

These two criteria, in addition to a high geometric resolution for the shower particles and a relatively high counting rate, constitute the principal differences of the experimental arrangement here described, with respect to those used recently by other authors. In order to clarify the importance of criterium 2) let us consider the case in which the generating layer is paraffin. Let us assume that the detection efficiency for the showers generated by the primary nucleons in collisions with the nuclei of hydrogen is very small in the absence of secondary interactions; whereas it increases by a factor $\gg 1$ if secondary interactions do take place (secondary interactions can increase both the mean number of ionizing particles emerging from the generating layer and their average angular spread). Since both the probability of generating a primary shower and the probability of a secondary interaction are proportional to the thickness of the generating layer (for small thicknesses), the rate of the observed events will be proportional to the *square* of the thickness (7). If, on the other hand, the detection efficiency of the primary shower does not depend upon the presence of secondary collisions, the rate should, in first approximation show a linear variation with thickness. We would like to emphasize that the application of this criterium seems essential (at least a priori) also if the probability of a secondary interaction is small, but not small with respect to the « direct » detection efficiency of the primary p.s..

2. – Experimental Apparatus.

The experimental arrangement used is shown in Fig. 1. It consists essentially of three parts: the shower generator, the penetrating shower detector, formed by the two trays of counters D and E in a lead housing, and a 48-channel hodoscope (one channel for each of the counters B and C). The counters of tray A are connected to circuits which permit to discriminate among the following three possibilities: no counter discharged (A_0), a single counter discharged (A_1), two or more counters discharged ($A_{>2}$). The two lateral groups of counters A', together with two other similar groups not represented in the figure and placed in front of and behind the generator, are in anticoincidence. The diameter of all the counters is 4 cm; the effective length is 100 cm for the counters B, C, D, E, 135 cm for the counters A and A'. The area of the generating layer Σ is 105×104 cm^2.

(7) See however the discussion of the effect of the presence of π^0-mesons among the secondaries of the primary p.s. in section 3·3.

The hodoscope information is displayed on a panel of neon lamps; the 48 lamps for counters B and C, and a few lamps for auxiliary informations (for example, the number of counters discharged in tray A). A photograph

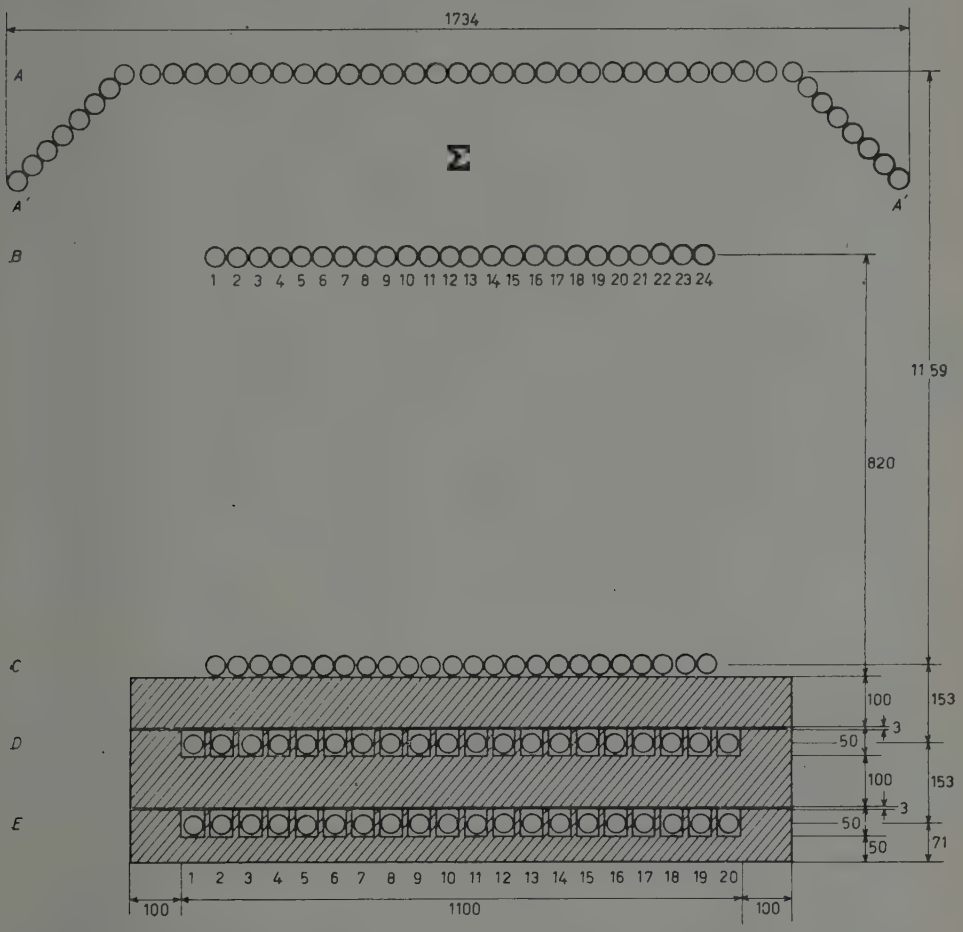

Fig. 1. – Experimental arrangement. Length of counters: 100 cm for trays B, C, D, E; 135 cm for trays A and A'; each counter of trays B and C is connected to a neon bulb through a 48-channel hodoscope. Triggering requirement $\overline{A}'\, A_{\leq 1} B_{\geq 1} C_{\geq 3} D_{\geq 3} E_{\geq 2}$.

of the panel and of some subsidiary instruments (clock and mechanical registers for various combinations of coincidence and anticoincidence) is taken whenever there is an event corresponding to the combination $A'\, A_{\leq 1}\, B_{\geq 1}\, C_{\geq 3}\, D_{\geq 3}\, E_{\geq 2}$ (« master » event).

The choice of the minimum order of coincidence in each counter tray was determined essentially by the requirement of a negligible background of chance coincidences. We have evaluated this background in a direct way, comparing,

in part of the measurements, the rate of coincidences given by the master pulse coincidence circuit (see the block diagram, Fig. 2) with the rate obtained with an auxiliary coincidence system, in which the resolving time of all the

MS = mixing circuit
F = pulse shaping circuit
S = adding circuit
DS = discriminator
C = coincidence
AC = anticoincidence
OD = hodoscope channel
P = « charged « primary neon bulb circuit.

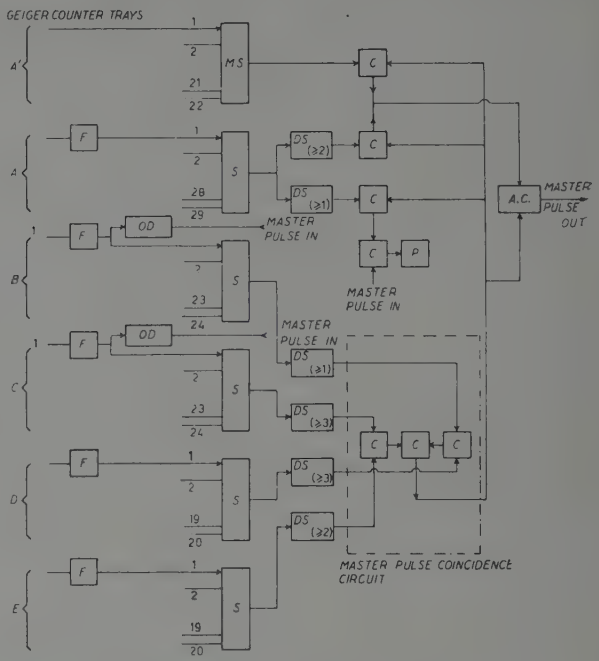

Fig. 2. - Simplified block diagram of the circuits used.

twofold coincidence elements was reduced by a factor of 3. From the difference between the two counting rates one gets easily an upper limit for the rate of chance coincidences: the values obtained are given, for the various types of runs, in columns 4 and 7 of Table I.

TABLE I.

Σ (g cm^{-2})	Time min	Neutral primary (A_0) $\times 10^{-3}$ m^{-1} Master Coincid.	Neutral primary (A_0) $\times 10^{-3}$ m^{-1} Random Coincid.	Time min	Charged primary (A_1) $\times 10^{-3}$ m^{-1} Master Coincid.	Charged primary (A_1) $\times 10^{-3}$ m^{-1} Random Coincid.
0.0	18 852	140 ± 3	24 ± 3	3 992	313 ± 9	26 ± 4
8.1 G	22 086	253 ± 3	27 ± 3	22 086	445 ± 4	25 ± 4
8.9 P	22 105	280 ± 4	31 ± 5	22 105	482 ± 5	32 ± 5
16.2 G	41 003	374 ± 3	25 ± 4	13 324	581 ± 7	24 ± 4
18.1 P	57 202	434 ± 3	28 ± 5	57 202	632 ± 5	27 ± 5
28.3 Pb	1 205	306 ± 16	29 ± 4	1 205	488 ± 20	26 ± 6
29.1 Fe	914	383 ± 21	19 ± 6	914	601 ± 26	29 ± 7

The symbols F, G and P indicate the measurements carried out without the generator ($\Sigma = 0$) and with a generator of Graphite or Paraffin, respectively. The suffixes indicate the thickness of the generating layers in g cm^2. Considering that for the analysis of the results only the rates G-F, P-F and P-G are interesting, one can conclude that the contribution of chance coincidences is, in every case, negligible. We would like to emphasize that a direct evaluation of this contribution (as well as of every other possible spurious effect) is very important for the interpretation of experiments of this type, in which the electronic analysis of the counter signals is complicated, and the number of different combinations that can give rise to random coincidences is very large.

The measurements have been carried out alternating frequently the various types and thicknesses of the generating layer Σ. To simplify the comparison, we have attempted to build layers of Paraffin that would have the same surface density of carbon as the corresponding layers of Graphite. However the paraffin blocks used are slightly thinner (about 5 %) than the calculated value. Correction for this have been calculated from the slope of the rate vs. thickness curve for the Graphite, and the corrected rates are shown in Table II together with the measured rates.

TABLE II.

	Charged primary	Neutral primary
$G_{8.1}$ — F	$132 \pm 10 \cdot 10^{-3}$ m^{-1}	$113 \pm 4 \cdot 10^{-3}$ m^{-1}
$(G_{8.1}$ — F$)_{int}$ (*)	124 ± 9	106 ± 4
($P_{8.9}$ — F)	169 ± 10	140 ± 4
$G_{16.2}$ — F	268 ± 11	234 ± 4
$(G_{16.2}$ — F$)_{int}$ (*)	255 ± 10	223 ± 4
($P_{18.1}$ — F)	319 ± 10	294 ± 4
($Pb_{28.3}$ — F)	175 ± 22	166 ± 16
($Fe_{29.2}$ — F)	270 ± 27	237 ± 21

(*) Interpolated rates.

The chemical composition of the paraffin was determined from various samples, and is: 85.19 % C, 14.21 % H, 0.60 % impurities (principally sulphur). The graphite used contains about 1 % impurities (principally Ca and Si) and can be considered completely dry.

The background (F) measurements were carried out leaving in position the supports used for the layer of paraffin and graphite. A good deal of care and labour was spent to reduce to a minimum the mass of these supports, particularly of that immediately under the generating layer. This is important

in view of the possible generation of electron showers by π^0-mesons generated in the primary interactions. In our case, the mass of the supports immediately underneath the generating layer is about 0.6 g/cm^2 (aluminium and steel), negligible with respect to the thickness of the brass walls of the counters B, evaluated at 2.60 g/cm^2 (and corresponding to about 0.20 radiation units).

The average duration of each run was about 20 hours with a maximum of about 40 hours. All parts of the apparatus were carefully checked before and after each measurement, and very severe tolerance criteria were applied.

On the other hand, no measurement has been eliminated in the analysis of the results except on the basis of a break-down of the apparatus, clearly and directly identified in the tests between runs. The results of a few runs in which one or more of the counting rates of the various types of coincidences recorded appeared to deviate from the average values more than twice the statistical error, have been analyzed separately before being included in the statistics: the partial means are in very good agreement with the general mean.

Barometric coefficients for the counting rates G(16.2) and P(18.1) of Table I have been calculated using the barograms of the local metereological station of the Aeronautica Militare, and the formulas of Jánossy and Rochester (corrected for an obvious printing error) ([8]). The values obtained are $B_N = (8.4 \pm 0.8) \cdot 10^{-3}$ mb^{-1} for the events produced by neutral primaries, and $B_P = (11.2 \pm 4.0)\ 10^{-3}$ mb^{-1} for events produced by charged primaries. All measurements have been reduced to a standard pressure using a barometric coefficient equal to the weighted average of B_N and B_P.

3. – Experimental Results and Discussion.

The results of the measurements carried out with Paraffin and Graphite are summarized in Tables I and II and in Figs. 3 and 4, together with the results of some measurements made with Pb and Fe generators.

3·1. *Nature of the primaries.* – The distinction between events produced by neutral primaries and by charged primaries is based, as already pointed out, on a purely instrumental criterium, that is, the number of counters discharged in tray A. Considerable care has to be applied if one wants to attach to this distinction a physical meaning: *a*) because the efficiency of tray A is not 100%; *b*) because an interaction in Σ due to a neutral primary can give rise to ionizing particles traveling upwards and capable of discharging one or

([8]) L. JÁNOSSY and G. D. ROCHESTER: *Proc. Roy. Soc.*, A **183**, 186 (1944).

more counters in tray A. The second effect is difficult to evaluate, but can be important (see section 3·5).

Because of the possibility of secondary interactions in the Pb above the counters D and E we cannot say definitely that the events recorded must

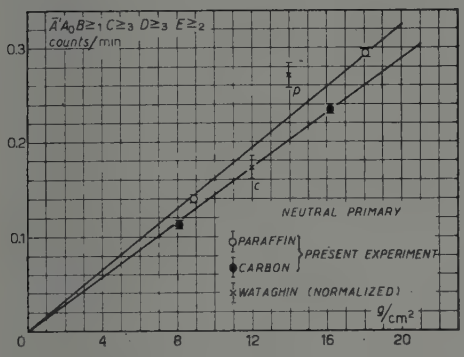

Fig. 3: events from « neutral primaries ».

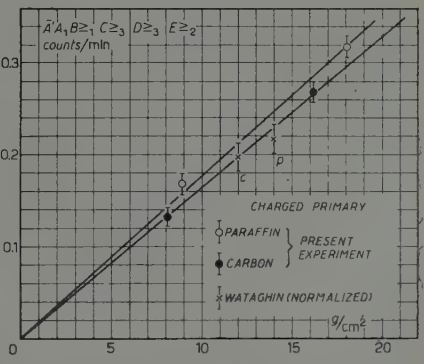

Fig. 4: events from « charged primaries ».

Fig. 3 and 4. – Rate of recorded p.s. vs. thickness of generating layer Σ. The points obtained by WATAGHIN and coworkers (6) are also shown for comparison (normalized to our Graphite lines).

contain at least three penetrating particles. However, one can show that only nuclear interactions in Σ of protons and neutrons of high energy are responsible for the counting rates G-F and P-F. All other components of the cosmic radiation give negligible contributions. The nuclear nature of the primaries of the recorded events is confirmed by the values found for the barometric coefficients, whose mean value corresponds to an absorption path in air $L_a = 119 \pm 15$ g/cm², in very good agreement with that determined in the same way by SCHULTZ (4) and with the results on the absorption of the N component in the atmosphere summarized by ROSSI (9).

3·2. *Background effect.* – The ratios of the counting rates obtained with and without generator are very satisfying for an experiment of this kind, taking into account the small thicknesses used for Σ. The background counts are nevertheless rather numerous and sensibly more so for the events produced by charged primaries than for those produced by neutral primaries. Whithout going into a detailed discussion of this effect, we can now only point out that of the background counts due to neutral primaries, about 18 % is

(9) B. ROSSI: *High Energy Particles* (New York, 1952), p. 438 and 490.

due to chance coincidences, while $\sim 40\%$ can, in a first approximation, be accounted for by p.s. produced in the walls of counters A and B.

3·3. *The difference method and the dependence of the counting rates on the thickness of the generator.* – In order to discuss the dependence of the counting rates on the thickness of the generating layer and the validity of the difference method it is convenient to separate the recorded events into various groups, according to the minimum number of successive interactions necessary for recording. Thus, for example, we shall indicate with H the interactions of the incident nucleons with the hydrogen nuclei in the Paraffin that are directly recorded, with HC those which instead are recorded *only* by way of *one* secondary interaction with a nucleus of carbon, with CH the primary interactions with carbon nuclei that are recorded *only* by way of *one* secondary interaction (also, for example, an elastic scattering) with the nuclei of hydrogen, and so forth. The usefulness of this nomenclature, which does not have a precise physical meaning, will appear from the following discussion.

Indicating with O the interactions which take place in the walls of the counters and in the supports immediately below Σ, the events recorded and originating in these and in Σ can be listed as follows:

for the Graphite generator: C, O; CC, CO, OO; CCC, ...;
for the Paraffin generator: C, O, H; CC, CO, OO, CH, HC, HH, HO; ....

The validity of the difference method is based on the hypothesis that, for equal masses of carbon, the partial rates due to processes having the same symbol are the same for the two materials. This hypothesis is obviously the more correct the thinner the two generators, but it is easily seen that the partial rates for a layer of Paraffin can never be greater than the corresponding rates for the equivalent layer of Graphite. It follows that, *wherever it is correct to neglect all events of order greater than the first*, the difference of the total rates yelds a lower limit for the counting rate H. Similar considerations hold for the subtraction of the back-ground; in this case, however, one has to remember that a large fraction of the background events originate from materials situated outside the solid angle covered by the generating layer Σ.

For the purpose of our analysis, the relevant property of the above list of events is that those of the first order give contributions that vary linearly with the thickness Σ (except obviously O, which is constant, to a first approximation); while those of second order depend on the square of the thickness, except OO (constant) and CO, HO for which the dependence is again linear.

From Table II and from Figs. 2 and 3 one can see that for Graphite the term proportional to the square of the thickness contributes certainly less than 15% of the counting rate at the greater thickness. As regards the CO events,

the contribution of the *nuclear* interactions in the walls of the counters B is certainly negligible, because the total thickness (including the supports) corresponds to only 0.03 nuclear interaction paths. The same thickness corresponds to about 0.3 radiation units; therefore, one can not a priori exclude the effect (increase of the detection efficiency) of the electron cascades generated by the π^0-mesons of the primary shower. This effect, however, implies the generation of a p.s. in the primary C interaction and therefore the corresponding counting rate can be included in the C contribution for the purpose of the present analysis.

Let us now consider the difference Paraffin-Graphite. In the spirit of the difference method, this shoulds represent the generation of p.s. in hydrogen. Taking into account, again, only the events of first and second order, we find that H, CH, HC, HH, HO can equally well contribute to the counting rates, and one could not a priori exclude that the bulk of the rates is due, for instance, to the p.s. produced in a primary interaction with a carbon nucleus but recorded by the apparatus only as a result of one or more elastic collisions of the shower particles with the hydrogen nuclei.

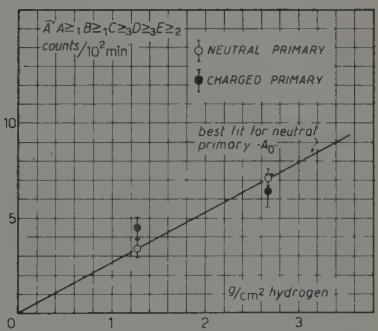

Fig. 5. – Rate of p.s. from Hydrogen (difference P — G) vs. thickness of generating layer.

The dependence of the counting rate on the thickness (Fig. 5) shows that « quadratic » processes cannot account for all of the events; the statistically most likely assumption is that their contribution is negligible, but a mixture of the type $0.5(H+HO)+0.5(CH+HC+HH)$ for the largest thickness would still be compatible with the experimental values, within 2.5 times the standard deviation (this would correspond, for a normal distribution, to a 2% probability lower limit). Of the HO contribution, the part due to electron cascades of the π^0-mesons can be, as before in the case of Graphite, included in the H counting rate; a truly spurious effect would instead be given by elastic collisions of the high energy incident nucleons with a hydrogen nucleus, followed by the generation of p.s. in the

TABLE III.

	g cm^{-2}	$\times 10^{-3}$ min^{-1} Charged Primary	$\times 10^{-3}$ min^{-1} Neutral Primary
(P–G)	2.67	64 ± 9	71 ± 4
(P–G)	1.27	45 ± 6	34 ± 5

walls of the counters below Σ. One can show that this effect can not contribute more than 5% of the counting rates of Table III.

3·4. *Production of penetrating showers in hydrogen and the mean free path in* Pb, Fe, C *and* H. – In the following, for the sake of simplicity, we shall assume that the rates of Table III represent penetrating showers generated in the hydrogen of the paraffin.

From the ratios of the rates G-F and P-G and the corresponding generating thicknesses, one can calculate the ratio of the *apparent* interaction mean free paths in carbon and hydrogen. The reciprocals of the mean free paths found are represented in Fig. 6 on an arbitrary logarithmic scale, together with those for Pb and Fe, calculated from the rates of Table II. The correction due to the finite thickness of the generating layers has been accounted for in the calculation. The straight line represents the $A^{-\frac{1}{3}}$ law corresponding to the « geometric » cross-sections of the nuclei. Another correction, which will be discussed qualitatively in section 3·5 and which can modify the counting rates due to charged and neutral primaries differently for different generators, has not been taken into account.

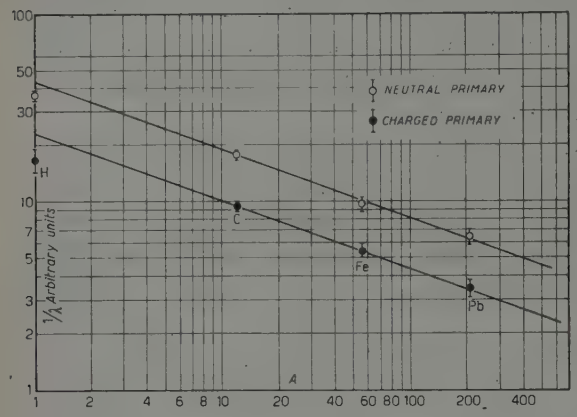

Fig. 6. – Dependence of interaction mean free path on mass number A. Ordinates in arbitrary units. The straight lines represent the $A^{-\frac{1}{3}}$ law, normalized to the Carbon point; only the ratios of ordinates belonging to the same line are meaningful.

If we assume that the mean free path for Pb is « geometric » (160 g/cm²) (there seems to be a general agreement among the results of many authors on this value), one gets for carbon $\lambda_C = 61.5 \pm 8$ g/cm² ($\lambda_{geom} = 60$ g/cm²). A comparison with the values (often quite different) found by others does not seem to us to be very significant, because the results seem to depend very critically on the instrumental bias ([10,11]).

It appears more difficult to reconcile our results with those obtained recently by SCHULTZ ([4]), who finds mean free paths essentially independent of A. He uses an arrangement of counters very similar to ours; the discrepancy

([10]) W. HEISENBERG: *Kosmische Strahlung* (Berlin, 1953), p. 101.
([11]) B. ROSSI: *High Energy Particles* (New York, 1952), p. 500.

may perhaps be attributed to the difference in the geometry of the generating layers.

As for the interactions in hydrogen, the results of Fig. 6 would seem to indicate cross-sections rather greater that those estimated by REDIKER ([5]) and close to « geometric » ($60 \cdot 10^{-27}$ cm^2). It seems reasonable to assume that a comparison between results *obtained with the same arrangement* should yeld a lower limit for the ratio of the cross-sections of hydrogen to heavier nuclei. The fact that we find for this limit a higher value than others did, can be understood on the basis of a less strong dependence of the detection efficiency on the size and angular spread of the showers produced in the two cases. On the other hand, since a cross-section much greater than « geometric » does not seem reasonably possible for the collisions between high energy nucleons, our results show that in appropriate experimental conditions the detection efficiency for the showers generated in elementary collisions is not much less than for those emerging from collisions involving complex nuclei.

3·5. *The ratio protons to neutrons at high energies.* – As has already been noted, for a reliable comparison between the rates of generation of p.s. by protons and by neutrons it is necessary to correct the observed counting rates for the two opposing effects of the inefficiency of the counter tray A and the possible projection of ionizing particles from the interaction in Σ towards the same counters.

The comparison is particularly interesting for the p.s. generated in Graphite. Because of the symmetry of the C nucleus and the generally admitted charge symmetry of the nuclear forces the ratio of the recorded p.s. should give a good approximation for the ratio P/N of the fluxes of protons and neutrons in the appropriate energy interval. Unfortunately, it is not easy to assign a lower limit to this interval: ionization loss only gives a minimum energy of about 2 GeV for a shower of 3 penetrating particles; the effective energy cut-off is probably very much higher.

The ratios P/N deduced from our measurements are shown in Table IV

TABLE IV. – *The ratio* P/N.

Σ	Uncorrected value	Corrected value $p=0.10$ $k=0$	Corrected value $p=0.10$ $k=0.14$
$G_{16.2} - F$	1.14 ± 0.05	1.46 ± 0.07	1.30 ± 0.06
$G_{8.1} - F$	1.17 ± 0.10	1.50 ± 0.12	1.35 ± 0.11
$H_{2.67}$	0.90 ± 0.13	1.11 ± 0.15	—
$H_{1.27}$	1.3 ± 0.3	1.7 ± 0.3	—

([12]) J. GREEN: *Phys. Rev.*, **80**, 832 (1950).

The values P'/N' represent the uncorrected ratios, that is the ratios of the counting rates of p.s..

The corrections have been calculated using the first approximation formula:

$$P/N = \frac{(P'/N')(1-k)-k}{(1-k-p)-P'p/N'},$$

where p represents the inefficiency of counter tray A, and k the probability that an ionizing particle of the p.s. generated in Σ strikes one of the counters A. The loss p has been measured independently and turned out to be $p=0.10$. It is more difficult to assign a value for k; however, one verifies immediately that P/N is, for a given value of p, a decreasing function of k, so that $k=0$ gives directly an upper limit for P/N. In order to evaluate also a lower limit we have used the results of GREEN ([12]), according to which the average number (per p.s. produced in carbon) of ionizing particles emerging from the target at angles greater than 90° with respect to the vertical is 0.14. This value probably gives an upper limit for the fraction k. The corresponding lower limits for the ratio P/N are listed in column 4 of Table IV.

Our experimental ratios are not easily reconciled with the value 0.81 ± 0.09 which can be deduced from the measurements with Graphite by WATAGHIN and coworkers ([6]), while they are in agreement with the value found by SCHULTZ ([4]), within the rather large errors of this last measurement. One has however, to bear in mind that in our evaluation, as in the others quoted, no account has been taken of the effect due to the possible association of the incident nucleons with other ionizing particles (f.i. electrons) capable of discharging one or more of the counters in tray A.

Similar considerations can be made for the p.s. produced in hydrogen. An estimate of the fraction k is, however, even more problematical, because of the lack of any direct information on the angular distribution; it is plausible that in this case the value of k is rather less than that corresponding to Graphite and lacking a better estimate we have used the value $k=0$. The corrected values of the ratio P/N are reproduced in Table IV; from the comparison with those for Graphite one could, in principle, draw some information on the relative probabilities of the processes pn and pp but this procedure does not seem significant to us, because the detection efficiencies depend on the characteristics of the experimental arrangement and of the p.s. produced in such a complicated way that it seems practically impossible to make any quantitative estimate.

The conclusions which WATAGHIN and coworkers have arrived at concerning this question seem therefore rather premature, even from a purely experimental point of view. Also a comparison with the probability tables

of the final states as calculated by FERMI ([13]) for collisions between nucleons with multiple meson production appears to be difficult at the present state of our analysis of the results.

4. – Acknowledgements.

We wish to express our thanks to Prof. E. AMALDI and Prof. B. FERRETTI, who participated in the original planning of the experiment, for their help and constant advice and encouragement. We are also indebted to Dr. R. GATTO for helpful discussions, and to Dr. G. SCHWACHHEIM, who ran the apparatus for part of the measurements. Finally, we wish to acknowledge the work of Mr. R. BERARDO, and of the many other technicians, whose skill and ingenuity helped us greatly to overcome the difficulties of installing such a big and complicated apparatus in the high altitude Laboratory.

([13]) E. FERMI: *Phys. Rev.*, 92, 452 (1953).

RIASSUNTO

È stata studiata la generazione di sciami penetranti (s.p.) da parte dei nucleoni veloci della Radiazione Cosmica a 3 500 m sul l.d.m. in Paraffina, Grafite, Ferro e Piombo. L'apparecchio impiegato consta essenzialmente di un rivelatore di s.p. a grande area e di un grande odoscopio di contatori di Geiger, e si differenzia dagli altri recentemente impiegati da vari Autori per una migliore risoluzione angolare rispetto alle particelle dello sciame e per l'impiego di strati di generazione molto sottili. Si discute la validità del procedimento « di differenza » (fra gli eventi osservati con Paraffina e quelli osservati con Grafite) ai fini dello studio delle interazioni in Idrogeno. Dalle frequenze attribuite all'Idrogeno e da quelle osservate con gli strati di generazione di Grafite, Ferro e Piombo si deducono i rapporti dei corrispondenti cammini liberi medi di interazione per generazione di s.p.. Le corrispondenti sezioni d'urto risultano seguire bene la legge « geometrica » di proporzionalità alla potenza 2/3 del numero di massa A. Anche la sezione d'urto apparente relativa all'idrogeno risulta poco inferiore alla sezione d'urto « geometrica » ($60 \cdot 10^{-27}$ cm^2), in contrasto con quanto trovato da altri Autori, la discrepanza viene attribuita alle diverse selezioni strumentali. Le frequenze degli s.p. generati in idrogeno da primari carichi e neutri vengono confrontate e discusse: i risultati empirici non mostrano alcuna sostanziale differenza fra i due casi, ma una interpretazione in termini delle sezioni d'urto elementari dei processi np e pp appare prematura.

Emissione di particelle α da parte di nuclei eccitati con protoni di 50, 100, 150 e 450 MeV.

M. Grilli e B. Vitale

Istituto di Fisica dell'Università - Padova
Istituto Nazionale di Fisica Nucleare - Sezione di Padova

P. E. Hodgson

University College - London

M. Ladu (*)

Istituto di Fisica dell'Università - Cagliari

(ricevuto il 17 Dicembre 1954)

Riassunto. — Sono presentati dati sperimentali sulla distribuzione angolare ed energetica delle particelle α e dei protoni emessi da nuclei dell'emulsione fotografica eccitati da protoni monoenergetici. Si osserva un eccesso di particelle α emesse in avanti rispetto al primario e si discutono alcune possibili interpretazioni di questo fenomeno.

Introduzione.

Molti autori hanno analizzato con la tecnica delle emulsioni nucleari le disintegrazioni dei nuclei fortemente eccitati, causate sia dalla radiazione cosmica sia, più recentemente, da particelle accelerate artificialmente. I dati sperimentali ottenuti possono essere interpretati in modo adeguato, nell'insieme, descrivendo il processo di disintegrazione mediante due stadi successivi. Nel primo di essi si inizia, ad opera del primario, una cascata nucleonica nell'interno del nucleo che dà luogo alla emissione di nucleoni (rami di emissione diretta);

(*) Attualmente presso l'Istituto Nazionale di Fisica Nucleare, Sezione di Milano.

nel secondo il nucleo residuo eccitato si diseccita mediante l'emissione di nucleoni o piccoli raggruppamenti di nucleoni di bassa energia (rami evaporativi). Ambedue questi stadi possono essere analizzati in dettaglio; il primo con metodi statistici (Montecarlo), il secondo in base alle teorie evaporative. Il confronto tra i dati sperimentali ed i risultati prevedibili con il modello ora descritto per le disintegrazioni nucleari mostra che, in genere, i primi sono in soddisfacente accordo con i secondi.

Alcuni lavori hanno, tuttavia, dato indicazioni su comportamenti anomali nella emissione di particelle α da parte di nuclei fortemente eccitati. HARDING *et al.* [1] ritrovarono una forte collimazione delle particelle α nella direzione opposta a quella del nucleo di rinculo e interpretarono questo fenomeno nell'ipotesi che le α fossero emesse, in un primo stadio della disintegrazione, da parte di una piccola zona della superficie del nucleo che fosse stata eccitata ad una temperatura anormalmente alta. In seguito PERKINS [2] ha ritrovato una anomalia nella distribuzione angolare delle α. In un lavoro analogo SÖRENSEN [3] ha osservato un notevole numero di α emesse, spesso con grande energia, nella direzione in avanti rispetto al primario; e ne ha interpretato il comportamento considerandole come particelle di emissione diretta. Altri interessanti risultati, riguardanti α di alta energia, sono stati ottenuti da CRUSSARD [4], sempre in stelle generate da raggi cosmici.

Le accurate condizioni sperimentali rese possibili dall'uso di fasci monoenergetici di particelle artificialmente accelerate ci hanno permesso di estendere questa analisi anche alle più basse energie. In questo lavoro presentiamo i risultati di una tale ricerca sulla emissione delle particelle α da parte di nuclei eccitati con protoni di 50, 100, 150 e 450 MeV.

1. – Condizioni sperimentali.

Le condizioni sperimentali sono state già discusse in un lavoro precedente (GRILLI *et al.* [5]). La discriminazione tra particelle con carica singola (protoni, deutoni e tritoni) e con carica doppia (particelle α) è stata resa possibile anche nelle Ilford G5 dall'opportuno sottosviluppo al quale queste emulsioni sono state assoggettate. Perchè la identificazione delle α fosse sicura abbiamo però preferito limitare la nostra analisi, nelle stelle della III e IV categoria (150 MeV

---

[1] J. B. HARDING, S. LATTIMORE e D. H. PERKINS: *Proc. Roy. Soc.*, A **196**, 325 (1949).

[2] D. H. PERKINS: *Phil. Mag.*, **41**, 138 (1950).

[3] S. C. O. SÖRENSEN: *Tesi*, Oslo, 1951; *Phil. Mag.*, **42**, 188 (1951).

[4] J. CRUSSARD: *Thèse* (Paris, 1952).

[5] M. GRILLI, P. E. HODGSON, M. LADU e B. VITALE: *Nuovo Cimento*, **12**, 889 (1954).

e 450 MeV, rispettivamente), a quelle tracce che formavano con il piano dell'emulsione un angolo non superiore ai 30°. L'angolo solido utilizzato è stato quindi metà dell'angolo solido totale e, considerando in prima approssimazione come isotropi i rami di bassa energia, circa metà delle particelle uscenti da stelle è stato identificato. Non riteniamo che la selezione così compiuta possa aver alterato in modo sensibile i dati ottenuti per le distribuzioni energetiche ed angolari.

Tutte le disintegrazioni osservate sono state suddivise in quelle dovute alla disintegrazione di nuclei leggeri dell'emulsione ed in quelle dovute alla disintegrazione di nuclei pesanti mediante un criterio sviluppato da uno di noi (HODGSON [6]). Questo criterio garantisce una buona separazione statistica tra i due tipi di stelle ma può essere impreciso nella attribuzione di un singolo evento ad una delle due categorie; questa considerazione deve essere tenuta continuamente presente nella discussione dei dati qui esposti.

Le particelle di carica unitaria le cui distribuzioni energetiche ed angolari sono in questo lavoro confrontate con quelle analoghe per le α corrispondono ai « rami neri N » del lavoro precedente [5]; si tratta quindi di particelle che, se protoni, avrebbero una energia massima di 20 MeV. La massima energia per le α risulta di circa 40 MeV.

Il numero di stelle in nucleo leggero o pesante raccolte e studiate per le varie energie del primario è dato in tabella I.

TABELLA I.

Energia	50	100	150	450
Numero di stelle:				
in nucleo leggero	136	70	69	71
in nucleo pesante	89	111	143	201

2. – Distribuzioni energetiche ed angolari.

Chiameremo nel seguito, per semplicità, « protoni » tutte le particelle di carica unitaria e di ionizzazione corrispondente ad un protone di energia minore di 20 MeV.

La tabella II dà i valori dell'energia media $\bar{E}$ delle particelle α e dei protoni emessi da nuclei leggeri e pesanti, per le differenti energie dei primari. Le $\bar{E}$ sono calcolate, separatamente, per i rami in avanti ed indietro rispetto alla direzione del primario. In parentesi è dato il numero assoluto di eventi.

(6) P. E. HODGSON: *Phil. Mag.*, **41**, 190 (1954).

TABELLA II. – *Valori di E* (in MeV).

	α				protoni			
	in avanti		indietro		in avanti		indietro	
A) Nuclei leggeri:								
I - 50 MeV . . .	5,8	(237)	4,3	(94)	4,6	(61)	4,3	(42)
II - 100 MeV . . .	5,4	(182)	4,0	(70)	5,6	(45)	3,4	(21)
III - 150 MeV . . .	8,5	(48)	7,0	(25)	9,6	(24)	8,7	(19)
IV - 450 MeV . . .	9,9	(50)	9,2	(29)	11,5	(16)	10,4	(11)
B) Nuclei pesanti:								
I - 50 MeV . . .	15,2	(48)	13,7	(25)	6,2	(53)	5,7	(40)
II - 100 MeV . . .	15,9	(50)	13,1	(32)	6,8	(75)	6,7	(58)
III - 150 MeV . . .	17,0	(55)	15,9	(26)	9,4	(127)	9,0	(75)
IV - 450 MeV . . .	21,6	(66)	17,8	(49)	10,9	(120)	10,1	(72)

In fig. 1 e 2 sono dati gli spettri energetici, per le stelle in nucleo pesante prodotte da primari di 450 MeV, delle particelle α in avanti e indietro rispetto alla direzione del primario.

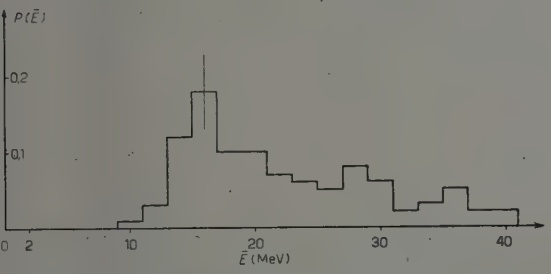

Fig. 1. – Stelle delle IV cat. (450 MeV). Spettro delle particelle α in avanti.

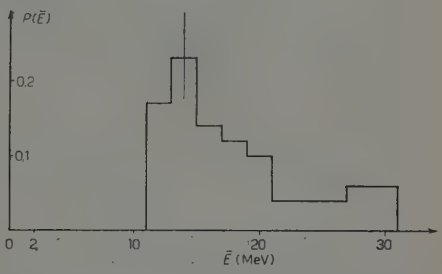

Fig. 2. – Stelle della IV cat. (450 MeV). Spettro delle particelle α indietro.

La tabella III dà i valori del rapporto F (v. (6)) tra i rami in avanti e tutti i rami al variare dell'energia del primario e, separatamente, per le particelle α ed i protoni.

Dai dati raccolti nelle tabelle II e III si deduce che il numero di particelle che va in avanti rispetto al primario è maggiore di quello che va indietro (anisotropia angolare) e che l'energia media delle particelle emesse in avanti è maggiore di quella delle particelle emesse indietro. È stato mostrato in un lavoro precedente (6) che nel caso dei nuclei pesanti il moto del nucleo eccitato è del tutto insufficiente per spiegare questo andamento; nel caso dei nuclei

TABELLA III. – *Valori del rapporto F.*

	Nuclei leggeri		Nuclei pesanti	
	α	protoni	α	protoni
I - 50 MeV	$0{,}74 \pm 0{,}07$	$0{,}70 \pm 0{,}09$	$0{,}65 \pm 0{,}11$	$0{,}65 \pm 0{,}07$
II - 100 MeV	$0{,}74 \pm 0{,}09$	$0{,}69 \pm 0{,}09$	$0{,}66 \pm 0{,}11$	$0{,}61 \pm 0{,}05$
III - 150 MeV	$0{,}66 \pm 0{,}17$	$0{,}58 \pm 0{,}20$	$0{,}68 \pm 0{,}17$	$0{,}64 \pm 0{,}10$
IV - 450 MeV	$0{,}63 \pm 0{,}16$	$0{,}59 \pm 0{,}25$	$0{,}57 \pm 0{,}12$	$0{,}63 \pm 0{,}11$

leggeri una analisi analoga è stata fatta da MUIRHEAD (7). Egli ha usato un valor medio per l'impulso ceduto dal primario al nucleo, calcolato mediante una analisi statistica (tipo « Montecarlo »), per trovare il valore di F come funzione dell'energia delle particelle α; i valori così ottenuti sono minori di quelli ritrovati sperimentalmente. È del resto chiaro che una tale ipotesi non può completamente spiegare l'eccesso in avanti osservato, perchè esso porta a un eccesso che decresce all'aumentare dell'energia dell'α, contrariamente a quanto osservato.

L'anisotropia angolare dei protoni può essere facilmente spiegata mediante un modello di cascata nucleonica che dia luogo a rami di emissione diretta, anche di bassa energia, collimati in avanti rispetto al primario. Il tentativo di spiegare il comportamento delle α con un modello analogo, tuttavia, dà luogo ad alcune difficoltà che saranno discusse nel seguito.

3. – Correlazioni angolari con il rinculo.

La tabella IV dà i valori del rapporto C (v. GRILLI *et al.* (8) e (5)) tra i rami che formano con il rinculo un angolo maggiore di 90° e quelli che formano un angolo minore di 90° (gli angoli considerati sono in proiezione sul piano del-

TABELLA IV. – *Valori del rapporto C.*

	α	protoni
I - 50 MeV	$3{,}3 \pm 1{,}1$	$1{,}7 \pm 0{,}3$
II - 100 MeV	$5{,}6 \pm 2{,}1$	$2{,}0 \pm 0{,}3$
III - 150 MeV	$2{,}8 \pm 1{,}4$	$1{,}6 \pm 0{,}5$
IV - 450 MeV	$2{,}3 \pm 0{,}8$	$2{,}1 \pm 0{,}6$

(7) H. MUIRHEAD: Comunicazione privata.
(8) M. GRILLI e B. VITALE: *Nuovo Cimento*, **10**, 1047 (1953).

l'emulsione) per le disintegrazioni in nucleo pesante, al variare dell'energia del primario e, separatamente, per le particelle α ed i protoni.

In figg. 3 a 6 sono date le distribuzioni in $(\vartheta - \vartheta_r)$ (angolo in proiezione tra

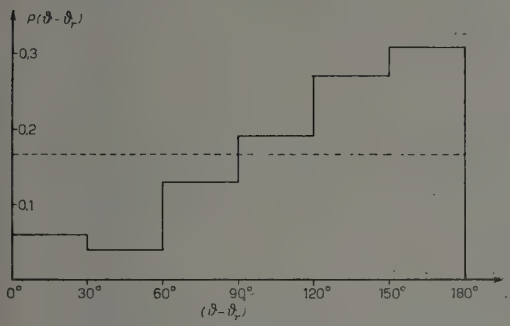

Fig. 3. – Stelle della I cat. (50 MeV). $(\vartheta - \vartheta_r)$ per le particelle α.

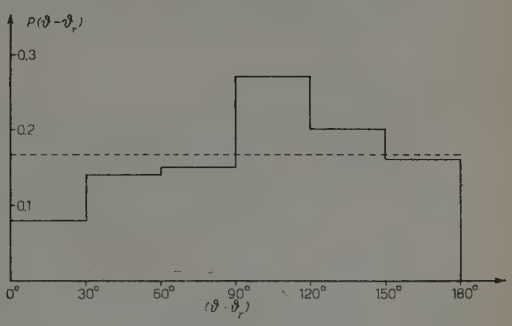

Fig. 4. – Stelle della I cat. (50 MeV). $(\vartheta - \vartheta_r)$ per i protoni.

ramo e rinculo) per le particelle α ed i protoni in stelle prodotte da primari di 50 MeV e 450 MeV, rispettivamente.

La anisotropia è molto più marcata per le particelle α che per i protoni. Questo è in accordo con la teoria sulla formazione del rinculo data in [8], quando si considerino tutte le particelle α come evaporative. I valori ottenuti

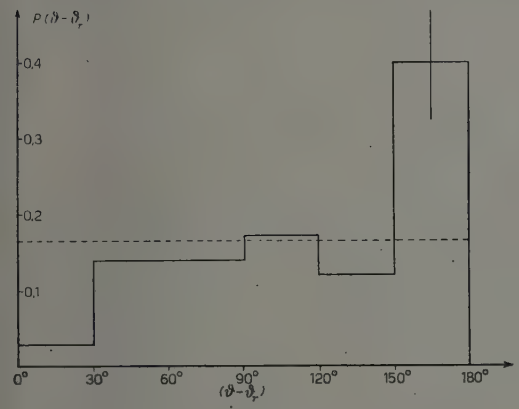

Fig. 5. – Stelle della IV cat. (450 MeV). $(\vartheta - \vartheta_r)$ per le particelle α.

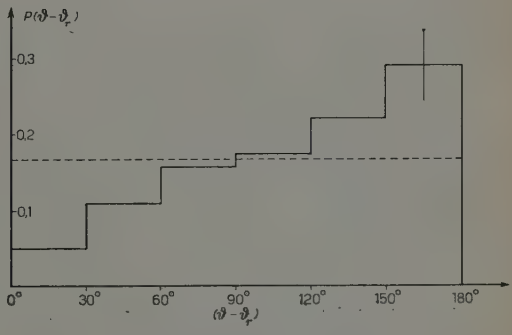

Fig. 6. – Stelle della IV cat. (450 MeV). $(\vartheta - \vartheta_r)$ per i protoni.

per il rapporto C potrebbero quindi indicare che almeno la maggior parte delle particelle α è prodotta in processi di tipo evaporativo.

Poichè l'energia media delle particelle secondarie evaporative aumenta molto più lentamente dell'energia del primario e il rinculo dovuto alla emis-

sione diretta diviene sempre più isotropo al crescere dell'energia del primario (v. § 2, [5]) l'anisotropia dei secondari evaporativi rispetto al rinculo dovrebbe diminuire al crescere dell'energia. I dati sperimentali non sono sufficientemente accurati per poter mettere in luce un effetto di questo genere.

4. – Rapporto $\alpha/(p + \alpha)$.

La tabella V dà i valori della percentuale di particelle α: $P_\alpha = \alpha/(p + \alpha)$ in disintegrazioni di nuclei leggeri e pesanti al variare dell'energia del primario.

TABELLA V. – *Valori di* P_α.

	Nuclei leggeri		Nuclei pesanti	
	avanti	indietro	avanti	indietro
I - 50 MeV	$0{,}63 \pm 0{,}06$	$0{,}58 \pm 0{,}08$	$0{,}27 \pm 0{,}04$	$0{,}27 \pm 0{,}06$
II - 100 MeV	$0{,}56 \pm 0{,}06$	$0{,}49 \pm 0{,}08$	$0{,}21 \pm 0{,}03$	$0{,}18 \pm 0{,}05$
III - 150 MeV	$0{,}61 \pm 0{,}15$	$0{,}50 \pm 0{,}15$	$0{,}26 \pm 0{,}05$	$0{,}22 \pm 0{,}06$
IV - 450 MeV	$0{,}69 \pm 0{,}17$	$0{,}67 \pm 0{,}22$	$0{,}31 \pm 0{,}05$	$0{,}36 \pm 0{,}07$

Non si nota alcuna variazione sensibile di P_α con l'energia del primario; P_α risulta inoltre indipendente, entro gli errori statistici, dalla direzione dei rami rispetto al primario.

5. – Correlazioni angolo-energia per le particelle α ed i protoni.

Sono state costruite le distribuzioni « angolo con il primario/energia » per le particelle α ed i protoni alle varie energie del primario, utilizzando sia gli angoli in proiezione che gli angoli nello spazio (per le α di energia maggiore di 15 MeV e per i soli nuclei pesanti). In nessuna delle distribuzioni ottenute è presente una correlazione significativa tra l'energia della particella ed il suo angolo di emissione rispetto al primario.

6. – Discussione dei dati sperimentali.

La discussione che segue è basata, principalmente, sui risultati in nucleo pesante. Nei paragrafi precedenti sono stati presentati anche i risultati in nucleo leggero, essenzialmente per un confronto qualitativo tra questi dati e quelli ottenuti per i nuclei pesanti dell'emulsione.

L'anomalia più evidente mostrata dai dati sperimentali rispetto ai risultati prevedibili in base al modello brevemente discusso nell'Introduzione è l'anisotropia angolare delle particelle α, anisotropia che non può essere giustificata tenendo conto del moto del nucleo eccitato residuo. Vi sono diverse spiegazioni possibili di questa anomalia:

a) Le particelle α partecipano alla cascata e parte di esse è da classificarsi tra i rami di emissione diretta.

Si può ammettere che nel nucleo esistano delle sotto-strutture o dei piccoli raggruppamenti di nucleoni, che continuamente si formano e si distruggono. La vita media e la frequenza di una particolare sotto-struttura dipendono dalla sua energia di legame e dal numero di nucleoni che la compongono: più bassa è l'energia di legame e maggiore è il numero di particelle che la compongono, più labile sarà una tale sotto-struttura. Se una particella incidente collide con essa può espellerla fuori del nucleo, purchè la sotto-struttura sia sufficientemente stabile per sopravvivere alla collisione; se un processo di questo tipo può aver luogo esso può giustificare l'osservata anisotropia delle α. A causa della sua grande stabilità, la particella α è infatti la sotto-struttura che ha la maggiore probabilità di prendere parte a questo processo.

Per verificare questa ipotesi è utile vedere se c'è qualche correlazione tra l'energia E_α della particella α e il suo angolo di emissione ϑ rispetto alla particella primaria. Nel caso di collisione con una particella α libera e ferma ad energie non relativistiche le due grandezze sono collegate dalla relazione:

$$E_\alpha = (16/25)E_p \cos^2 \vartheta ,$$

dove E_p è l'energia della particella incidente.

I risultati esposti in § 5 non mostrano alcuna correlazione. Questa osservazione, tuttavia, non può inficiare l'ipotesi di emissione diretta delle α, perchè vi sono molte cause che possono deformare la dipendenza prevista. In primo luogo, la sotto-struttura può essere emessa come conseguenza di una collisione con un ramo secondario della cascata. In secondo luogo, la sotto-struttura può essere anch'essa in moto nel nucleo prima che la collisione avvenga. Infine la collisione può essere influenzata dalla presenza di altri nucleoni vicini. Le distribuzioni « angolo con il primario/energia » per i protoni, tra i quali sono presenti certamente rami di emissione diretta, non mostrano alcuna correlazione sensibile; questo dimostra che le cause precedentemente elencate possono essere sufficienti a mascherare ogni correlazione del genere previsto.

In casi particolari, specie per particelle α di alta energia, sono state messe in luce correlazioni tra l'angolo di emissione e l'energia (v. SÖRENSEN [3], CRUSSARD [9], MUIRHEAD [7]).

---

(9) J. CRUSSARD: *Compt. Rend. Acad. Sci.*, **233**, 611 (1951).

b) *Evaporazione locale.* – KIND *et al.* [10], seguendo HARDING *et al.* [1], hanno studiato la possibilità di eccitazione di una parte del nucleo ad una temperatura più alta che il resto del nucleo. Essi hanno mostrato che, se una piccola parte del nucleo è eccitata ad alta temperatura, il tempo necessario perchè l'eccitazione si ripartisca in modo uniforme su tutto il nucleo può essere maggiore di quello necessario perchè si inizi un fenomeno di evaporazione locale, e che questo avviene quando l'energia di eccitazione eccede i 7 MeV. È possibile che la parte inferiore del nucleo (rispetto al primario), quando la cascata si è completamente sviluppata, si ecciti in tal modo, così che da essa si inizi un processo di evaporazione locale; una obiezione a questa ipotesi è nell'osservazione che più particelle dovrebbero evaporare da un nucleo la cui energia di eccitazione è così alta, mentre l'eccesso di particelle α in avanti ha luogo anche nelle stelle più piccole con solo due o tre rami ionizzanti. L'influenza di un processo di evaporazione locale, quindi, può forse giustificare solo una piccola parte della osservata anisotropia delle particelle α.

c) « *Pick-up* » *multiplo.* – È possibile che due o più particelle della cascata, muovendosi molto vicine in direzioni quasi parallele, possano unirsi per formare una particella composta. Anche un tale processo potrebbe spiegare l'anisotropia osservata, ma sembra estremamente improbabile che tanto frequentemente tre o quattro particelle si uniscano per dar luogo ad una particella di carica doppia.

d) *Emissione delle* α *da parte di frammenti di fissione.* – Frammenti di fissione possono essere emessi nella direzione in avanti e successivamente spaccarsi, dando luogo a un eccesso in avanti di particelle α. I frammenti di fissione sono però emessi, nei nuclei considerati in questo lavoro, solo a temperature molto alte, che non sono praticamente raggiungibili con le basse energie usate per le particelle primarie.

7. – Conclusioni.

Sono stati esposti dei dati sperimentali che mettono in luce una notevole anisotropia angolare delle particelle α emesse durante la disintegrazione sia di nuclei leggeri che di nuclei pesanti, componenti l'emulsione fotografica. Sono state suggerite alcune spiegazioni di questo effetto, e ci sembra che sia probabile che una parte di queste particelle α in avanti sia dovuto alla emissione diretta di sotto-strutture preesistenti nel nucleo urtate dai rami della cascata nucleonica che si sviluppa nel nucleo durante il primo stadio della disintegrazione; anche gli altri meccanismi considerati nel § 6 possono avere una certa

---

([10]) A. KIND e G. PATERGNANI: *Nuovo Cimento*, **10**, 1375 (1953); **11**, 106 (1954).

importanza nel determinare l'andamento osservato. Una più completa analisi sperimentale e teorica è necessaria perchè si possa stabilire la validità di questa conclusione in modo quantitativo.

Ringraziamo vivamente i proff. N. Dallaporta, A. Kind e G. Puppi per l'interesse dimostrato verso il nostro lavoro e per le utili discussioni; i proff. G. Frongia e A. Rostagni per aver reso possibile la nostra collaborazione; il sig. D. Narciso per l'intelligente aiuto prestato durante le misure.

Uno di noi (P. E. H.) è grato al D.S.I.R. per un « Senior Research Award ».

P.S. – Quando questo lavoro era già completato ci sono stati gentilmente comunicati dal dott. Lock (comunicazione privata) alcuni dati preliminari di una analisi sistematica in corso di elaborazione sulle particelle α emesse da nuclei pesanti eccitati con protoni di 950 ± 50 MeV. Per le α di energia minore di 30 MeV, si ritrova l'eccesso in avanti e una energia media un po' maggiore per le particelle in avanti rispetto a quelle indietro rispetto al primario; per le α più energiche si è osservato qualche caso in cui una particella α di alta energia (100-200 MeV) è emessa in avanti con un piccolo angolo con il primario.

SUMMARY

The photographic emulsion technique is used to investigate the disintegration of nuclei excited by monoenergetic protons. The angular and energy distributions of the secondary particles show an excess in the forward direction, and this excess is greater for the secondary particles of high energy than for those of low energy. A correlation was found between the directions of emission of the secondary particles and that of the recoil fragments from the heavy nuclei, but no significant correlation was found between the energies and angles of emission of the secondary particles. These features of the disintegrations can be accounted for by the cascade-evaporation process, with the exception of the forward excess of α-particles. Several possible explanations of this effect, including direct knock-on, emission from a part of the nucleus excited to an abnormally high temperature, and multiple pick-up, are discussed.

Influence of Ions on the Nucleation Processes in Liquids.

II. - Liquids Under Positive Pressure in Metastable Thermodynamical Equilibrium (Overheated liquids).

L. Bertanza and G. Martelli (*)

Istituto di Fisica dell'Università - Pisa
Istituto Nazionale di Fisica Nucleare - Sezione Aggregata di Pisa

(ricevuto il 20 Dicembre 1954)

Summary. — The behaviour of liquids in metastable equilibrium under positive pressure has been investigated, and an expression for the total flux of « critical » bubbles carrying different number of ions has been found. A comparison between our results and the data of some experiments shows that in some cases the contribution of the ions at the nucleation processes in overheated liquids cannot be neglected. The total flux of bubbles is larger than that obtained when the effect of the ions is neglected: the waiting times are therefore shorter and, in some cases, become zero effectively.

1. – Introduction.

In a previous paper (1) the problem as to whether the presence of ions may influence the nucleation processes in liquids has been formulated under very general assumptions, and some results have been applied to study the particular case of nucleation of vapour bubbles in liquids in *stable thermodynamical equilibrium*. However, it seems difficult at present to check experimentally, for liquids in these conditions, whether the predictions of the theory are valid, whereas for liquids in a metastable state there are some quantities (waiting time, fracture pressure, etc.), whose values may be evaluated theoretically and compared with the results of experiments.

(*) At present at Physics Department of the University, Birmingham.
(1) G. Martelli: *Nuovo Cimento*, 12, 250 (1954).

This second paper is mainly concerned with the quantitative theory of the nucleation of vapour bubbles in liquids in *metastable equilibrium under positive pressure* (overheated liquids), when the contribution of the ions is taken into account. The formulae have been worked out in such a form, that it is easy to make direct comparison between the results predicted by theory and those obtained experimentally.

In the present paper we shall use some results which have been obtained in ref. [1]. We may recall that the equilibrium condition for an N-charged bubble of radius R is

$$(1)\qquad \begin{cases} p_n(R,N) = P + \dfrac{2\sigma}{R} - \dfrac{C_1^2}{R^4} & \text{for} \quad N > \bar{N} \\ \text{or} \\ p_n(R,N) = P + \dfrac{2\sigma}{R} + \dfrac{C_2^2}{R^4} & \text{for} \quad N < \bar{N} \end{cases}$$

where $p_n(R, N)$ is the internal pressure in a bubble containing n molecules and N ions, σ is the surface tension on a vapour-liquid surface, P the hydrostatic pressure on the liquid. The meaning of the constants $\bar{N}$, C_1^2 and C_2^2 is specified in the appendix.

The equation of state of the vapour in the bubble may therefore be written as

$$(2)\qquad \begin{cases} n(R,N) = \dfrac{4\pi}{3KT} R^3 \left\{ P + \dfrac{2\sigma}{R} - \dfrac{C_1^2}{R^4} \right\} & \text{for} \quad N > \bar{N} \\ \text{or} \\ n(R,N) = \dfrac{4\pi}{3KT} R^3 \left\{ P + \dfrac{2\sigma}{R} + \dfrac{C_2^2}{R^4} \right\} & \text{for} \quad N < \bar{N} \end{cases}$$

where K is the Boltzmann constant and T the absolute temperature.

Next, let us call « equilibrium nucleus » the spherical bubble for which

$$(3)\qquad \begin{cases} p_k = P + \dfrac{2\sigma}{R_k} - \dfrac{C_1^2}{R_k^4} & \text{if} \quad N > \bar{N} \\ \text{or} \\ p_k = P + \dfrac{2\sigma}{R_k} + \dfrac{C_2^2}{R_k^4} & \text{if} \quad N < \bar{N} \end{cases}$$

and

$$\mu_k = \mu_l ,$$

where R_k, μ_k and p_k are the radius, the chemical potential and the vapour pressure inside the nucleus itself, μ_l the chemical potential in the liquid phase. In Fig. 1 the behaviour of the functions

$$(4)\qquad f_1(R) = \frac{2\sigma}{R} - \frac{C_1^2}{R^4}, \qquad f_2(R) = \frac{2\sigma}{R} + \frac{C_2^2}{R^4}, \qquad f_3(R) = \frac{2\sigma}{R}.$$

is shown.

2. – For liquids in metastable equilibrium we can distinguish some different cases, depending upon the values of P and N.

A) If $N > \overline{N}$, for each value of $p_k - P$ and for each N, we can find a particular value of R smaller than that corresponding to the maximum of the curve $f_1(R)$ of Fig. 1, which corresponds to the radius of the « initial aggregates » which, for simplicity's sake, are supposed to be spherical (2).

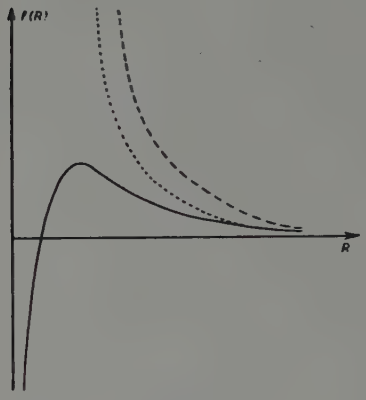

Fig. 1.

Full line $f_1(R) = (26/R) - (C_1^2/R^4)$, $N > \overline{N}$;
Dashed line $f_2(R) = (26/R) + (C_2^2/R^4)$, $N < \overline{N}$;
Dotted line $f_3(R) = (26/R)$, $N = 0$.

If we call $R_a(N)$ the values of their radii, n_a the number of molecules present in each of them and μ_i the chemical potential of a bubble having i molecules, the total work for the reversible formation of a mechanical stable bubble of radius R having N ions and $n(R, N)$ molecules, may be written as

$$(5) \qquad \sum_{n_a+1}^{n_i} (\mu_i - \mu_l) = kT \int_{n_a}^{n} \ln \frac{p_i}{p_k} \, \mathrm{d}i = W_n(R, N) - W_{n_a}(N) ,$$

where

$$(6) \qquad W_n(R, N) = nkT \ln \frac{p_n}{p_k} + \frac{4}{3} \pi \sigma R^2 + \frac{16}{3} \pi \frac{C_1^2}{R} ,$$

as may be checked by performing the integration.

The functions $p_n(R, N)$ and $n(R, N)$ are given by eq.'s (1) and (2). $W_{n_a}(N)$ are the values of the functions $W_n(R, N)$ for $R = R_a$.

Since the values W_{n_a} correspond to the minima of the functions $W_n(R, N)$, bubbles whose radii have a value near R_a are stable against the change of their size.

Eq.'s (1), to (6) enable us to investigate some general properties of ionized liquids in metastable states. Let us first study the curves $D_n(R, N) = W_n(R, N) - W_{n_a}(R, N)$, in the cases when $N > \overline{N}$ and $R \geqslant R_a$. There are two different possibilities:

---

(2) In view of the fact that some of these « initial bubbles » may consist only of one or few ions surrounded by a few molecules, it will be preferable to refer to them as to « initial aggregates ».

I-*A*) $p_k - P$ is smaller than the maximum of $f(R)$ (for each N). The functions $D_n(R, N)$ increase from zero up to a maximum for $R = R_k$, and then decrease monotonically with increasing R (see Fig. 2).

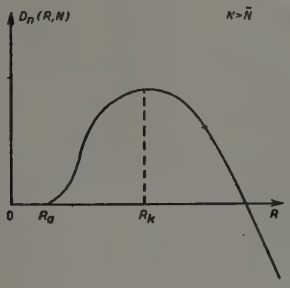

Fig. 2.

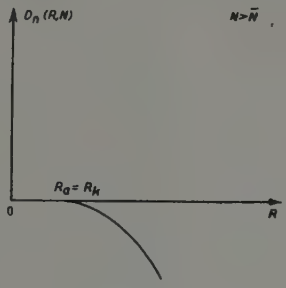

Fig. 3.

II-*A*) $p_k - P$ is equal to the maximum of $f(R)$. The functions $D_n(R, N)$ decrease monotonically with increasing R, from the zero value which they possess for $R = R_a = R_k$ (see Fig. 3).

B) If $N < \bar{N}$, R_a and n_a may no longer be obtained as in the foregoing cases but the $W_{n_a}(N)$'s still keep their meaning, i.e. they still are the values assumed by the functions $W_n(R, N)$ at their relative minima. Under these assumptions eq.'s (5) and (6) are valid in this case too. (In eq. (6) the term C_1^2 has obviously to be replaced by C_2^2).

Let us call $R_0(N)$ the values of R for which $\mathrm{d}n(R, N)/\mathrm{d}R = 0$.

I-*B*) If $R_0 < R_k$ the functions $D_n(R, N)$ increase from zero (at $R = R_0$) up to a maximum for $R = R_k$, and then decrease monotonically with increasing R (see Fig. 4).

II-*B*) If $R_0 = R_k$ [3] the functions $D_n(R, N)$ decrease monotonically with increasing R, from the zero value which they possess at $R = R_0 = R_k$ (see Fig. 5).

The radii of the bubbles having a size for which the functions $D_n(R, N)$ are maximum will be referred to hereafter as *critical radii* and indicated as $R'(N)$, and the bubbles satisfying this condition will be referred to as *critical bubbles*.

Bubbles with radii smaller than $R'(N)$ still require free energy to grow

---

[3] This happens when approaching the critical temperature. More generally, we may remark that in both cases ($N > \bar{N}$ and $N < \bar{N}$) there exists for a given $P < p_k$ a certain value of T for which $R_a = R_k$. This fact sets an upper limit to maximum attainable superheats.

further, whereas those whose radii have reached the critical size grow freely with a decrease of their energy. In view of the statistical nature of the pro-

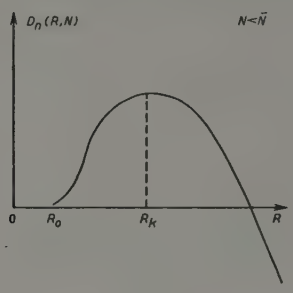

Fig. 4.

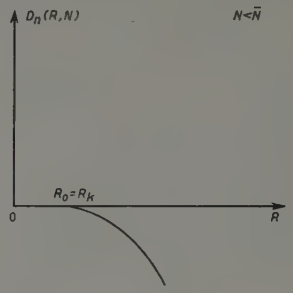

Fig. 5.

cesses, where only one molecule at a time is exchanged between bubble and liquid, only a favourable chain of fluctuations may bring a bubble up to the critical size. However, when this does happen, the metastable equilibrium is broken and the bubble grows until the total pressure balances the vapour pressure of the liquid (4). In this case the growth becomes eruptive, and *the processes may no longer be treated as reversible.* In order to investigate liquids in these conditions, it is useful to know the *waiting time*, i.e. the time one has to wait from the moment when the liquid is brought in the metastable state until it gives rise to a critical bubble. As a matter of fact, such a quantity may be measured very easily and is the most suitable for a *direct* control of the theoretical predictions.

3. – Calculation of the Waiting Time.

In order to investigate the dependence of the waiting time from the degree of ionization of the liquid, we shall start the calculation of the *rate of formation of critical bubbles*, hereafter indicated as $J(N)$.

Let $Z_{n_a}(N)$ be the number of initial aggregates and $n_a(N)$ the total number of molecules in each of them. Next, let us call:

$Z_i(N)$ the number of bubbles with i molecules and N ions;

A_i the surface area of a bubble having i molecules;

(4) For the growth of bubbles beyond the critical size, see for instance: H. K. FORSTER and N. ZUBER: *Journ. Appl. Phys.*, **25**, 474 (1954); M. S. PLESSET and S. A. ZWICK: *Journ. Appl. Phys.*, **25**, 493 (1954).

A_i' the effective area of a bubble having i molecules for the capture of one molecule (or the effective area of a bubble having $i+1$ molecules for the loss of one molecule);

$H_I A_i'$ the probability per unit time for a molecule to pass from the phase I (liquid) into a bubble having n molecules;

$H_{II(i+1)} A_i'$ the probability per unit time for a bubble having $n+1$ molecules to lose one molecule ([5]).

Since the first critical bubble to form perturbs the metastable equilibrium of the liquid, we assume it is possible to remove it from the liquid as soon as it forms: the number of such critical bubbles removed from the liquid per unit time is by definition the rate $J(N)$. Furthermore, to compensate for the loss of molecules and ions (which occurs when the bubbles are removed) we suppose it is possible to reintroduce them into the liquid. Under these assumptions every process occurring in the liquid can be regarded as stationary. Therefore

$$
(7) \qquad \begin{cases} J(N)\,\mathrm{d}t = [Z_{n_a}(N) H_I A'_{n_a} - Z_{(n_a+1)}(N) H_{II(n_a+1)} A'_{n_a}]\,\mathrm{d}t \\ \quad \cdots\cdots\cdots\cdots\cdots\cdots\cdots\cdots \\ J(N)\,\mathrm{d}t = [Z_{(n_a+i)}(N) H_I A'_{(n_a+i)} - Z_{(n_a+i+1)}(N) H_{II(n_a+i+1)} A'_{(n_a+i)}]\,\mathrm{d}t \\ \quad \cdots\cdots\cdots\cdots\cdots\cdots\cdots\cdots \\ J(N)\,\mathrm{d}t = [Z_{(s-1)}(N) H_I A'_{(s-1)}]\,\mathrm{d}t \end{cases}
$$

where $J(N)$ is the total flux of bubbles per unit time, which has been defined above, s is a number larger than $n(R')$ and Z_s, according to the foregoing statement, is zero.

In order to express $J(N)$ as a function only of the macroscopic parameters defining the state of the liquid, we can follow a procedure which is somewhat similar to that developed by VOLMER ([6]).

With the substitution

$$
\frac{H_I}{H_{II(i)}} = \beta_i ,
$$

([5]) For the definition of effective area see: M. VOLMER: *Kinetik der Phasenbildung* (Dresden und Leipzig, 1939).

([6]) M. VOLMER: loc. cit..

we obtain, from the system (7)

$$Z_{n_a}(N)\,\frac{J(N)}{H_1}\sum_{n_a}^{s-1} 1/A_n' \prod_{n_a+1}^{n}{}_i\,\beta_i\,.$$

On the other hand, since

$$\beta_i = \exp\left[\frac{\mu_l - \mu_i}{kT}\right],$$

we have

$$\prod_{n_a+1}^{n}{}_i\,\beta_i = \exp\left[-\frac{1}{kT}\,(W_n - W_{n_a})\right].$$

Hence, replacing the sum with an integral, we can write

$$J(N)\,\mathrm{d}t = Z_{n_a}(N)H_1\,\frac{1}{\int_{n_a}^{s-1}(1/A_n')\,\exp\left[(1/kT)(W_n - W_{n_a})\right]\mathrm{d}n}\,\mathrm{d}t\,.$$

To calculate the integral

$$B \equiv \int_{n_a}^{s-1} \frac{1}{A_n'}\exp\left[\frac{1}{kT}\,(W_n - W_{n_a})\right]\mathrm{d}n\,,$$

we must follow different methods, according to the different cases established in the foregoing paragraph.

I-*A*) The functions $D_n(R, N)$ show a maximum for $R = R_k$. With the help of the substitutions

$$x = \frac{R}{R_k}\,; \qquad a = \frac{p}{p_k}\,; \qquad b = \frac{2\sigma}{R_k p_k}\,; \qquad c = \frac{C_1^2}{R_k^2 p_k}\,,$$

we get

$$B = \frac{n_k}{A_k'}\left\{\exp\left[-\frac{W_{n_a}}{kT}\right]\right\}\int_{x(n_a)}^{x(s-1)}\left(3a + \frac{2b}{x} + \frac{c}{x^4}\right)\exp\left[n_k x^3 \ln\left(a + \frac{b}{x} - \frac{c}{x^4}\right) + \right.$$

$$\left. + \frac{4}{3}\,\frac{\pi}{kT}\,\sigma R_k^2 x^2 + \frac{16\pi}{3}\,\frac{C_1^2}{R_k kT}\right]\cdot\frac{1}{x}\,\mathrm{d}x \equiv$$

$$\equiv \frac{n_k}{A_k'}\left\{\exp\left[-\frac{W_{n_a}}{kT}\right]\right\}\int_{x(n_a)}^{x(s-1)}\left(3a + \frac{2b}{x} + \frac{c}{x^4}\right)\exp\left[F(x, N)\right]\mathrm{d}x\,,$$

where $F(x, N)$ is the function in the exponent, and n_k and A_k are respectively the number of molecules and the surface area of the equilibrium nucleus. The function $F(x, N)$ shows a sharp maximum for $x = 1$. We can develop it

into a power series in the neighbourhood of this point. Neglecting the terms after the third and with the help of the substitution $y = x - 1$, we obtain (7)

$$B = \frac{n_k}{A_k'} \exp\left[\frac{1}{kT}(W_k - W_{n_a})\right] \int_{y(n_a)}^{y(s-1)} \left(3a + \frac{2b}{1+y} + \frac{c}{(1+y)^4}\right) \cdot \exp\left[-\frac{1}{2} n_k (3-L) L y^2\right] \mathrm{d}y ,$$

where $W_k - W_{n_a}$ is the work for the formation of an equilibrium nucleus, and $L = b - 4c$ satisfies the conditions $0 < L < 3$. Under our assumptions these conditions are not restrictive.

Finally we get

$$B \cong \frac{n_k}{A_k'} (3-L) \sqrt{\frac{2\pi}{n_k L (3-L)}} \exp\left[-\frac{1}{kT}(W_k - W_{n_a})\right],$$

and hence

$$J(N)\,\mathrm{d}t = Z_{n_a}(N) H_I A_k' \sqrt{\frac{L}{2 n_k \pi (3-L)}} \exp\left[-\frac{1}{kT}(W_k - W_{n_a})\right] \mathrm{d}t , \tag{8}$$

which is the required expression for $J(N)$ (8).

II-*A*) In this case, the foregoing procedure is not suitable for the calculation of B. Since $p_k - P$ is equal to the maximum of the function $f(R, N)$ (i.e. $R_a = R_k$), the bubbles grow freely. (Obviously, this also happens when $p_k - P$ is larger than the maximum of $f(R, N)$. From this consideration the principle of operation of a bubble chamber may be easily deduced).

I-*B*) The condition $0 < L < 3$ is always fulfilled in this case. (In this case L becomes $(2\sigma/R_k p_k) + (4C_2^2/R_k^4 p_k)$). The result is therefore the same as that obtained in the case I-*A*, provided the $W_{n_a}(N)$'s are taken as the values of $W_n(R, N)$ in the points $R = R_0$.

II-*B*) In this case the procedure used for the calculation of $J(N)$ is not valid. But, on the other hand, the functions $D_n(R, N)$ decrease monotonically with increasing R, so that in this case the bubbles grow freely.

(7) We shall not give here an exact calculation of this integral between the limits $y(n_a)$ and $y(s-1)$, but only remark that since the function $F(x, N)$ has a very sharp maximum for $x = 1$, the main contribution to the integral will thus come from the neighboroud of this point, and so the use of the method of steepest descent is legitimate.

(8) The calculation of H_I, which is independent from the presence of ions in the initial aggregates, may be carried out following the procedure used by D. TURNBULL and J. C. FISHER (*Journ. Appl. Chem.*, **17**, 71 (1949)).

4. – Discussion.

The behaviour of the functions $n(R, N)$ and $W(R, N)$ when the hydrostatic pressure has a value $0 < P < p_k$ does not differ very much, at small values of R, from that of the same functions for liquids in stable equilibrium. The behaviour of the liquid *as a whole* is nevertheless very different, owing to the instability conditions. To investigate the influence of the ions on the behaviour of a liquid in a metastable state it is necessary to specify the way the liquid has been ionized, and brought to the metastable state. We shall confine ourselves to the analysis of two cases, which are the most significant and useful for many practical purposes.

1st *case.* – Let us suppose the liquid to be initially ionized and in stable equilibrium. When we reduce the hydrostatic pressure to a value $P < p_k$, the distribution $Z_{n_a}(N)$ of the initial aggregates in the liquid will be established, if the characteristics of the ionizing radiation are known. A trivial application of the formulae (8) enables us to find, for each N, the corresponding $J(N)$ ($N = 0, 1, 2, ...$). Hence we can evaluate the resulting frequency J' of formation of critical bubbles, without any reference to the number of ions carried by any particular one of them. *J' is always larger than the frequency $J(0)$ of formation of critical bubbles calculated under the assumption that the effect of the ions is negligible.*

If we consider the condition in which one critical bubble is formed every t seconds, the waiting time may be expressed as

$$t = \frac{1}{J'} .$$

The waiting time decreases with increasing degree of ionization of the liquid. The discrepancies observed by several authors, who neglected ionization, between calculated and measured waiting times ([9]) may be probably explained in terms of this effect.

If an initial aggregate contains a sufficiently large number of ions ($\overline{N} > N$), when $p_k - P$ is equal to the maximum of the functions $f(R, N)$, the integral B of § 3 vanishes. The waiting time becomes zero effectively and the metastable equilibrium is broken as soon as the pressure is released. (This is also true, of course, if $p_k - P$ becomes larger than the maximum of $f(R, N)$ during the expansion).

This has been observed experimentally ([10]): eruptive bubbles are formed in

([9]) See, for instance: S. TAKAGI: *Journ. Appl. Phys.*, **24**, 1453 (1953).

([10]) D. A. GLASER: *Phys. Rev.*, **87**, 665 (1952); *Suppl. Nuovo Cimento*, **12**, 361 (1954). L. BERTANZA, G. MARTELLI and A. ZACUTTI: *Nuovo Cimento*, **11**, 692 (1954).

overheated liquids under the effect of radioactive sources, as soon as the pressure was reduced.

2nd *case.* – We assume the liquid is only weakly ionized. If a charged particle crosses the liquid after the release of the pressure, two processes may occur, both leading to the formation of ionized bubbles ([11]):

a) the radiation ionizes the molecules of vapour in the existing uncharged bubbles;

b) some bubbles are nucleated on the ions, which are formed on the path of the particle.

Let us first suppose the particle crossing the liquid is relativistic.

With the help of a procedure similar to FÜRTH's ([12]), we can evaluate the average radius of the bubbles just after the release of the pressure. The probability for a bubble to acquire a given number N of ions and the probability for N ions to be formed on a path unit of liquid equal to an average bubble diameter may be calculated from the specific ionization of the particle with the help of the Poisson law. We assume, of course, that the probability for the formation of a bubble on a cluster of ions is very near unity, as may be seen from eq. (5). Hence the distribution with respect to N of the bubbles on the path of the particle may be found. If we suppose $p_k - P$ to be larger than the maximum of $f(R, N)$, the first critical bubble gives rise to an eruptive boiling. Thus, if we know the rate of the impinging particles, it will be sufficient to calculate the probability of getting *one* bubble with a number N of ions larger than $\overline{N}$, in the whole liquid. *The waiting time depends upon the total number of ionizing particles crossing the liquid per unit time*, for every value of P and T.

Experimentally, GLASER has found a track density of about 25 bubbles per cm for relativistic particles in diethyl ether at 145 °C ([13]). We have calculated the track density of bubbles for this case, according to our theory, on the assumption that the energy loss is 2 MeV/g·cm² (the average radius of the bubbles at this temperature is ~ 30 Å), and have obtained a value of 30 bubbles per cm, in good agreement with the experimental figure.

The probability for a heavily ionizing particle (e.g. α-particle at the end of its range) to give rise to at least one bubble with $N > \overline{N}$ is extremely near unity. In this case the waiting time is reduced to the interval of time measured between the moment of release of the pressure and the moment when the particle is crossing the liquid.

([11]) G. MARTELLI: loc. cit..

([12]) R. FÜRTH: *Proc. Camb. Phil. Soc.*, **37**, 252 (1951).

([13]) D. A. GLASER: *Suppl. Nuovo Cimento*, **12**, 361 (1954).

5. – Conclusions.

The most important points which emerge from the present work are:

1) The contribution of ions to the nucleation processes in overheated liquids may modify very strongly the thermodynamical behaviour predicted by usual theories. In certain conditions even very few ions may give rise to rupture of the metastable equilibrium.

2) Discrepancies between theoretical values and results of previous experiments performed by several authors, may be explained on this basis.

The case of ionized liquids under tension (negative pressure) will be treated in a further paper.

6. – Acknowledgments.

The authors like to acknowledge some interesting discussions on the subject with Prof. M. CONVERSI.

APPENDIX

In ref. ([1]) the electrostatic energy of a charged bubble has been evaluated in an approximate form, which is very convenient for numerical calculation. A more precise calculation may be carried out in the following way.

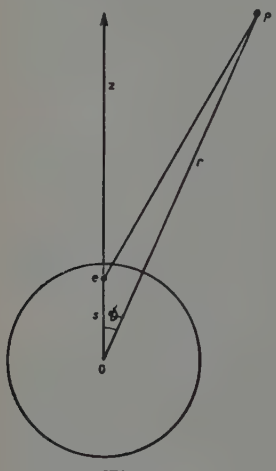

Fig. 6.

A spherical bubble of radius R, in a liquid of dielectric constant ε, contains a single ion carrying a charge e. Let us call s (see Fig. 6) the distance (slightly smaller than R) of this ion from the center of the bubble. We take the z-axis of the co-ordinate system through the point charge, and assume the center of the bubble as origin O.

The potential V_1 due to the charge e at the point P outside the bubble is given in polar coordinates r and ϑ by

$$V_1 = \frac{e}{r} \sum_{l=0}^{\infty} \frac{2l+1}{l+(l+1)\varepsilon} \left(\frac{s}{r}\right)^l P_l(\cos\vartheta) ,$$

where $P_l(\cos\vartheta)$ are the Legendre polynomials of order l.

If the dielectric medium has a dielectric constant $\varepsilon = 1$ (vacuum), we have

$$V_0 = \frac{e}{r} \sum_{l=0}^{\infty} \left(\frac{s}{r}\right)^l P_l(\cos\vartheta) .$$

Therefore the electrostatic energy of the bubble in the liquid (i.e. the energy which has to be spent to bring the dielectric medium in the space surrounding the bubble), is given by

$$U = -\frac{1}{8\pi}\int_{\tau} \boldsymbol{E}_0 \times \boldsymbol{E}_1(\varepsilon - 1)\,\mathrm{d}\tau\,,$$

where $\boldsymbol{E}_0$ and $\boldsymbol{E}_1$ are respectively the electric field before and after the change of the dielectric, and the integral is taken over all space outside the bubble. E_0 and E_s may be calculated with the help of the relations

$$E_{0r} = -\frac{\partial V_0}{\partial r}\,, \qquad E_{0\vartheta} = -\frac{1}{r}\frac{\partial V_0}{\partial \vartheta}\,,$$

$$E_{1r} = -\frac{\partial V_1}{\partial r}\,, \qquad E_{1\vartheta} = -\frac{1}{r}\frac{\partial V_1}{\partial \vartheta}\,.$$

Taking into account the orthogonality of the Legendre polynomials and the values of their normalization factors, we have

$$U(1) = \frac{e^2}{2R}(1-\varepsilon)\sum_{l=0}^{\infty}\left(\frac{s}{R}\right)^{2l}\frac{l+1}{l+(l+1)\varepsilon}\,. \tag{01}$$

In this case $\mathrm{d}U/\mathrm{d}R$ is always positive ([13]).

In the case when the bubbles contain two ions in symmetric positions with respect to the center of the bubble, a similar procedure gives, for the electrostatic energy

$$U(2) = \frac{1}{2}\frac{e^2}{R} + \frac{e^2}{2R}(1-\varepsilon)\sum_{l=0}^{\infty}\left(\frac{s}{R}\right)^{2l}[1+(-1)^l]^2\,\frac{l+1}{l+(l+1)\varepsilon}\,. \tag{02}$$

At this point further precise calculations are of little physical significance, because under the action of the electrostatic forces the bubble becomes deformed, and may be no longer regarded as spherical.

For very large N, however, we can immagine the ions to be uniformly distributed, on the surface of the bubble, and write

$$U(N) = \frac{(Ne)^2}{2\varepsilon R}\,. \tag{03}$$

In this case $\mathrm{d}U/\mathrm{d}R$ is always negative.

From eq.'s (01), (02) and (03) we see that there exists a certain value N of N, for which $\mathrm{d}U/\mathrm{d}R$ changes its sign (being N a value somehow related to ε). Thus, for $N > \bar{N}$, we can write

$$p_n = P + \frac{2\sigma}{R} - \frac{C_1^2}{R^4}\,,$$

and, for $N < \bar{N}$

$$p_n = P + \frac{2\sigma}{R} + \frac{C_2^2}{R^4},$$

where C_1^2 and C_2^2 are constants which depend both upon N and ε. For very large N, we have

$$C_1^2 = \frac{(Ne)^2}{8\pi\varepsilon}.$$

As can be seen from numerical calculations $\bar{N}$ is, for most liquids, of the same order of magnitude as ε. The approximate formulae used in ref. [1] and containing the factor $(1 - \varepsilon/N)$ are therefore legitimate.

RIASSUNTO

Si studia il comportamento di liquidi in equilibrio metastabile sotto pressioni positive. Si ricava il lavoro $D_n(R, N)$ necessario per la formazione di una bolla di raggio R contenente un numero N qualsiasi di ioni, a partire dagli « aggregati iniziali » definiti in § 2. Si ricava la frequenza di formazione di « bolle critiche » a partire da questi aggregati, avendo chiamato « bolle critiche » le bolle che hanno raggiunto un valore del raggio tale che crescono liberamente con diminuzione della loro energia (§ 3). Si discutono i risultati e si mostra (§ 4) che tale frequenza è in generale piú grande di quella che si ottiene trascurando l'effetto degli ioni. Si confrontano i risultati con alcuni dati sperimentali, che mostrano che in alcuni casi non è lecito trascurare il contributo degli ioni nei processi di nucleazione di liquidi surriscaldati.

LETTERE ALLA REDAZIONE

(La responsabilità scientifica degli scritti inseriti in questa rubrica è completamente lasciata dalla Direzione del periodico ai singoli autori)

Remarks on the Existence of Derivatives of Propagation Kernels with Respect to the Interaction Strength.

E. R. Caianiello

Istituto di Fisica e Scuola di Perfezionamento in Fisica Nucleare dell'Università - Roma
Istituto Nazionale di Fisica Nucleare - Sezione di Roma

(ricevuto il 18 Dicembre 1954)

Recently equations involving derivatives of the propagation kernels of a field theory with respect to the coupling constant λ, considered in the real domain, have been derived with different methods ([1-3]). These equations do not imply any hypothesis on an analytical dependence of the kernels on λ; the existence of the λ-derivatives of the kernels which appear in them is, however, obviously assumed a priori. Although correspondential considerations may give some degree of plausibility to such assumption ([4]), it is hard to see how they may lead, alone, to a strict proof of it; it would seem, indeed, that arguments of this sort may at most justify assumptions on the continuity of the kernels of the type introduced below.

We propose here to show that all the λ-derivatives of the propagation kernels of a renormalized field theory do actually exist in the point $\lambda=0$ (λ real), provided that the kernels themselves exist and are continuous functions of λ in the origin. It is then meaningful to calculate them with the standard renormalization procedure, applied to the formulae of ref. ([1]). This statement, to be rigorous, requires some further specifications which are indicated later. We shall prove it under the assumption that the overall space-time volume of integration Ω is finite; this restriction may be conceivably dispensed with, but it seems a convenient one to retain, whenever possible, both for physical and for mathematical reasons.

Regarding the assumption that the kernels be continuous functions of λ in the origin — or rather, in a right (or left) neighborhood of the origin — we notice that it is necessarily satisfied, at least in the case of electrodynamics, if the field equations have solutions at all and if these equations are such as to fulfil the principle of correspondence; in this case, indeed, physical quantities (and thereby kernels) calculated with an interaction of infinitesimal strength must differ from the cor-

([1]) E. R. Caianiello: *Nuovo Cimento*, **11**, 492 (1954).
([2]) B. Ferretti: *Nuovo Cimento*, **10**, 1179 (1953).
([3]) D. J. Candlin: *Nuovo Cimento*, **12**, 380 (1954).
([4]) B. Ferretti: *Lecture at the Congress of the It. Phys. Soc.*, Parma, 1954.

responding free-field ones by infinitesimal amounts; a pole in the origin, say, would be incompatible with this requirement.

The proof given here is only valid for the point $\lambda=0$; this is, though, the most interesting one to investigate, both because it is the only point in which we can actually calculate the derivatives of the kernels, and because the fact that kernels satisfy integro-differential relations (5) which become singular for $\lambda=0$ may lead to expect trouble, if at all, just there (for λ small).

Some further remarks are necessary. First, we should not speak of « derivatives » with respect to λ in the origin, but of « right » or « left » derivatives, according to the convention adopted for the sign of λ; this turns out to be unnecessary, however, because, as is seen from the work of ref. (1), it suffices to restrict the proof to the case of purely fermionic kernels, which depend only upon λ^2; we shall thus consider derivatives with respect to λ^2, which are certainly right-derivatives, since we restrict λ to be real. (This we are obliged to do, because, if $\lambda=0$ is actually a singular point, an infinitesimal imaginary increase $\delta\lambda$ might produce, say, discontinuous changes in some quantities, thus impairing our arguments). Then, the theorem cannot, strictly speaking, be enunciated for kernels, but only for matrix elements of these kernels among arbitrary particle states (or for some suitable averages on these matrix elements); the kernels are indeed singular functions of space and time, and renormalization kills only the « internal » singularities, while the « external » ones disappear trivially on taking the matrix elements. We shall, however, refer to kernels for short, reminding that this is to be regarded only as a symbolic, concise way of considering all matrix elements with the same particle numbers (we prefer not to introduce distribution theory in this trivial connection). Finally, rather than the matrix elements or the kernels of ref. (1), we use the corresponding quantities normalized to unity vacuum-vacuum transition amplitude; this restriction is almost immaterial, since, in most cases, the quantities of interest are defined just in this manner.

We begin with considering eq.'s (51) of ref. (1). Writing $K/K_0=G$, the first of them reads:

$$\text{(i)} \qquad G\begin{pmatrix} x \\ y \end{pmatrix} = (xy) - \lambda^2 \int \sum_{1,2} \gamma^1\gamma^2 (x\xi_1)[\xi_1\xi_2] G\begin{pmatrix} \xi_1\ \xi_2 \\ y\ \ \xi_2 \end{pmatrix}.$$

As it stands, this equation does not take renormalization into account; but, in principle, it is possible to see how it can be changed into its renormalized version, if one takes the view that renormalization is to be performed with a subtractive procedure (the fact that subtraction techniques have been thus far demonstrated effective only in the case of perturbative expansions is not, in our opinion, an objection against this point of view; it stands to reason that such techniques may be made general enough to allow their direct application to the eq.'s of ref. (1), regardless of the methods used in their solution. This question is now being studied in detail). Eq. (i) becomes:

$$\text{(ii)} \qquad G_r\begin{pmatrix} x \\ y \end{pmatrix} = (xy)_r - \lambda_r^2 \int_r \sum_{1,2} \gamma^1\gamma^2 (x\xi_1)_r [\xi_1\xi_2]_r G_r \begin{pmatrix} \xi_1\ \xi_2 \\ y\ \ \xi_2 \end{pmatrix},$$

where the label r denotes that all quantities involved have now their renormalized

(5) E. R. CAIANIELLO: *Nuovo Cimento*, **12**, 561 (1954).

values, and $\int_r$ denotes the convergent part of the whole integral, taken with some criterion which need not concern us here (this may be actually quite complicated: in particular, a symbol $\int_r \int_r$ arising from iteration may *not* denote two distinct $\int_r$ performed successively) (6). Things are particularly neat in electrodynamics, because then λ may be taken as the renormalized interaction constant λ_r to start with (7). What only interests us here is the fact that, after renormalization, the square of the coupling constant which appears explicitly in our equation will still be there, having a finite quantity as factor; our conclusion could be reached as well, formally, by using the unrenormalized symbols. Clearly, then:

$$\text{(iii)} \qquad \frac{G_r\begin{pmatrix} x \\ y \end{pmatrix} - (xy)_r}{\lambda_r^2} = -\int_r \sum_{1,2} \gamma^1 \gamma^2 (x\xi_1)_r [\xi_1 \xi_2]_r G_r \begin{pmatrix} \xi_1 \, \xi_2 \\ y \;\; \xi_2 \end{pmatrix}.$$

Under our assumptions that the 4-volume of integration Ω is finite and that (iii) is symbolic of like relations among matrix elements which are continuous in $\lambda_r = 0$ it is then easily surmised that the limit of the l.h.s. is given by the value of the r.h.s. for $\lambda_r = 0$: this is $\left.\dfrac{\mathrm{d}G_r\begin{pmatrix} x \\ y \end{pmatrix}}{\mathrm{d}(\lambda_r^2)}\right|_{\lambda_r = 0}$ whose existence is thus proved, and whose value can be calculated (1,6).

Consider, next, the following equation of the set (51) of ref. (1); it reduces, using (ii), to:

$$\text{(iv)} \qquad G_r\begin{pmatrix} x_1 \, x_2 \\ y_1 \, y_2 \end{pmatrix} = (x_1 y_1)_r G_r \begin{pmatrix} x_2 \\ y_2 \end{pmatrix} - (x_1 y_2)_r G_r \begin{pmatrix} x_2 \\ y_1 \end{pmatrix} - \lambda_r^2 \int_r \sum_{1,2} \gamma^1 \gamma^2 (x_1 \xi_1)_r [\xi_1 \xi_2]_r G_r \begin{pmatrix} \xi_1 \, x_2 \, \xi_2 \\ y_1 \, y_2 \, \xi_2 \end{pmatrix} =$$

$$= \begin{pmatrix} x_1 \, x_2 \\ y_1 \, y_2 \end{pmatrix}_r - \lambda_r^2 \int_r \sum_{1,2} \gamma^1 \gamma^2 \left\{ (x_2 \xi_1)_r [\xi_1 \xi_2]_r \left[G_r \begin{pmatrix} \xi_1 \, \xi_2 \\ y_2 \, \xi_2 \end{pmatrix} (x_1 y_1)_r - G_r \begin{pmatrix} \xi_1 \, \xi_2 \\ y_1 \, \xi_2 \end{pmatrix} (x_1 y_2)_r \right] - \right.$$

$$\left. - (x_1 \xi_1)_r [\xi_1 \xi_2]_r G_r \begin{pmatrix} \xi_1 x_2 \xi_2 \\ y_1 y_2 \xi_2 \end{pmatrix} \right\}.$$

The same argument shows that $\left.\dfrac{\mathrm{d}G_r\begin{pmatrix} x_1 \, x_2 \\ y_1 \, y_2 \end{pmatrix}}{\mathrm{d}(\lambda_r^2)}\right|_{\lambda_r = 0}$ exists, and, therefore, that $\left.\dfrac{\mathrm{d}^2 G_r\begin{pmatrix} x \\ y \end{pmatrix}}{\mathrm{d}\,(\lambda_r^2)^2}\right|_{\lambda_r = 0}$ exists. An obvious procedure of iteration leads readily to establish the same result for the derivatives of arbitrary order of all the purely fermionic kernels. The extension of this result to more general kernels is trivially afforded by the renormalized counterpart of eq.'s (48) of ref. (1), which need not be written here. Our theorem is thus proved. It should be added, though, that some further restrictions may be introduced by a mathematically rigorous study of renormalization, such as requirements on the behavior of the space-time derivatives of the kernels; we think it very unlikely that troubles may arise this way.

---

(6) A. SALAM: *Phys. Rev.*, **82**, 217 (1951); **84**, 426 (1951).

(7) S. N. GUPTA: *Proc. Phys. Soc. (London)*, A **64**, 426 (1951); F. J. DYSON: *Phys. Rev.*, **83**, 608 (1951).

A proof of similar simplicity does not seem feasible for values of λ other than the origin; it is hoped that the present results may render more acceptable the hypothesis, when needed, that such derivatives exist also in a neighborhood of the origin.

This result makes perhaps the question whether the perturbative expansions of some matrix elements may actually converge more interesting; it cannot, clearly, answer it, since it is very well known that the existence of all the derivatives of a function in the origin is far from sufficient to secure the convergence of its McLaurin expansion.

The author gratefully acknowledges his indebtedness to Prof. B. Ferretti for fruitful and stimulating discussions on this argument.

IL NUOVO CIMENTO Vol. I, N. 2 1° Febbraio 1955

Dosage de radioéléments par la distribution des intervalles entre désintégrations. Efficacité des estimations.

D. Hirschberg

Laboratoire de Physique Nucléaire - Université Libre de Bruxelles

(ricevuto il 27 Dicembre 1954)

Dans une note précédente [1] nous avons décrit une méthode de dosage du RdTh (et du RdAc), basée sur les couples de désintégrations successives Tn $\xrightarrow{\alpha}$ ThA $\xrightarrow{\alpha}$ (et An $\xrightarrow{\alpha}$ AcA $\xrightarrow{\alpha}$).

La méthode d'analyse que nous y avons décrite consiste en la sélection de tous les intervalles inférieurs à un temps τ. Ce temps est choisi de façon à rendre minimum l'erreur statistique. Nous avons adopté cette méthode d'analyse pour sa simplicité, mais on peut se demander si elle ne fait pas perdre trop d'information.

Calculons la quantité d'information contenue dans un intervalle, telle qu'elle est définie par R. A. Fisher [2].

Fisher définit g, la quantité d'information relative à un paramètre λ, apportée par une mesure, comme étant:

$$g = E\left\{\left(\frac{\partial \ln \varphi}{\partial \lambda}\right)^2\right\}$$

où E est l'espérance mathématique et φ la densité de probabilité de la grandeur mesurée.

Soient: ϑ l'intervalle moyen des couples Tn-ThA (0,23 s) ou An-AcA ($2.6 \cdot 10^{-3}$ s);

n_1 le nombre moyen d'α comptés par unité de temps;

n_2 le nombre moyen de couples réels émis par unité de temps dans le volume sensible du compteur;

x la durée d'un intervalle.

Nous supposons n_1 connu avec une erreur négligeable.

---

[1] D. Hirschberg: *Nuovo Cimento*, **12**, 733 (1954).

[2] R. A. Fisher: *Phil. Trans. of Roy. Soc. of London*, A **222**, 309 (1921); *Proc. Phil. Soc.*, **22**, 700 (1925).

Le paramètre à estimer est n_2.

Notre méthode de dosage n'est utile que dans le cas de faibles activités, soit $n_1\vartheta \ll 1$. Dans ce cas, la densité de probabilité d'un intervalle x est:

$$\varphi(x; n_2) = (n_1 - n_2)\left(\exp\left[-n_1 x\right] + \frac{1}{\mu}\exp\left[-\frac{x}{\vartheta}\right]\right)$$

où

$$\mu = \frac{n_1(n_1 - n_2)\vartheta}{n_2}.$$

Dans le cas de $\mu \ll 1$, l'estimation par le procédé décrit est très bonne, mais nous pourrions craindre qu'il n'en soit plus ainsi pour des valeurs de μ plus grandes. Pour de telles valeurs, obtenues quand $n_2 \ll n_1$; la densité de probabilité peut s'écrire:

$$\varphi(x; n_2) = n_1\left(\exp\left[-n_1 x\right] + \frac{1}{\mu}\exp\left[-\frac{x}{\vartheta}\right]\right).$$

La quantité d'information g, relativement à n_2, contenue dans une mesure d'intervalle, est:

$$g = E\left\{\left(\frac{\partial \ln \varphi}{\partial n_2}\right)^2\right\}.$$

Soit, après calcul

$$g = g(\mu) = \frac{1}{n_1 n_2}\left(1 - \mu \ln \frac{1+\mu}{\mu}\right).$$

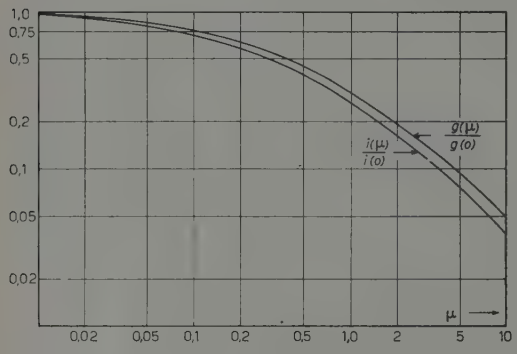

Fig. 1.

D'autre part, la quantité d'information i par intervalle, de l'estimation décrite dans la note précédente est

$$i = \frac{1}{n_1 t \sigma^2_{n_2}} = \frac{1}{n_1 n_2}\,\frac{1}{f^2(\mu; \tau/\vartheta \text{ opt})}$$

quand le nombre de couples est suffisamment élevé. Ici, $\sigma^2_{n_2}$ est la variance de cette estimation, t la durée du comptage et $f(\mu; \tau/\vartheta \text{ opt})$ une fonction de μ déjà définie (1).

La fig. 1 montre $i(\mu)/i(0)$ et $g(\mu)/g(0)$ en fonction de μ. Pour des $g(\mu)/g(0)$ compris entre 1,0 et 0,05 l'efficacité e, définie par:

$$e = \frac{i(\mu)}{g(\mu)}$$

est comprise entre 1,0 et 0,8.

Nous voyons que tout en n'étant pas exhaustive, l'estimation proposée suffit dans la pratique. La seule utilité d'une connaissance plus détaillée de la longueur des intervalles réside dans la possibilité de contrôle qu'elle offre.

L'enregistrement des intervalles pourrait se faire à l'aide d'un circuit à coïncidences retardées à canaux multiples. Nous avons construit pour la mesure du RdTh,

un appareil basé sur un principe différent. La fig. 2 représente le schéma de principe de cet appareil.

Le faisceau du tube à rayons cathodiques est normalement coupé. Chaque α détecté par le compteur rend le spot visible en envoyant une première impulsion positive de courte durée sur la grille d'intensité. Une deuxième impulsion positive est envoyée ensuite sur la grille du tube T, qui est normalement non conducteur; cette dernière impulsion a pour effet de décharger la capacité.

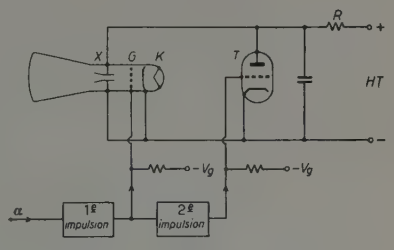

Fig. 2.

Un appareil dont l'objectif est ouvert en permanence photographie l'écran. Chaque point lumineux représente un intervalle, la longueur étant déterminée par la coordonnée X. Une tension périodique (par exemple, 50 Hz) appliquée aux plaques Y permet d'utiliser une plus grande partie de l'écran. Plutôt que de nous fier à la loi (exponentielle) du balayage, nous étalonnons les temps à l'aide d'un générateur d'impulsions.

Comme nous l'avons dit plus haut, un tel dispositif permet de contrôler la bonne marche d'un comptage, mais le gain d'information qu'il procure par rapport au dispositif simple décrit antérieurement n'est pas appréciable.

Nous remercions M. M. Huybrechts pour de nombreuses discussions et M. le Professeur P. Gillis pour l'intérêt qu'il a porté à cette note.

ERRATA CORRIGE

D. Hirschberg: **Dosage de radioéléments par la distribution des intervalles entre désintégrations. Application au** RdTh, *Nuovo Cimento*, 12, 733 (1954).

Page 741, ligne 3, il faut lire:

$$N'' = (n_1 - n_2)t(1 - \exp[-n_1\tau]) \approx n_1(n_1 - n_2)\tau t$$

au lieu de

$$N'' = n_1 t(1 - \exp[-(n_1 - n_2)\tau]) \approx n_1(n_1 - n_2)\tau t\,.$$

Many Body Forces and Non-Linear Interactions.

E. Clementel and C. Villi

Istituti di Fisica delle Università di Padova e di Trieste

Istituto Nazionale di Fisica Nucleare - Sezione di Padova

(ricevuto il 30 Dicembre 1954)

The moderate success of two body exchange interactions, with or without repulsive core, to account for saturation in heavy nuclei has suggested many body (1) and non-linear interactions (2) as new clues both to explain saturation without collapse and to harmonize the assumptions of strong nuclear forces with the shell model.

It is known that these two approaches lead to the same sort of physical effects: in fact, either because of the balance between even-body attractive and odd-body repulsive forces or because of the smoothing mechanism of the non-linearities, nuclear correlations are weakened, so that the interaction of a number of nearby nucleons is less than the sum of the pair interactions. However, although quantitative results are in agreement, it is not clear, mainly because of the widely different mathematical treatments, under which assumptions and to which extent the two approaches can be considered as substantially equivalent.

This is the point we want to discuss in this note. With this aim in view we shall make analytical developments as simple as possible in favour of the physical content of the arguments.

It has been shown (3), on the basis of ordinary forces approximation and by means of non-linear interactions, that the saturation of the nuclear binding energy can be obtained to a large extent. It is easy to see that the same result can be also achieved using Wigner many body forces only.

Let V_0 be the average many body potential well and b the mean range of the particles averaged over all n-body clusters. Then, if $p(R, b)$ is the probability (4) of finding two particles within the range b of each other in a nucleus of radius R, the expectation value of the total potential energy is:

$$\langle V \rangle = - V_0 \sum_{k=2}^{A} (-1)^k \frac{A!}{k!\,(A-k)!}\, p^{k-1}(R, b)\,, \tag{1}$$

(1) S. D. Drell and K. Huang: *Phys. Rev.*, **91**, 1527 (1953).

(2) L. J. Schiff: *Phys. Rev.*, **84**, 1 (1955); W. Thirring: *Zeits. Naturfor.*, **7a**, 63 (1952); **9**, 804 (1954)

(3) B. Malenka: *Phys. Rev.*, **86**, 68 (1952); P. Mittelstaedt: *Zeits. Phys.*, **137**, 545 (1954).

(4) J. M. Blatt and M. F. Weisskopf: *Theor. Nuclear Physics* (ed. 1952).

where the function $p(R, b)$, given essentially by $(b/R)^3$, makes higher oder ($k > 5$) contributions negligible. The series (1) can be summed up and the result reads:

$$\langle V \rangle = - V_0 \frac{A p(R, b) - 1 + [1 - p(R, b)]^A}{p(R, b)} . \tag{2}$$

By adding the kinetic energy term, it is found that the minimum of the total energy occurs at a value of the nuclear radius given by

$$R = \left[\frac{3\pi}{20}\left(\frac{3}{\pi}\right)^{\frac{1}{3}} \frac{\hbar^2 b^3}{M V_0}\right]^{\frac{1}{5}} A^{\frac{1}{3}} = r_0 A^{\frac{1}{3}} . \tag{3}$$

Thus, as in the case of non-linear interactions, the saturation prescriptions are fulfilled provided two constants are properly determined. For example, with $r_0 = 1.4 \cdot 10^{-13}$ cm we find a binding energy per nucleon of the same order of that given the usual non-linear treatment ($(\sim 13$ MeV), choosing $b = 1.95 \cdot 10^{-13}$ cm and $V_0 = 39$ MeV. Without emphasizing this agreement, we shall only point out that the previous argument can be considered as the many body counterpart of a similar non-linear calculation only as far as Wigner forces are concerned. Apart from this, there is a basic difference between the two procedures, mainly due to the assumptions: (i) that the classic scalar field with time independent nucleon source is characterized by a non linearity of the kind $F[\varphi(\boldsymbol{r})] \sim \varphi^n(\boldsymbol{r})$, where $\varphi(\boldsymbol{r})$ is the meson field in the nucleus, and (ii) that the linear term is negligible with respect to the non-linear one. Since saturation can be obtained only if $n > 5/2$, two cases have been so far considered, i.e. $n = 3$ and $n = 4$. It is seen that the assumptions (i) and (ii) lead to a dependence of the nucleus potential energy on the 1/3 respectively 1/4 power of the nuclear density, whereas the many body forces potential energy depends on all integer powers of the nuclear density up to A. Furthermore, the assumption (ii) has as physical consequence the suppression of two body forces, and therefore the situation in this way described gets clearly out of the many body picture.

On the contrary, it can be shown that the state of affairs described by a non-linear equation of the kind

$$\Delta\varphi(\boldsymbol{r}) - \mu^2\varphi(\boldsymbol{r}) - F[\varphi(\boldsymbol{r})] = - g\varrho(\boldsymbol{r}) , \tag{4}$$

leads to the same result of Eq. (2), provided one assumes that the non-linear function $F[\varphi(\boldsymbol{r})]$ is a uniformingly convergent series of φ of the form $F(\varphi) = \sum_{n=2} \alpha_n \varphi^n$. In this case the potential energy is

$$\langle V \rangle = \int \left\{ \frac{(\nabla\varphi)^2}{2} + \sum_{n=1} \frac{\alpha_n \varphi^{n+1}}{n+1} - g\varphi\varrho \right\} \mathrm{d}\boldsymbol{r} , \tag{5}$$

where $\alpha_1 = \mu^2$ ($\mu =$ inverse Compton meson wave length). The linear term in (4) is closely related to two body short range forces, whereas contributions to many body forces come out from all other non-linear terms ($n \geqslant 2$). Assuming in (4) all α's but α_1 equal to zero and assuming to the first approximation $\varphi(\boldsymbol{r}) = \varphi_0$ and $\varrho(\boldsymbol{r}) = \varrho_0$, Eq. (5) gives $\langle V \rangle = - (3/4\pi b^3)(g/\mu)^2 (A^2/2)(b/R)^3$, which, for large A, corresponds to the two body forces term in Eq. (1) provided $V_0 = (3/4\pi b^3)(g/\mu)^2$.

With the values $V_0 = 25$ MeV and $b = 2.2 \cdot 10^{-13}$ cm, consistent with the deuteron ground state, one has $g^2 = 2.9$ ($\mu^{-1} = 1.4 \cdot 10^{-13}$ cm).

In the general case all α's are different from zero and Eq. (5) reads

$$\langle V \rangle = -\frac{A}{\varrho_0} \sum_{n=1} \frac{n\alpha_n}{n+1} \varphi^{n+1} . \tag{6}$$

Applying now to Eq. (4) the series reversion technique, φ_0 can be expressed as a function of ϱ_0, and therefore, after rearrangement and relabelling, one gets

$$\langle V \rangle = -A \sum_{k=2} (-1)^k \beta_{k-1} \varrho_0^{k-1} , \tag{7}$$

where the constants β_k are known functions of the α's. Since $\beta_k \ll 1$, only the first $A - 1$ terms of the infinite series (7) can be retained: then, the expansions (7) and (1) can be compared, and both exhibit the same dependence on the nuclear density, as far as heavy nuclei are concerned. Although to work out constants seems at the present to be pointless, it is seen that Eq. (7) identifies with Eq. (1) on writing

$$\beta_k = V_0 \left(\frac{4\pi}{3}\right)^k \left(\frac{b^3}{A}\right)^k \binom{A-1}{k+1} . \tag{8}$$

In this way the constants α are determined. Although this identification is rather artificial, it corresponds just to the ad hoc determination of arbitrary constants which any non-linear theory cannot at the present avoid. Thus, Eq. (4) describes, under the assumptions we have supposed valid, just the situation envisaged by the many body approach in the Wigner forces approximation. It is clear that the previous correspondence can be established also without starting from average values of depth and range of many body potential wells.

A valuable criticism of Dr. A. SALAM is gratefully acknowledged.

Sull'equazione del positone nell'elettrodinamica classica.

P. Caldirola

Istituto di Scienze Fisiche dell'Università - Milano
Istituto Nazionale di Fisica Nucleare - Sezione di Milano

(ricevuto il 7 Gennaio 1955)

È noto come l'elettrodinamica classica, nella sua forma più ampia datale da Feynman, possa essere dedotta da un principio variazionale dovuto a Fokker e generalizzato dallo stesso Feynman.

Tale principio permette di descrivere anche il comportamento dell'elettrone positivo, le cui equazioni del moto si ottengono da quelle dell'elettrone ordinario (negativo) considerando l'azione del campo proprio anticipato anzichè di quello ritardato ed operando un'inversione dell'orientamento della linea oraria (nel cronotopo minkowskiano) della particella.

Nella teoria dell'elettrone da noi proposta ([1,2]) si ha la seguente equazione del moto:

$$(1) \qquad -\frac{m_0}{\tau_0}\left[u_\alpha(\tau-\tau_0)+\frac{u_\alpha(\tau)\,u_\beta(\tau)}{c^2}\,u_\beta(\tau-\tau_0)\right]=\frac{e}{c}\,F^{(\mathrm{ext})}_{\alpha\beta}(\tau)\,u_\beta(\tau)\,,$$

che viene stabilita ammettendo che l'azione sull'elettrone del suo campo proprio sia a carattere ritardato. Assumendo invece che tale azione sia a carattere anticipato, l'equazione del moto si scrive:

$$(2) \qquad \frac{m_0}{\tau_0}\left[u_\alpha(\tau+\tau_0)+\frac{u_\alpha(\tau)\,u_\beta(\tau)}{c^2}\,u_\beta(\tau+\tau_0)\right]=\frac{e}{c}\,F^{(\mathrm{ext})}_{\alpha\beta}(\tau)\,u_\beta(\tau)\,,$$

o anche

$$\frac{e}{c}\left[F^{(\mathrm{self}+)}_{\alpha\beta}+F^{(\mathrm{ext})}_{\alpha\beta}\right]u_\beta=0\,,$$

essendo

$$(3) \qquad F^{(\mathrm{self}+)}_{\alpha\beta}(\tau)=\frac{m_0}{e\tau_0 c}\left[u_\alpha(\tau+\tau_0)\,u_\beta(\tau)-u_\alpha(\tau)\,u_\beta(\tau+\tau_0)\right]$$

il campo proprio anticipato dell'elettrone.

([1]) P. Caldirola: *Nuovo Cimento*, **10**, 1747 (1953).
([2]) P. Caldirola e F. Duimio: *Nuovo Cimento*, **12**, 699 (1954).

Scomponiamo questo in due parti ([3]):

$$F_{\alpha\beta}^{(\mathrm{self}+)} = F_{\alpha\beta}^{(\mathrm{reaz}+)} + F_{\alpha\beta}^{(\mathrm{diss}+)},$$

di cui la prima:

$$(4)\quad F_{\alpha\beta}^{(\mathrm{reaz}+)}(\tau) = \frac{m_0}{2e\tau_0 c}\{[u_\alpha(\tau+\tau_0) - u_\alpha(\tau-\tau_0)]u_\beta(\tau) - u_\alpha(\tau)[u_\beta(\tau+\tau_0) - u_\beta(\tau-\tau_0)]\}$$

ha carattere conservativo ed è esattamente eguale a quella $F_{\alpha\beta}^{(\mathrm{reaz}-)}$ che si ha quando si considerino le azioni ritardate, mentre la seconda

$$(5)\quad F_{\alpha\beta}^{(\mathrm{diss}+)}(\tau) = \frac{m_0}{2e\tau_0 c}\{u_\beta(\tau)[u_\alpha(\tau-\tau_0) + u_\alpha(\tau+\tau_0)] - u_\alpha(\tau)[u_\beta(\tau-\tau_0) + u_\beta(\tau+\tau_0)]\}$$

ha carattere dissipativo ed è eguale ma di segno contrario a quella $F_{\alpha\beta}^{(\mathrm{diss}-)}$ che si ha quando si considerino le azioni ritardate.

Prendendo ora in considerazione i moti di particelle che descrivono linee orarie rivolte verso il passato (per cui $\mathrm{d}x^0/\mathrm{d}\tau < 0$), opereremo nelle espressioni precedenti la sostituzione:

$$\frac{\mathrm{d}x^\alpha}{\mathrm{d}\tau} \to -\frac{\mathrm{d}x^\alpha}{\mathrm{d}\tau}.$$

Come conseguenza del fatto che nello sviluppo in serie delle potenze di τ_0 dell'espressione (4) di $F_{\alpha\beta}^{(\mathrm{reaz})}$ compaiono solo le derivate dispari di $u_\alpha(\tau)$, mentre in quello dell'espressione (5) di $F_{\alpha\beta}^{(\mathrm{diss})}$ solo quelle pari, si ha con tale sostituzione:

$$F_{\alpha\beta}^{(\mathrm{reaz}+)} \to -F_{\alpha\beta}^{(\mathrm{reaz}+)} = -F_{\alpha\beta}^{(\mathrm{reaz}-)},$$
$$F_{\alpha\beta}^{(\mathrm{diss}+)} \to \quad F_{\alpha\beta}^{(\mathrm{diss}+)} = -F_{\alpha\beta}^{(\mathrm{diss}-)}.$$

Con ciò l'equazione del moto della particella nel verso invertito della linea cronotopica diventa:

$$\frac{e}{c}\left[-F_{\alpha\beta}^{(\mathrm{reaz}-)} - F_{\alpha\beta}^{(\mathrm{diss}-)} + F_{\alpha\beta}^{(\mathrm{ext})}\right]u_\beta = 0,$$

o anche in forma esplicita

$$-\frac{m_0}{\tau_0}\left[u_\alpha(\tau-\tau_0) + \frac{u_\alpha(\tau)\,u_\beta(\tau)}{c^2}u_\beta(\tau-\tau_0)\right] = -eF_{\alpha\beta}^{(\mathrm{ext})}(\tau)u_\beta(\tau)$$

che è appunto l'equazione, sotto l'azione dell'ordinario campo proprio ritardato, di

---

([3]) P. Caldirola: *Nuovo Cimento*, **1**, 269 (1955).

una particella di carica $-e$ (positone). Tale equazione risulta quindi equivalente a quella che descrive il moto di una particella di carica e (elettrone) sotto l'azione del campo proprio anticipato e descrivente una linea oraria cronotopica diretta verso il « passato ». Osserviamo che avendosi:

$$eF_{4\beta}^{(\text{reaz}+)} u_\beta \sqrt{1-\beta^2} = -\frac{\mathrm{d}}{\mathrm{d}t}\left(\frac{m_0 c^2}{\sqrt{1-\beta^2}}\right) - \dots ,$$

l'energia (cinetica + correzioni radiative) di una siffatta particella (di carica e) nel suo moto verso il « passato » risulta negativa.

I risultati precedenti, stabiliti per via diretta, possono comprendersi anche ricordando che, come si è dimostrato in [2], l'equazione del moto (1) è deducibile, in una teoria da campo, dal principio variazionale di Fokker-Feynman. Con ciò i tensori dei campi propri dell'elettrone, ritardato $F_{\alpha\beta}^{(\text{self}-)}$ o anticipato $F_{\alpha\beta}^{(\text{self}+)}$, vengono derivati rispettivamente dai potenziali:

$$\text{(6)} \qquad \begin{aligned} \tilde{A}_\alpha^{(-)}(x) &= e\int_{-\infty}^{\infty} \tilde{G}^{(-)}(\sigma^2;\tau_0)\, u_\alpha(\tau')\,\mathrm{d}\tau' \\ \tilde{A}_\alpha^{(+)}(x) &= e\int_{-\infty}^{\infty} \tilde{G}^{(+)}(\sigma^2;\tau_0)\, u_\alpha(\tau')\,\mathrm{d}\tau' \end{aligned} \qquad (\sigma^2 = |x(\tau) - x(\tau')|^2) .$$

Si ha inoltre:

$$\begin{aligned} F_{\alpha\beta}^{(\text{reaz}\mp)} &= \tfrac{1}{2}\left[F_{\alpha\beta}^{(\text{self}+)} + F_{\alpha\beta}^{(\text{self}-)}\right], \\ F_{\alpha\beta}^{(\text{diss}\mp)} &= \mp\,\tfrac{1}{2}\left[F_{\alpha\beta}^{(\text{self}+)} - F_{\alpha\beta}^{(\text{self}-)}\right]. \end{aligned}$$

Ricordiamo ancora che si ha approssimativamente [4]:

$$\begin{aligned} \tilde{G}^{(-)}(\sigma^2;\tau_0) &\simeq \delta_-(-\sigma^2+\lambda^2) \\ \tilde{G}^{(+)}(\sigma^2;\tau_0) &\simeq \delta_+(-\sigma^2+\lambda^2) \end{aligned} \qquad \left(\lambda = \frac{3}{8}c\tau_0\right),$$

dove:

$$\delta_-(-\sigma^2+\lambda^2) = \begin{cases} = 2\delta(-\sigma^2+\lambda^2) & \text{per} \quad \sigma < 0 \\ = 0 & \text{»} \quad \sigma > 0 \end{cases}$$

$$\delta_+(-\sigma^2+\lambda^2) = \begin{cases} = 0 & \text{per} \quad \sigma < 0 \\ = 2\delta(-\sigma^2+\lambda^2) & \text{»} \quad \sigma > 0 . \end{cases}$$

---

[4] Cfr. [2] a pag. 728. Prendiamo l'occasione per correggere alcuni banali errori contenuti in detta pagina:

nella formula a riga 10 anzichè $=(4/3)R$ va letto $=4/3R$;

la formula a riga 14 anzichè $\lambda = \frac{3}{8}R$ va letta $\lambda = \frac{3}{4}R$;

le funzioni indicate impropriamente con $\delta(-r^2+\lambda^2)$ e $\delta(-\sigma^2+\lambda^2)$ sono in realtà le $\delta_-(-r^2+\lambda^2)$ e $\delta_-(-\sigma^2+\lambda^2)$ come definite in questa lettera.

Con queste espressioni del fattore $\widetilde{G}$, i potenziali (6) si riducono per $\lambda \to 0$ alle formule di Wiechert-Liénard:

$$A_\alpha^{(-)}(x) = 2e \int_{-\infty}^{\bar{\tau}} \delta(\sigma^2)\, u_\alpha(\tau')\, d\tau' = e \left[\frac{u_\alpha}{(x_\beta - z_\beta^*) u_\beta} \right]_{\text{rit}}$$

$$A_\alpha^{(+)}(x) = 2e \int_{\bar{\tau}}^{\infty} \delta(\sigma^2)\, u_\alpha(\tau')\, d\tau' = e \left[\frac{u_\alpha}{(x_\beta - z_\beta^*) u_\beta} \right]_{\text{ant}}$$

essendo z_β^* le coordinate del punto ove è situato l'elettrone e $\bar{\tau}$ un valore arbitrario del tempo proprio, compreso fra quelli corrispondenti ai due zeri di σ^2.

Vogliamo infine osservare come la possibilità di descrivere, nel modo detto, il moto del positone e la circostanza che l'energia intrinseca di una particella a riposo risulta nella nostra teoria data da

$$m_0 c^2 = \frac{1}{2} e\varphi(0) = \frac{1}{2} \frac{e^2}{\lambda},$$

permettono anche di interpretare classicamente la creazione e l'annichilazione di una coppia di elettroni di segni opposti.

Effetti di diffusione nell'assorbimento di ultrasuoni in miscele di gas.

S. Petralia

Istituto di Fisica dell'Università - Bologna

(ricevuto il 14 Gennaio 1955)

Si sono continuate (1) le misure di assorbimento di ultrasuoni in miscele di gas, con lo scopo di determinare il contributo che a tale assorbimento arrecano i processi di diffusione e termodiffusione, che hanno luogo quando i componenti della miscela differiscono in modo cospicuo nel peso molecolare.

Si sono adoperati ancora gas monoatomici quali elio, neon, argon e kripton, escludendo di proposito gas poliatomici, per la difficoltà, che si sarebbe incontrata in questi ultimi, di valutare il contributo all'assorbimento che ha origine nei processi molecolari. Tale contributo è infatti fortemente influenzato dalla presenza di gas estranei.

La tecnica e le condizioni sperimentali sono quelle descritte nella nota precedente. I gas, eccettuato l'argon, ci sono stati forniti puri in fiale. La frequenza della sorgente ultrasonora era di 3 MHz, la temperatura dell'interferometro di 25 °C e la pressione del gas poteva variare tra 15 e 40 cm Hg.

Le fig. 1-5 e le tabelle I e II riassumono i risultati per le cinque miscele elio-neon, elio-kripton, neon-argon, neon-kripton, argon-kripton. Nelle figure le curve continue danno i valori di α/f^2 (α coefficiente di assorbimento dell'ampiezza ultra sonora, f frequenza degli ultrasuoni), in funzione del componente più leggero che entra a far parte delle singole miscele, calcolati, a pressione normale e temperatura di 25 °C, in base all'espressione generale per l'assorbimento classico data da M. K. Kohler (2)

$$(1) \qquad \frac{\alpha}{f^2} = \frac{2\pi^2}{V^3}\left\{\frac{4}{3}\frac{\eta}{\varrho} + \frac{\gamma-1}{\gamma}\frac{\lambda}{C_v\varrho} + \frac{\gamma-1}{\gamma}\frac{\nu'_{12}\nu_{12}}{C_v\varrho} + \gamma D_{12}C_1C_2\left(\frac{M_2-M_1}{M_0}\right)^2 + 2(\gamma-1)\nu'_{12}C_1C_2\frac{M_2-M_1}{M_0}\right\}.$$

Le curve tratteggiate dànno α/f^2 quale risulta dalla somma dei primi due termini della (1), che sono i termini di G. G. Stokes e di G. Kirchhoff. Per costruire

(1) S. Petralia: *Nuovo Cimento*, **11**, 570 (1954).
(2) M. K. Kohler: *Ann. der Phys.*, **39**, 209 (1941).

tali curve, poichè non è stato possibile trovare i valori sperimentali per tutte le costanti interessate, come i coefficienti di viscosità, i coefficienti di conduzione termica e i coefficienti di diffusione, perché effettivamente determinazioni di tali costanti

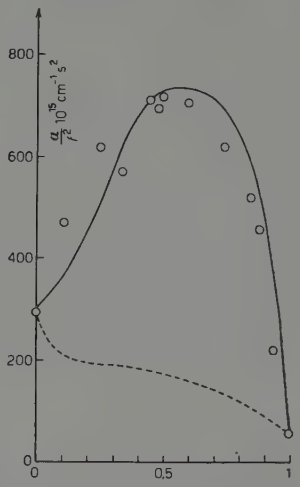

Fig. 1. – Frazione elio in elio-kripton.

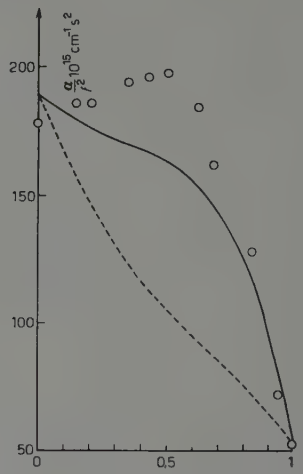

Fig. 2. – Frazione elio in elio-neon.

TABELLA I.

Miscela elio-kripton		Miscela elio-neon		Miscela neon-argon	
Concentrazione elio	$\alpha/f^2 \cdot 10^{15} cm^{-1}s^2$	Concentrazione elio	$\alpha/f^2 \cdot 10^{15} cm^{-1}s^2$	Concentrazione neon	$\alpha/f^2 \cdot 10^{15}\ cm^{-1}\ s^2$
0	293	0	178	0	185
0,11	472	0,15	186	0,11	196
0,25	620	0,21	186	0,16	195
0,34	570	0,36	194	0,25	198
0,45	710	0,43	196	0,39	208
0,48	695	—	—	—	—
0,50	717	0,51	198	0,50	217
0,60	705	0,62	184	0,59	205
0,74	618	0,69	162	0,63	205
0,84	520	0,84	128	0,72	193
0,88	456	—	—	0,80	194
0,93	270	0,94	72	—	—
1	52	1	52	1	178

non esistono per tutte le miscele qui esaminate, si è preferito ricavare le costanti stesse dalle espressioni che sono stabilite nella teoria molecolare dei gas, quali si trovano riportate da J. O. HIRSCHFELDER, C. F. CURTISS e R. B. BIRD [3].

[3] J. O. HIRSCHFELDER, C. F. CURTISS e R. B. BIRD: *Molecular Theory of Gases and Liquids* (New York, 1954).

TABELLA II.

Miscela argon-kripton		Miscela neon-kripton	
Concentrazione argon	$\alpha/f^2 \cdot 10^{15}$ cm^{-1} s^2	Concentrazione neon	$\alpha/f^2 \cdot 10^{15}$ cm^{-1} s^2
0	293	0	293
0,27	280	0,20	315
0,39	281	0,32	330
0,41	274	0,40	360
0,50	265	0,50	376
0,61	267	0,67	355
0,70	236	0,76	350
0,80	230	—	—
0,85	218	0,90	250
1	185	1	178

I cerchi nelle figure danno i valori sperimentali di α/f^2 ridotti a pressione normale. Nelle singole determinazioni l'errore commesso è inferiore al 5%. Può però accadere che misure ripetute su mescolanze a concentrazione pressochè uguale, ma in circostanze diverse, diano risultati discordanti, non mai però per più del 10%. Ciò è da imputare soprattutto alle piccole cause perturbatrici che intervengono nella preparazione delle miscele, e può render conto della dispersione dei punti sperimentali che si osserva in alcune figure.

Dall'esame dei risultati si possono trarre le seguenti conclusioni:

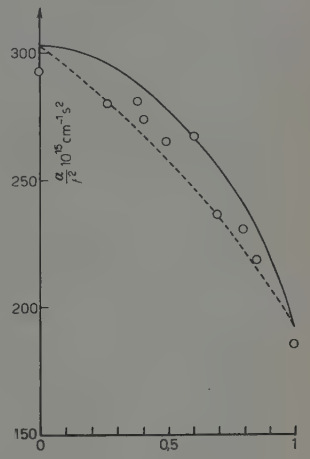

Fig. 3. – Frazione argon in argon-kripton.

1) I valori dei coefficienti di assorbimento, per i quattro gas puri qui studiati, sono d'accordo abbastanza bene con i valori previsti dalla teoria. Per il neon esistono determinazioni fatte da A. VAN ITTERBEEK e L. THYS [4]; esse però sembrano discostarsi alquanto dal valore classico. Non ci sono note determinazioni per il kripton.

2) L'assorbimento dovuto ai fenomeni di diffusione può essere notevole, specie se i gas della miscela sono di peso molecolare fortemente diverso, e può superare l'assorbimento dovuto alla viscosità e alla conduzione termica (caso elio-kripton).

3) Eccettuata la mescolanza argon-kripton, per le altre coppie di gas vi è un massimo nell'assorbimento misurato; esso massimo si ha circa per pari concentrazione dei due componenti.

[4] A. VAN ITTERBEEK e L. THYS: *Physica*, **5**, 889 (1938).

4) I valori sperimentali sono prossimi (entro il 10%) a quelli teorici per le miscele neon-argon, argon-kripton, neon-kripton; possono discostarsi fino a circa il 16% in eccesso per alcuni punti della curva teorica nel caso di miscele elio-neon

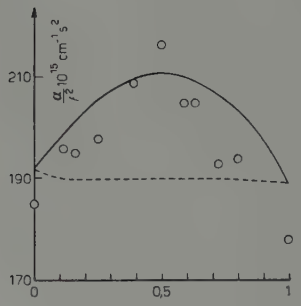

Fig. 4. – Frazione neon in neon-argon.

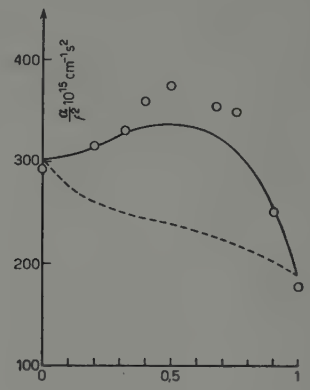

Fig. 5. – Frazione neon in neon-kripton.

ed elio-kripton. Per la miscela elio-neon la curva di Kohler ha un andamento diverso da quello della curva che può riunire i punti sperimentali. Il disaccordo cresce fino al 20% per la miscela elio-argon, precedentemente studiata, e per la quale sono state rifatte alcune misure, qui non riportate, e migliorati i calcoli.

Come si vede, l'accordo globale tra teoria e risultati sperimentali si può ritenere buono. Certo per poter conseguire una maggior precisione, bisognerebbe disporre di dati numerici più approssimati.

IL NUOVO CIMENTO Vol. I, N. 2 1° Febbraio 1955

Equivalence of the Lagrangian Formulations of Quantum Field Theory due to Feynman and Schwinger.

W. K. Burton

Department of Natural Philosophy, The University - Glasgow

(ricevuto il 17 Gennaio 1955)

Davison [1], Mathews and Salam [2], and Polkinghorne [3] have constructed a field theoretical generalization of Feynman's [4] action principle in quantum mechanics, and Polkinghorne [3] has deduced the canonical commutation relations and the operator equations of motion from it. The present note attempts to outline the proof that Schwinger's [5] dynamical principle may also be deduced from the amended Feynman principle, and hence that Heisenberg's equations of motion and thus Schrödinger's equation are consequences of that principle. The proof of the converse statement, that Schwinger's principle implies Feynman's, is considerably more difficult, but seems to have been achieved in its essentials by Symanzik [6].

Feynman's principle in its amended form presents the transformation function connecting the state on the space-like surface σ' in which the field functions φ have the values φ', with the state on the later space-like surface σ'' in which the φ have the values φ'', as an integral over Hilbert space:

$$(\varphi''\sigma''|\varphi'\sigma') = N^{-1}(\Omega)\int_{\sigma'\varphi'}^{\sigma''\varphi''} \delta\varphi \exp[iI[\varphi]] \tag{1}$$

where $I[\varphi]$ is the action integral

$$I[\varphi] = \int_{\sigma'}^{\sigma''} (\mathrm{d}x)\mathcal{L} \tag{2}$$

---

[1] B. Davison: *Proc. Roy. Soc.*, A **225**, 252 (1954).
[2] P. T. Mathews and A. Salam: *Phys. Rev.* (in press).
[3] J. C. Polkinghorne: *Proc. Roy. Soc.* (in press).
[4] R. P. Feynman: *Rev. Mod. Phys.*, **20**, 367 (1948).
[5] J. Schwinger: *Phys. Rev.*, **91**, 713 (1953).
[6] K. Symanzik: *Zeits. f. Naturfor.*, **9a**, 809 (1954).

for the given Lagrangian density $\mathcal{L}$ taken over the region Ω contained between the space-like surfaces σ' and σ'', and calculated for the field φ. The quantity $N^{-1}(\Omega)$ is a normalizing factor, and $\int_{\sigma'\varphi'}^{\sigma''\varphi''} \delta\varphi$ denotes an integration over all fields φ satisfying the boundary conditions that the φ take the values φ' on σ' and φ'' on σ''. These fields are c-numbers in the Bose case and anticommuting c-numbers ([3]) for Fermi fields. The normalization factors $N^{-1}(\Omega)$ satisfy the composition law ([3])

$$N^{-1}(\Omega+\Omega') = N^{-1}(\Omega)N^{-1}(\Omega'), \tag{3}$$

where the total region $\Omega+\Omega'$ is dissected into the parts Ω and Ω' with a common space-like boundary.

If we make a general variation in (1), we obtain

$$\delta(\varphi''\sigma''|\varphi'\sigma') = N^{-1}(\Omega)\int_{\sigma'\varphi'}^{\sigma''\varphi''} \delta\varphi\cdot i\delta I[\varphi]\,\exp\big[iI[\varphi]\big] = i(\varphi''\sigma''|\,\overline{T}(\delta\boldsymbol{I}[\boldsymbol{\varphi}])|\varphi'\sigma'), \tag{4}$$

where in the second version of the variation, we have used Polkinghorne's result ([3]) that

$$\big(\varphi''\sigma''|\,T(\boldsymbol{\varphi}(x_1)\ldots\boldsymbol{\varphi}(x_n))\,|\varphi'\sigma'\big) = N^{-1}(\Omega)\int_{\sigma'\varphi'}^{\sigma''\varphi''}\delta\varphi\cdot\varphi(x_1)\ldots\varphi(x_n)\,\exp\big[iI[\varphi]\big], \tag{5}$$

for the T-ordered product of the field operators $\boldsymbol{\varphi}$. The latter are defined by Polkinghorne in terms of their matrix elements:

$$(\varphi''\sigma''|\,\boldsymbol{\varphi}(x)|\varphi'\sigma') = N^{-1}(\Omega)\int_{\sigma'\varphi'}^{\sigma''\varphi''}\delta\varphi\cdot\varphi(x)\,\exp\big[iI[\varphi]\big], \tag{6}$$

where x lies on a surface intermediate between σ' and σ''. If derivatives appear on a φ on the right side of (5), the corresponding derivative appears outside the T-product on the left. The symbol $\overline{T}$ in (4) is defined by the requirement

$$\overline{T}\left(\boldsymbol{\varphi}(x_1)\ldots\boldsymbol{\varphi}(x_{j-1})\,\frac{\partial\boldsymbol{\varphi}(x_j)}{\partial x_{j\mu}}\,\boldsymbol{\varphi}(x_{j+1})\ldots\boldsymbol{\varphi}(x_n)\right) = \frac{\partial}{\partial x_{j\mu}}\,T(\boldsymbol{\varphi}(x_1)\ldots\boldsymbol{\varphi}(x_n)). \tag{7}$$

The effect of this in first order Lagrangians is to symmetrize the derivative term in the case of Bose fields, and to antisymmetrize it in the case of Fermi fields, if we use the definition

$$\varepsilon_\mu\partial_\mu\boldsymbol{\varphi}(x) = \lim_{h\to 0}\frac{\boldsymbol{\varphi}(x_\mu+\tfrac{1}{2}h\varepsilon_\mu)-\boldsymbol{\varphi}(x_\mu-\tfrac{1}{2}h\varepsilon_\mu)}{h}. \tag{8}$$

It is seen that equation (4) differs from Schwinger's dynamical principle only in notation: we have merely to put

$$\overline{T}(\delta\boldsymbol{I}[\varphi]) = \delta W, \tag{9}$$

to achieve complete agreement. Moreover the class of « admissible variations » in Schwinger's theory is explicitly indicated: they are the general variations of the « parameters » $\varphi(x)$ appearing in $I[\varphi]$. The result that the first order variation of the transformation function vanishes for variation of $\boldsymbol{\varphi}(x)$ at places between σ' and σ'' is effectively demonstrated in POLKINGHORNE's paper; he also deals with variations of φ' and φ''. The reasoning used in that case is easily extended to the coordinated variations $x_\mu \to x_\mu + \delta x_\mu$; the main result needed being that the change in the volume element $(\mathrm{d}x)$ in (2) is $\delta(\mathrm{d}x) = (\mathrm{d}x)\,\partial_\mu\,\delta x_\mu$. The result is, as might well be expected, that the eigenvectors out of which the transformation is constructed undergo unitary transformations with generator $G = \int_\sigma \mathrm{d}\sigma_\mu\, T_{\mu\nu}\,\delta x_\nu$, where $T_{\mu\nu}$ is the energy-momentum tensor and the integration is over the surfaces σ' and σ''. The remaining type of variation is that of the structure of $\mathcal{L}$, for example source variations.

More details will be given in a forthcoming paper written in collaboration with A. H. DE BORDE of this Department.

Thermodynamics and Quantum Mechanics.

A. Gamba

Istituto di Fisica dell'Università - Torino

(ricevuto il 18 Gennaio 1955)

The most complete discussion of the connections between thermodynamics and quantum mechanics is still to be found in von Neumann's book (1). However, in the light of the recently developed theory of information (2), not all the conclusions of von Neumann can be accepted as satisfactory, and in this letter we shall discuss how to supplement von Neumann's theory in order to get a more modern picture of the whole subject.

The main result of information theory as regards thermodynamics is the introduction of a quantitative measure for the concept of information, which turns out to be a negative entropy (negentropy) (3). The second principle of thermodynamics states that in a closed system the quantity «entropy minus information» either increases (irreversible processes) or remains constant (reversible processes). Therefore, if by means of an experiment we get some information, the entropy of the observed system is diminished. Of course, this has to be paid by a greater or at least equal increase in the entropy of the measuring apparatus, since the entropy of the observed system + measuring apparatus cannot decrease Examples may be found in the quoted papers by Brillouin (3). One has to be careful that the information which amounts to negentropy is only the information one gets through an actual experiment, which excludes some of the physically allowed states; the knowledge of a natural law, which limits the a priori possible states (4) is *not* to be counted as information. Of the first type is, for example, the reading of an ammeter (any position of the needle is a priori allowed, the experiment decides which it actually is); of the second type is the knowledge that three electrons cannot be in the same 1s state of an atom due to the exclusion principle.

We may say that, other things being

(1) J. v. Neumann: *Mathematische Grundlagen der Quantenmechanik* (Berlin, 1932), pp. 191-222.

(2) C. E. Shannon and W. Weaver: *Mathematical Theory of Communication* (University of Illinois Press 1949).

(3) L. Brillouin: *Journ. Appl. Phys.*, **24**, 1152 (1953); **25**, 595 (1954). The first quantitative discussion of the concept of information is due to L. Szilard: *Zeits f. Phys.*, **53**, 840 (1929); however, it is only after the development of the theory of communication. that the importance of this concept has been fully realized.

(4) A. Gamba: *Journ. Appl. Phys.*, **25**, 1549 (1954).

equal, the best experiment is the one, which reduces the most the entropy of the observed system (incidentally, no such means are given to decide on the goodness of a theory).

VON NEUMANN defines the entropy of a quantum mechanical system as

$$S = -Nk \,\mathrm{Spur}\,(U \ln U)\,,$$

where N is the number of individual systems, k the Boltzmann constant, and U the statistical matrix (von Neumann's notation will be used throughout this letter). Then he starts examining the various processes, which are liable to change U and therefore the entropy, in order to prove that the 2nd principle of thermodynamics holds true.

He finds two such processes:

$$(1) \qquad U \to U' = \sum_1^\infty{}_n \,(U\varphi_n, \varphi_n) P_{[\varphi_n]}\,,$$

which is due to the perturbation on the system when a measurement is made:

$$(2) \qquad U \to U_t = \\ = \exp\left[-\frac{2\pi i}{h} tH\right] U \exp\left[\frac{2\pi i}{h} tH\right],$$

which is due to the natural evolution of the system which satisfies a Schrödinger equation.

VON NEUMANN proves that process (2) does not change the entropy. The proof is straightforward since (2) is a unitary transformation, which leaves the spur invariant.

A more careful analysis is needed for process (1). VON NEUMANN proves that in this case the entropy either increases or remains constant. This seems rather suprising, since there is no need that the entropy of a system should increase or remain constant during a measurement, when it interacts with the measuring apparatus and therefore is not closed. And there is even something worse: according to what we said before a good experiment is one in which the entropy of the system is *decreased*.

In order to solve the paradox, let us go back to classical physics. Two kinds of experiments may be envisaged.

The first one is a measurement which simply verifies the predictions of a theory and is typical of the following idealized experiment. A body is given the position and momentum at the time t_0. Knowing the force law, one is able to predict theoretically the position and momentum at a later time t. An experiment is now designed to determine the position at the time t. If the theory were known to be correct and the precision of the experimenter were infinite, this could be more properly called a verification rather than a measurement; and, of course, we get no information (no reduction of the entropy of the observed system), since everything was already known before. We could possibly only loose some information by giving an unknown perturbation to the observed system, as a consequence of a too crude process of measurement. This is the type of experiment which is the classical analogue of von Neumann's process (1). We transform a statistical mixture U into statistical mixture U' by verifying experimentally that by measuring the observable R in a great number of individual states described by U we get the statistical mixture U'. This, however, was all predicted by the theory and we get no information. We may only add, in view of von Neumann's results, that in this case the analogue of a classical unaccurate measurement, which gives an unknown perturbation to the system, is also a measurement of an observable R which does not commute with U.

The second kind of experiment in classical physics is the one which is typical of the reading of an ammeter in order to know an a priori unknown current. In this case we get some information and the entropy is reduced. This

process, which is far more significant as a measurement, has a quantum analogue which has not been considered by VON NEUMANN. Let us call it process (1′): it is a measurement which transforms the statistical matrix U describing a *single* particle into the pure eigenstate corresponding to the experimentally found eigenvalue of the observed operator R. In other words, when we observe a single particle described by U with an operator R, the a priori possible results are given by the statistical matrix U' of process (1). However, this is only the first step of the process of measurement. Next we actually make the measurement and with it we further restrict the possibilities given by U' by bringing the particle into the pure state, corresponding to the experimentally found eigenvalue of R, in an unpredictable way. We gain some information and the entropy of the system is reduced from $-k\,\mathrm{Spur}\,(U \ln U) \geqslant 0$ to 0 (the entropy of a pure state). Of course, this is paid by an equal or greater increase in the entropy of the measuring apparatus.

In conclusion, by taking into account process (1′), information theory can be consistently fitted into the scheme of quantum mechanics as well as of classical physics.

IL NUOVO CIMENTO Vol. I, N. 2 1° Febbraio 1955

Field Equations in General Relativity.

C. W. Kilmister
Department of Mathematics, King's College - London

G. Stephenson
Department of Mathematics, Imperial College - London

(ricevuto il 18 Gennaio 1955)

The logical status of any of the usual derivations of the field equations of general relativity is very different from that of the foundations of the theory. There are three such derivations and each involves an argument in which there is considerable hiatus.

1. – In one derivation [1,2,3] the Riemann-Christoffel tensor occurs first in an integrability condition (« condition for flat space-time »), $B^i_{jkl}=0$. From this equation, the tensor B^i_{jkl} is abstracted; a symmetric tensor of rank two, S_{jk} is then sought, which will vanish whenever B^i_{jkl} vanishes. If we assume *arbitrarily* that S_{jk} is a linear function of the B^i_{jkl} which does not involve any new field variables, it is easy to prove that we may without loss of generality take S_{jk} as the contracted tensor R_{jk} $(=B^s_{jks})$. This process can, of course, only derive the field equations without a cosmical term.

2. – An alternative derivation [4,5] depends on the concept of parallel displacement. Since vectors at distant points cannot be compared, the effect of parallel displacement can only be measured by displacing a vector round a closed circuit. The resultant change is

$$\delta A^i = \iint_{\vee} B^i_{jkl} A^j \, \delta S^{kl}_{\vee} .$$

This is used to introduce B^i_{jkl} and avoids the criticism in (1) that the tensor is first introduced in the form of an equation $B^i_{jkl}=0$. The rest of the argument is as in (1). There is now the serious objection, however, that since $\delta S^{kl}_{\vee}$ is skew-symmetric, we also have

$$\delta A^i = \iint_{\vee} K^i_{jkl} A^j \, \delta S^{kl}_{\vee} ,$$

where $K^i_{jkl}=B^i_{jkl}+T^i_{j\underline{kl}}$; and $T^i_{j\underline{kl}}$ is any tensor symmetric in (k, l). The choice

(1) A. S. Eddington: *Mathematical Theory of relativity* (Cambridge, 1952), § 37.
(2) E. Schrödinger: *Space-Time Structure* (Cambridge, 1950), Chap. 8.
(3) R. C. Tolman: *Relativity, Thermodynamics and Cosmology* (Oxford, 1934).
(4) See (1), § 84.
(5) See (1), § 92.

of B^i_{jkl} for contraction is thus *arbitrary*. A variation of this treatment is to investigate the effect of interchanging the order in two-fold covariant differentiation. This avoids the ambiguity noticed here, at the expense of all intuitive obviousness.

3. – A method involving no appeal to the Riemann-Christoffel tensor ([6,7]) uses the result that the only symmetric tensor of rank two which is conserved, and is derived from the metric tensor and its derivatives, is $R_{ij} - \frac{1}{2}g_{ij}(R - 2\lambda)$, provided we apply to this tensor the *arbitrary* restrictions that it contains no derivatives of g_{ij} above the second, and is linear in the second derivatives. This tensor is then identified as a multiple of the energy tensor, and equated to zero in free space. The field equations with the cosmical term then result.

In each of these cases the arbitrary point constitutes a break in the argument. In some expositions ([3]), an attempt is made to overcome this by an appeal to experiment. Since the line elements involved in all known experiments have an exceedingly special form, this appeal is very weak. It is the purpose of this letter to direct attention to the need for improvement in the derivation of the theory at this point.

([6]) P. G. BERGMANN: *Introduction to the Theory of Relativity* (New York, 1946).

([7]) C. MØLLER: *Theory of Relativity* (Oxford, 1952).

LIBRI RICEVUTI E RECENSIONI

H. Bruining – *Physics and Applications of Secondary Electron Emission*; un vol. di XII+178 p. Ed. Pergamon Press, London 1954, 25 s..

Nella raccolta « Electronics and Waves » della Pergamon Press è uscito quest'anno un volumetto che tratta i problemi della emissione di elettroni secondari; l'opera è impostata prevalentemente da un punto di vista sperimentale e pratico, ma non trascura elementi di teoria che permettano al lettore di interpretare correttamente i fatti osservati.

L'alto livello scientifico e tecnico, la completezza della documentazione e la veste editoriale curata sono caratteristiche di questa raccolta e non hanno bisogno di presentazione; basti dire che questo volume è ricco di dati quantitativi, presentati in diagrammi e tabelle, e che l'elenco bibliografico comprende 33 citazioni di carattere scientifico, elencate in ordine cronologico, a partire dal 1902 fino al 1952, e molte altre che riguardano le applicazioni.

Ecco come è distribuita la materia nel testo: dopo brevi cenni introduttivi l'attenzione del lettore è richiamata prima sui metodi di studio e di misura della emissione secondaria, successivamente sulle caratteristiche della emissione da parte dei metalli e dei composti metallici. Un capitolo a parte tratta dell'influenza degli strati di ioni e di atomi adsorbiti, sulla produzione di elettroni secondari.

A questo punto trovano luogo considerazioni di carattere teorico, in un tentativo di paragonare le teorie sino ad ora proposte, nessuna delle quali spiega completamente tutti i fenomeni osservati.

Gli ultimi tre capitoli sono completamente dedicati alle applicazioni; notiamo in particolare le notizie sui fotomoltiplicatori e sui tubi dotati di « memoria ». Anche gli effetti dannosi, prodotti talvolta dalla emissione secondaria, sono esaminati, ad uno ad uno, e con essi i metodi per evitarli.

Nell'insieme il volume si presenta come un'ottima fonte di informazione, utile sia per chi desideri una introduzione generale sull'argomento, sia per chi cerchi particolari notizie aggiornate; ne è garanzia la competenza specifica dell'Autore, che è uno dei ricercatori dei laboratori Philips di Eindhoven.

F. A. Levi

Department of Scientific and Industrial Research – *Scientific Research in British Universities 1953-54*; un vol. di V+522 p. Ed. H. M. Stationary Office, 1954; 10 s..

Nel 1948 il British Council pubblicò un volume intitolato *Scientific Research in Britain* contenente un elenco dei lavori che si stavano svolgendo presso gli Istituti scientifici britannici. Di questa opera, che ebbe inizialmente una modesta tira-

tura, vennero pubblicate successive edizioni nel 1949-50 e nel 1950-51, limitando le notizie fornite al lavoro in corso presso gli Istituti universitari. Nel 1951-52 venne diffusa una edizione pubblicata dal H.M.S.O. e posta in vendita al pubblico; questo volume del 1953-54, che appare dopo un anno di interruzione, prosegue la raccolta.

Le notizie pubblicate sono state raccolte a cura del British Council e riguardano i lavori scientifici attualmente svolti dal personale di ruolo presso le Università britanniche; per ciascuna delle 24 Università, elencate in ordine alfabetico, sono pubblicati, per ogni disciplina, i nomi dei ricercatori, seguiti da brevi cenni indicativi degli argomenti trattati. Le informazioni risultano molto complete benchè di fronte a qualche nome si legga « no information ».

La consultazione del volume è resa pratica dai due indici che lo completano, uno dei nomi ed uno delle materie, il quale permette di trovare prontamente quali ricerche sono in corso su un determinato argomento.

Questa pubblicazione, che può apparire a prima vista arida e scarsamente particolareggiata, contiene in realtà una vasta messe di notizie di grande interesse e prende degnamente posto tra quei preziosi ausiliari del ricercatore scientifico che sono le raccolte ordinate di informazioni, come gli indici bibliografici e le tabelle dei dati numerici. Ci si deve quindi augurare che insieme alle successive edizioni di quest'opera, possibilmente più dettagliate almeno per alcune voci, vedano prossimamente la luce altre analoghe pubblicazioni che diano un quadro sempre più vasto e completo della ricerca scientifica mondiale.

F. A. Levi

GRIMSEHL – *Lehrbuch der Physik*, Ester Band: *Mechanik Wärmelehre, Akustik*. Fünfzehnte Auflage, 8s. x+622 mit 722 Abbildungen, B. G. Teubner, Leipzig 1954.

Della nuova edizione di questo classico trattato scolastico sono state già recensite qui le parti dedicate all'Elettromagnetismo (*Nuovo Cimento*, **9**, 380 (1952)) ed Ottica (*Nuovo Cimento*, **10**, 693 (1953)). Il rifacimento dell'opera, intrapreso nel 1945 dal prof. W. Schallreuter, prevede anche un quarto volume, sulla fisica atomica. Intanto è apparsa questa 15° edizione del primo, che comprende vari aggiornamenti e allargamenti, specialmente nei capitoli riguardanti la termologia e l'acustica, ed una utile appendice con le nozioni essenziali di calcolo vettoriale. Segue ad essa una quindicina di tabelle che riportano alcune velocità ed accelerazioni caratteristiche, le dimensioni nel sistema C.G.S. e le unità di misura delle grandezze meccaniche e termiche, le equazioni principali introdotte nel testo, ed altri dati di interesse pratico. Oltre agli indici dei nomi e degli argomenti, vi è infine un elenco cronologico dei grandi fisici, da Leonardo a Joliot e Anderson, che stranamente esclude il nome di Fermi.

V. Somenzi

Questo fascicolo è stato licenziato dai torchi il 28-I-1955

Direttore responsabile: G. POLVANI

Tipografia Compositori - Bologna